UNIVERSITÉ DU QUÉBEC À MONTRÉAL

EUTROPHISATION ET HYPOXIE DE L'ESTUAIRE MARITIME DU SAINT-LAURENT : ASPECTS GÉOCHIMIQUES

THÈSE

PRÉSENTÉE

COMME EXIGENCE PARTIELLE

DU DOCTORAT EN SCIENCES DE L'ENVIRONNEMENT

PAR

BENOIT THIBODEAU

NOVEMBRE 2010

AVANT-PROPOS

Cette thèse a été rédigée sous forme de trois articles publiés ou en préparation pour publication dans des journaux à comité de lecture. Chaque article est écrit en anglais et constitue un chapitre. La mise en page de ces trois chapitres suit donc les directives propres à chaque revue. Pour cette raison, les titres et figures de chacun ne sont pas numérotés selon le Guide de présentation des mémoires et thèses de l'UQÀM (Bouthat, 1993). À la place, les numéros tels qu'ils apparaissent dans les articles ont été conservés. De plus, les formats des références sont légèrement différents d'un chapitre à l'autre, afin de rester conformes aux revues dans lesquelles ils seront publiés.

Le premier chapitre est un article publié en 2010 dans la revue *Geophysical Research Letters* et ayant pour titre « *Twentieth century warming in deep waters of the Gulf of St. Lawrence : A unique feature of the last millennium* ». Il a pour co-auteurs Anne de Vernal, Claude Hillaire-Marcel et Alfonso Mucci. L'article confirme l'ampleur du réchauffement des masses d'eau profondes du Saint-Laurent et en précise la résolution temporelle. Cette étude est basée sur les résultats de la carotte CR02-23 que j'ai échantillonné en 2002. J'ai effectué la totalité des analyses géochimiques sur cette carotte. J'ai ensuite comparé les résultats avec ceux d'une carotte archivée au GEOTOP. J'ai interprété les résultats et écrit l'article avec l'aide des trois co-auteurs.

Le deuxième chapitre est un article publié en 2010 dans la revue *Estuarine, Coastal and Shelf Science* et ayant pour titre « *Benthic nutrient fluxes along the Laurentian Channel: Impacts on the N-budget of the St. Lawrence marine system* ». Les co-auteurs sont Moritz Lehmann, Jacqueline Kowarzyk, Alfonso Mucci, Yves Gélinas, Denis Gilbert, Roxane Maranger et Mohammad Alkhatib. L'article porte sur les variations spatiales des flux benthiques de nitrate et de leur rôle dans le cycle régional de l'azote dans l'estuaire et le golfe du Saint-Laurent. Cet article fait suite à deux missions en mer (2005 et 2006) auxquelles j'ai participé. J'ai donc prélevé la totalité des échantillons utilisés dans cette étude et j'ai effectué toutes les analyses des isotopes des nitrates. Les mesures de concentrations en nutriments ont été effectuées au GEOTOP par Sophie Xiu Phuong, celles de N_2 ont été réalisées à l'Université de Montréal par

Jacqueline Kowarzyk dans le laboratoire de Roxane Maranger. Les mesures isotopiques de l'ammonium ont été faites par Mark McCarthy dans le laboratoire de Wayne Gardner (Université du Texas, Austin). Les co-auteurs ont participé à au moins une des missions en mer et ont donc contribué à l'échantillonnage. Le texte a été rédigé par moi-même mais les co-auteurs ont eu l'occasion de se prononcer sur l'article avant qu'il ne soit soumis.

Le troisième chapitre est un article en préparation pour la revue *Biogeochemistry* et ayant pour titre « *Seasonal variations of nitrogen sources and cycling in the St. Lawrence River* ». Les co-auteurs seront Moritz Lehmann, Jean-François Hélie et Éric Rosa. Il expose les différentes sources possibles d'azote ainsi que les variations saisonnières des apports. La possibilité de production interne d'azote y est également évoquée. Pour la préparation de ce chapitre, j'ai effectué la totalité des analyses isotopiques sur les nitrates ainsi que l'interprétation et la rédaction. L'échantillonnage a été réalisé par Éric Rosa et Jean-François Hélie. La rédaction a été faite en collaboration avec Moritz Lehmann.

L'appendice D contient les données micropaléontologiques et géochimiques que j'ai produites à partir d'une carotte échantillonnée en 2006, à la tête du Chenal Esquiman (CR06-TCE). J'ai effectué le sous-échantillonnage ainsi que toutes les analyses subséquentes. Les analyses isotopiques ont été faites au GEOTOP avec l'aide de Jean-François Hélie, Agnieszka Adamowicz et Julie Leduc. Les données consignées dans l'appendice sont intéressantes, mais les résultats de mesures ^{14}C ont démontré des vitesses de sédimentation inférieures à 10 cm/10^3 ans, ce qui est peu compatible avec la problématique abordée dans cette thèse.

L'appendice E contient les mesures isotopiques des nitrates dissous pour les échantillons prélevés en 2005 et 2006 dans l'estuaire et le golfe du Saint-Laurent. J'ai effectué les prélèvements et produit la totalité des données présentées dans cette annexe.

L'appendice F contient un article dans lequel je suis co-auteur. Pour cette étude, j'ai contribué aux analyses de foraminifères benthiques ainsi qu'à l'interprétation des résultats et à la rédaction du manuscrit.

REMERCIEMENTS

Je remercie ma directrice de thèse, Anne de Vernal, de m'avoir donné l'opportunité de travailler sur le projet hypoxie et de m'avoir soutenu et encouragé.

J'ai aussi eu la chance de côtoyer des chercheurs qui ont influencé ma vision de la science chacun à leur manière. Merci notamment à Alfonso Mucci, Claude Hillaire-Marcel, Marc Lucotte, Yves Gélinas, Christophe Migon, Alain Véron, Denis Gilbert, Ana Carolina Ruiz-Fernandez, Alfred Jaouich, Catherine Jeandel et Frédérique Eynaud. Merci aussi à Moritz Lehmann, qui m'a permis de me bâtir une force de caractère et une détermination à toute épreuve.

Merci au personnel technique du GEOTOP-UQAM pour leur aide et leur soutien : Jean-François Hélie, Josée Savard, Maryse Henri, Bassam Ghaleb, Agnieszka Adamowicz, Julie Leduc, Sophie Xiu Phuong et Chantal Gosselin. Aussi, merci à Aurélie Dufour du Laboratoire d'Océanographie de Villefranche-sur-mer.

Aussi, merci aux chercheurs qui donnent vie à la prestigieuse école d'été d'Urbino et qui s'efforcent d'interagir avec les étudiants qui y participent, entre autres : Henk Brinkhuis, Thomas Cronin, Robert DeConto, Simone Galeotti, Matthew Hubert, Mark Leckie, Debbie Thomas et Richard Zeebe.

Merci aux organismes subventionnaires qui m'ont permis de réaliser cette étude: Le Fonds québécois de la recherche sur la nature et les technologies, le GEOTOP, l'Université du Québec à Montréal, le Conseil de recherche en sciences naturelles et en génie du Canada, Hydro-Québec et Québecor. Merci aussi au consortium européen et canadien de forage océanique (ECORD et CCORD) pour le financement qui m'a permis de participer à l'école d'été d'Urbino.

Finalement, merci à ma famille et à mes amis pour tout ce qu'il y a de réellement important.

TABLE DES MATIÈRES

LISTE DES FIGURES

INTRODUCTION

CHAPITRE I

CONCLUSION

LISTE DES TABLEAUX

APPENDICE A

RÉSUMÉ

Cette étude a été réalisée avec comme objectif principal d'identifier les processus mis en cause dans l'hypoxie récente de l'estuaire maritime du Saint-Laurent. Cette zone d'hypoxie existe depuis une vingtaine d'années et engendre des conséquences néfastes pour cet écosystème. Il devient donc critique de comprendre les mécanismes qui sont responsables du taux d'oxygénation dans l'optique de proposer des solutions d'adaptation réalistes. Pour ce faire, nous avons ciblé deux des processus qui ont probablement le plus d'impact sur les concentrations en oxygène dissous de cet écosystème, c'est-à-dire le réchauffement des eaux profondes et l'eutrophisation possible des eaux de surface de l'estuaire.

Pour bien comprendre le rôle du réchauffement sur l'hypoxie, il est important d'avoir accès à des séries temporelles plus étendues que celles que nous offrent les données instrumentales. L'étude de carottes de sédiment nous permet d'obtenir des renseignements précieux sur les conditions environnementales du passé. Nous avons étudié deux carottes sédimentaires provenant de l'estuaire du Saint-Laurent dans le but d'estimer les variations de température survenues depuis le dernier siècle voire même depuis le dernier millénaire. Dans ces carottes, nous avons mesuré la composition isotopique en oxygène ($\delta^{18}O$) des tests de foraminifères benthiques. Cette mesure enregistre, entre autres, la température de calcification de l'organisme, et donc de l'eau dans lequel il se trouve. En comparant le $\delta^{18}O$ avec les données de température instrumentales, nous avons validé l'utilisation du $\delta^{18}O$ comme paléothermomètre dans l'estuaire du Saint-Laurent. De ce fait, nous avons utilisé le $\delta^{18}O$ pour reconstruire les variations de température du dernier millénaire. Les résultats nous permettent de conclure que les eaux de fond de l'estuaire du Saint-Laurent se sont réchauffées d'environ 1.7°C depuis le dernier siècle. Cela constitue le plus important réchauffement des 1 000 dernières années.

L'eutrophisation des eaux de surface en milieu estuarien est généralement due à un apport accru en nitrate, nutriment limitant dans ce type de milieu. Les sources d'azote ayant déjà été étudiées, nous avons donc mesuré les puits de façon à pouvoir établir un bilan régional. Deux approches ont été privilégiées: 1) une série de mesures de dénitrification sédimentaire ponctuelles et 2) une approche intégratrice se basant sur les concentrations d'azote et de phosphore dans la colonne d'eau. Les mesures nous permettent de conclure que la majorité de la dénitrification benthique est produite par le couplage nitrification-dénitrification. De plus, les résultats sont cohérents avec l'hypothèse que le processus de bioirrigation joue un rôle très important dans l'élimination sédimentaire de l'azote. L'approche intégratrice semble indiquer que le bilan régional de l'azote est proche de l'équilibre, ce qui suggère que cette région ne peut être considérée comme globalement soumise au phénomène d'eutrophisation. Ceci impliquerait donc que si l'augmentation de la productivité

primaire observée dans l'estuaire du Saint-Laurent est due à une augmentation de l'apport en azote, celui-ci est par la suite éliminé naturellement par le système sans avoir d'impact en aval.

Dans l'optique de proposer des solutions au problème de l'hypoxie, nous devons mieux connaître les sources d'azote qui fertilisent le Saint-Laurent ainsi que le taux de recyclage *in situ*. Par conséquent, nous avons mesuré la composition isotopique des nitrates dissous dans la ville de Québec pour identifier les différentes sources d'azote qui se retrouvent dans le Saint-Laurent. De plus, cette méthode nous permet d'identifier les mécanismes du cycle de l'azote qui sont actifs dans cette région. Les résultats sont typiques d'un environnement ou la composition isotopique des nitrates est principalement contrôlée par la saisonnalité et où les processus internes ne semblent pas avoir un impact significatif. Par contre, le peu de données sur la signature isotopique des différentes sources potentielles nous empêche de quantifier leur importance dans le flux de nitrate du Saint-Laurent.

INTRODUCTION

1. Motivation

1.1. Hypoxie et eutrophisation en milieu estuarien et côtier

Aucune variable environnementale, d'une importance écologique aussi capitale pour les écosystèmes estuarien et côtier, n'a changé aussi radicalement, sur une période de temps aussi courte, que la concentration d'oxygène dissous (OD) (Diaz, 2001). Pour définir le seuil où les concentrations d'OD deviennent trop faibles pour le fonctionnement normal de l'écosystème et des organismes y vivant, nous utilisons le terme hypoxie, emprunté aux sciences médicales. Comme ce seuil peut varier d'un écosystème à l'autre et dépend du contexte géographique, il n'y a pas de définition officielle de l'hypoxie. Ainsi,, nous nous baserons sur le seuil le plus couramment utilisé de 2 mg L^{-1} (équivalent à 63 µmol L^{-1}, ou 30% de saturation) (Diaz, 2001; Rabalais et al., 2009). La présence d'environnements hypoxiques et anoxiques (où l'OD est complètement absent) n'est pas nouvelle lorsque l'on considère l'histoire de la Terre (Gilbert et al., 2009; Rabalais et al., 2009). Le déficit est créé lorsque l'OD présent dans la colonne d'eau est consommé à un rythme plus élevé que son ajout. Les voies par lesquelles l'OD peut être ajouté sont l'échange d'O_2 entre l'eau et l'atmosphère, la production photosynthétique *in situ*, ou l'advection d'eau contenant de l'OD. La plupart du temps, l'hypoxie se produit dans une masse d'eau isolée par une barrière de densité, appelée pycnocline (causée par la température et/ou la salinité), qui empêche l'apport d'OD par diffusion ou mélange. Le risque d'hypoxie est spécialement élevé si le temps de séjour de la masse d'eau isolée est élevé, comme dans le cas du fjord de Saanich Inlet (Tunniclife, 1981). L'hypoxie peut aussi être induite par l'advection de masses d'eau déjà appauvries en OD. Par exemple, des changements dans la contribution de la masse d'eau intermédiaire, faible en OD, provoquent des variations temporelles des concentrations d'OD dans l'est de l'Océan Pacifique (Chan et al., 2008; Bograd et al., 2008). La baie

de Yaquina, en Oregon, est aussi sujette à des épisodes d'hypoxie lorsqu'une masse d'eau pauvre en OD pénètre par advection dans la baie (Bown et al., 2007). L'advection de masses d'eau pauvres en OD peut aussi être induite par le vent, comme c'est le cas dans les baies de Donkai et Ise, au Japon (Nakata et al., 1997; Ueda et al., 2000) et dans la baie de Chesapeake (Breitburg, 1992).

Selon plusieurs études, l'apparition des zones hypoxiques est plus importante à notre époque et serait probablement engendrée par les activités humaines (Diaz, 2001; Cloern, 2001; Gilbert et al., 2009). Une synthèse effectuée par Diaz (2001) démontre que le budget d'OD de plusieurs systèmes estuariens et côtiers est affecté principalement par une augmentation de la consommation locale d'OD due au phénomène d'eutrophisation. En milieu estuarien, la source de carbone qui permet la respiration de l'OD peut être autochtone (productivité primaire locale) et allochtone (d'origine terrestre, naturelle ou anthropique). Peu importe sa source, ce carbone sera dégradé par l'activité bactérienne via la réaction de respiration (1), qui consomme de l'OD, diminuant ainsi la concentration d'OD résiduelle dans la masse d'eau.

$$CH_2O + O_2 \Rightarrow CO_2 + H_2O \qquad (1)$$

L'eutrophisation est l'augmentation de l'apport de carbone entraînant une augmentation de la consommation d'OD et donc une diminution importante de la concentration d'OD de la masse d'eau. La principale cause d'eutrophisation en milieu estuarien et côtier est l'apport excessif de nitrate qui engendre une hausse de la productivité primaire. Cependant, la cause peut aussi être liée à des changements hydrologique ou dans l'activité biologique (Turner and Rabalais, 1994; Diaz and Rosenberg, 1995; Cloern, 2001; Rabalais et al., 2009). Les zones estuariennes étant souvent limitées en nitrate, elles sont donc particulièrement sensibles à ces apports. Les rejets anthropiques de nitrate ont considérablement augmenté durant le dernier siècle notamment par la fixation du N_2 pour fabriquer des fertilisants et l'émission

d'oxydes nitreux par la combustion d'énergie fossile (Galloway et al., 2004). Le rejet de ces nitrates dans l'environnement a augmenté 20 fois entre les années 1860 et 1995, et a continué de croître 156 Tg N an^{-1} en 1995 à 187 Tg N an^{-1} en 2005 (Galloway et al., 2008). Cette augmentation de l'apport en nitrates a résulté en une amplification de la productivité primaire dans les environnements qui étaient préalablement limités en nitrates, engendrant donc une hausse de l'exportation de carbone organique vers les sédiments, et conséquemment une augmentation de la consommation en OD. Un des mécanismes naturels pouvant améliorer la situation est la dénitrification (2), réaction qui transforme les nitrates en N_2, qui diffusent alors vers l'atmosphère. Cette réaction est dépendante de plusieurs facteurs, notamment la production de nitrate par la nitrification (3) qui est dépendante à son tour du taux d'OD. La dénitrification est donc un paramètre difficile à évaluer sans une étude circonstanciée de l'écosystème.

$$NO_3^- + CH_2O \Rightarrow N_2 + CO_2 + H_2O \quad (2)$$

$$NH_4^+ \Rightarrow NO_2^- \Rightarrow NO_3^- \quad (3)$$

Les conséquences écologiques de l'hypoxie sont importantes et sont proportionnelles à son intensité et à sa durée (Diaz, 2001; Levin et al., 2009). Les conséquences les plus fréquentes sont une migration des espèces vivantes dans la colonne d'eau, ainsi qu'un changement dans la structure des communautés benthiques par la mortalité des espèces à mobilité réduite et la migration des espèces mobiles. Les modifications des communautés benthiques peuvent aussi avoir des conséquences indirectes sur la chaîne alimentaire (Diaz, 2001). De plus, les faibles concentrations d'OD peuvent avoir des impacts physiologiques, par exemple en réduisant le taux de croissance des poissons (Taylor et Miller, 2001) et en diminuant la capacité de reproduction de certaines espèces (Marcus et al., 2004). Ces effets ont déjà eu des répercussions majeures sur certains écosystèmes, comme en témoignent le

déclin de la langoustine en Mer de Kattegat (Baden et al., 1990) et de plusieurs espèces de poissons de fond en Mer Baltique et en Mer Noire (Breitburg et al., 2001; Diaz et al., 2004). Les zones hypoxiques et anoxiques sont communément qualifiées de *dead zones* (zones mortes) vu le désastre écologique qu'elles représentent. Depuis les années 60, le nombre de ces zones mortes a doublé chaque décennie (Diaz and Rosenberg, 2008). À ce jour, 400 zones mortes ont été déclarées, pour une surface totale affectée de plus de 245 000 km^2.

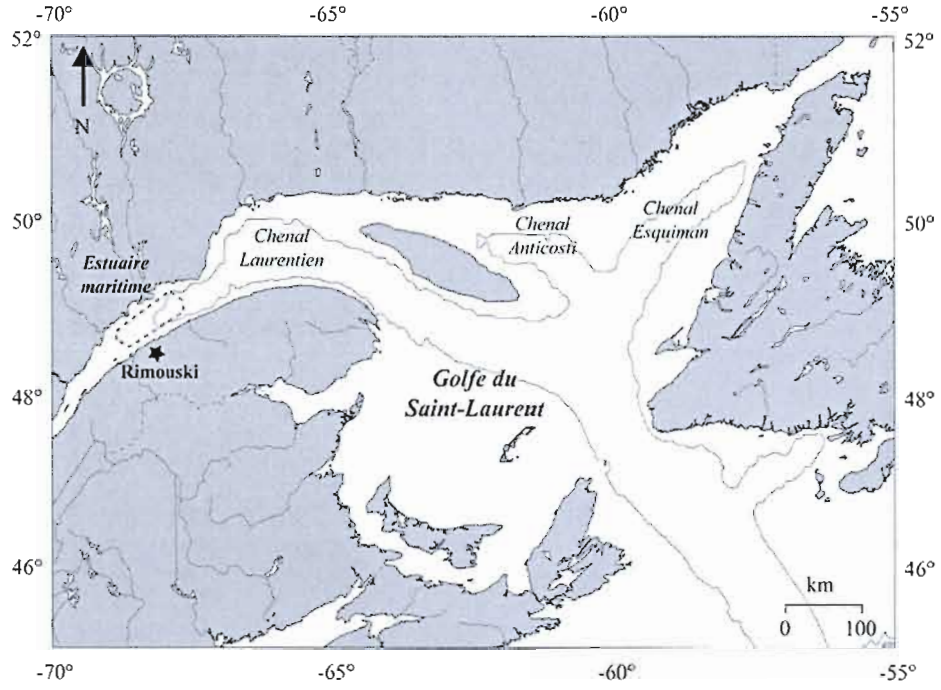

Figure 1. Carte de l'estuaire maritime et du golfe du Saint-Laurent. La zone grisée représente environ l'étendue de la zone d'hypoxie. L'isobathe est celle de 300 m.

1.2. L'hypoxie de l'estuaire du Saint-Laurent.

Une étude récente a mis en évidence qu'une zone hypoxique est présente dans l'estuaire maritime du Saint-Laurent (Figure 1) et recouvre une surface d'environ 1300 km^2 (Gilbert et al., 2005). À l'aide de données instrumentales, il a été démontré

que les concentrations d'OD ont diminué de 50% en l'espace de 70 ans, passant d'environ 40% de saturation en 1930 à moins de 20% lors des deux dernières décennies (Gilbert et et al., 2005). La zone hypoxique est restreinte à l'estuaire maritime dû à la forte productivité locale, mais aussi dû à la stratification des masses d'eau. En effet, l'estuaire maritime est caractérisé par une circulation de type estuarienne, c'est-à-dire par une couche d'eau douce en surface provenant du ruissellement du bassin versant et une couche d'eau salée en profondeur, provenant de l'océan Atlantique. Dû à leurs densités très différentes, très peu d'échanges s'effectuent entre les deux masses d'eau (Figure 2). La différence d'OD observée dans les eaux de fond entre l'estuaire et le détroit de Cabot est donc principalement le résultat de l'effet cumulatif de la consommation d'OD par la dégradation de la MO, puisque l'OD des eaux de fonds ne peut pas être renouvelé par mélange vertical (Figure 3).

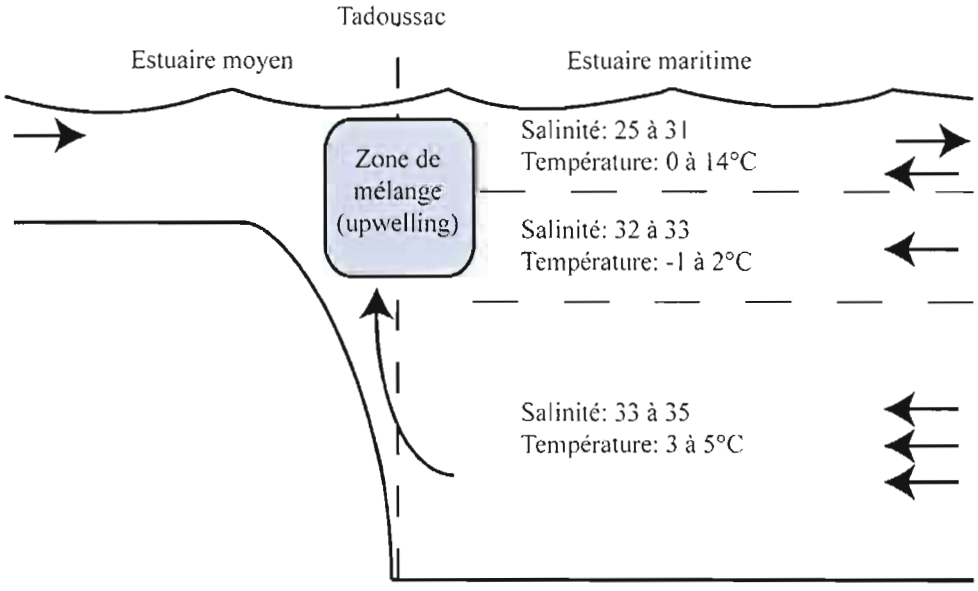

Figure 2. Représentation des différentes masses d'eau et de la circulation dans l'estuaire moyen et maritime.

Des répercussions de l'hypoxie des eaux de fond aux environs de Rimouski ont déjà été mises en évidence, notamment par un changement de diversité de la faune benthique qui est maintenant caractérisé par des organismes tolérants de faibles concentrations d'OD, comme la classe des polychètes aux dépens des crustacés et des mollusques (Bourque, 2009). Un gradient faunistique a aussi été déterminé (Belley et al., 2010) le long du gradient d'OD, ce qui nous laisse croire que l'OD est un facteur déterminant de la biodiversité du benthos dans le Saint-Laurent.

Le déclin des concentrations en OD dans l'estuaire du Saint-Laurent peut être relié à plusieurs phénomènes: a) des changements océanographiques comme une augmentation du temps de séjour de la couche d'eau de fond ou une diminution de la concentration initiale d'OD de la masse d'eau profonde lors de son entré par le détroit de Cabot et b) une augmentation de la demande totale en OD par la dégradation de la MO.

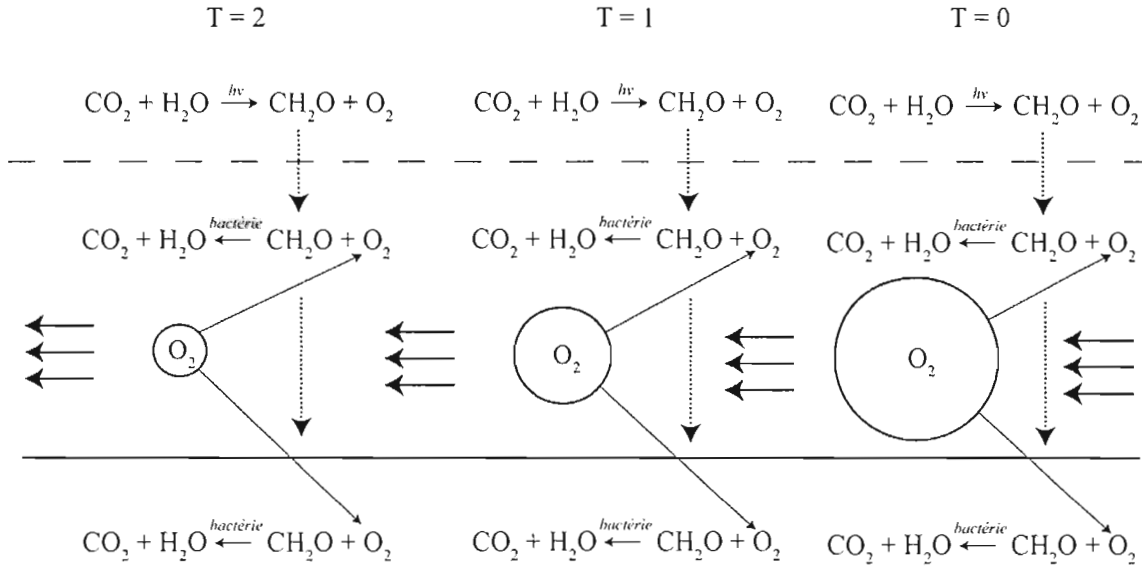

Figure 3. Représentation schématique de l'effet cumulatif de la consommation d'oxygène dissous par la respiration de la matière organique (dans la colonne d'eau et dans le sédiment) sur la concentration en oxygène dissous de la masse d'eau profonde à t = 0, t = 1 et t = 2.

1.3. Causes possibles de l'hypoxie de l'estuaire maritime du Saint-Laurent

Présentement, nous ne possédons pas d'indice pour reconstituer les variations du temps de séjour de la masse d'eau profonde. Par contre, des approximations de la vitesse d'advection ont été faites par Budgen (1988) et Gilbert et al. (2005). Les résultats tendent à démontrer qu'elle aurait augmenté, ce qui entraînerait l'effet opposé sur le bilan d'OD. La stratification des masses d'eau dans l'estuaire du Saint-Laurent est telle que la masse d'eau profonde est isolée par une ou deux autres masses d'eau dépendamment de la saison (Dickie et Trites, 1983) (Figure 2). Cette masse d'eau profonde provient des eaux du Labrador et de l'Atlantique Nord qui se mélangent au niveau du plateau continental de la Nouvelle-Écosse (Lauzier et Trites, 1958; Bugden, 1991). Les caractéristiques de la masse d'eau profonde du Saint-Laurent varient donc en fonction de la proportion de chacune des masses d'eau qui la constitue et de leurs caractéristiques propres (Bugden, 1991, Gilbert et al., 2005). Selon une analyse de la température, de la salinité et de la densité des masses d'eau impliquées, Gilbert et al. (2005) ont suggéré que les eaux de fonds du Saint-Laurent sont présentement formées sur l'isopycnale de densité 27,27 kg m^{-3}, ce qui signifie qu'elles sont formées de l'eau du Labrador située entre 100 et 300 m de profondeur et des eaux de l'Atlantique Nord d'une profondeur de 700 à 1000 m. À ces profondeurs, ces deux masses d'eau sont caractérisées par des conditions physico-chimiques très différentes: l'eau du Labrador est froide (~ 2°C), peu salée (~ 34) et bien oxygénée (~ 300 µmol L^{-1}) tandis que l'eau de l'Atlantique Nord est chaude (~ 9°C), plus salée (> 35) et peu oxygénée (~ 60 µmol L^{-1}). Au vu de ces différences marquées, il apparaît donc qu'un changement de la proportion des masses d'eau se mélangeant pour former la masse d'eau profonde du Saint-Laurent aura des répercussions sur la température et la salinité de celle-ci (Bugden, 1991). Gilbert et al. (2005) ont donc utilisé les variations de température et de salinité dans les eaux de fond du Saint-Laurent pour

estimer les proportions respectives des masses d'eaux parentes. En suggérant que la proportion de la masse d'eau peu oxygénée de l'Atlantique Nord a augmenté d'environ 20% en 70 ans, Gilbert et al. (2005) proposent également que ce changement a contribué de façon importante à la baisse en OD observé dans l'estuaire maritime. Par contre, cette approche considère les propriétés des masses d'eau parentes comme constantes. Les masses d'eau parentes étant situées dans deux régions qui ont subi des changements climatiques importants (Grey et al., 2000; Dickson et al, 2002), il paraît important de vérifier le rôle de ces changements sur les variations de température, salinité et OD dans l'estuaire maritime du Saint-Laurent.

L'influence des apports de MO sur le bilan d'OD fut l'objet d'une modélisation qui confirme la sensibilité du système et suggère que l'oxydation de la matière organique a joué un rôle important dans le développement récent de l'hypoxie (Benoît et al., 2006). De plus, un enrichissement de la composition isotopique de la matière organique ainsi que des variations des assemblages de microfossiles suggèrent une augmentation de productivité primaire au cours des dernières décennies (Thibodeau et al., 2006), ce qui laisse supposer que l'eutrophisation peut avoir joué un rôle sur la diminution des concentrations d'OD. Malgré la concomitance du déclin de l'OD et des ventes de fertilisants (Thibodeau et al., 2006), une connaissance plus approfondie du cycle de l'azote est souhaitable avant de pouvoir tirer des conclusions définitives.

En résumé, le développement de la zone hypoxique du Saint-Laurent est un phénomène récemment observé qui a déjà des impacts sur l'écosystème du Saint-Laurent. Plusieurs hypothèses sur les causes ont été avancées, mais elles doivent être vérifiées avant d'élaborer un plan de réhabilitation adéquat.

2. Objectifs de l'étude

Au vue de l'état des connaissances actuelles, cette thèse s'articule autour d'un grand thème, soit l'identification et la compréhension des mécanismes à l'origine de

l'hypoxie dans l'estuaire maritime du Saint-Laurent. Plus spécifiquement, les objectifs sont :

1. Reconstruire les variations de la température des eaux profondes du chenal laurentien, en portant une attention particulière à la proportion de la masse d'eau chaude et peu oxygénée de l'Océan Atlantique. Ce faisant, nous voulons mieux comprendre le rôle des changements océaniques sur l'hypoxie des environnements estuariens et côtiers. La composition isotopique des foraminifères benthiques sera utilisée, car elle enregistre la température ainsi que la composition isotopique de l'eau, cette dernière reflétant la proportion des différentes masses d'eau.

2. Dresser un portrait du cycle de l'azote dans la partie maritime du système Saint-Laurent. Une attention particulière sera portée au mode d'élimination de l'azote (la dénitrification), de façon à établir une première estimation complète du budget de l'azote dans ce système. Comme le degré d'hypoxie du Saint-Laurent n'a pas encore atteint le degré d'oxygénation qui permet la dénitrification dans la colonne d'eau, nous évaluerons l'élimination de l'azote faite par le sédiment au moyen de mesures précises de la concentration en nitrates des eaux porales. Ces données ponctuelles seront alors confrontées à un modèle plus général de l'élimination de l'azote dans l'estuaire et le golfe du Saint-Laurent. Il sera ensuite possible d'évaluer la capacité du système à éliminer les apports d'azote continentaux.

3. Dans l'optique d'estimer l'impact des apports d'azote continentaux, il est important d'identifier leur origine. Ceci permettra de mieux comprendre l'impact qu'ont les activités humaines dans le bassin versant du Saint-Laurent sur l'écosystème, et plus spécialement sur le bilan d'OD. Comme les différentes sources azotées possèdent une signature isotopique qui leur est

propre, il est possible de les différencier à l'aide des isotopes de l'oxygène et de l'azote. Une série de mesures isotopiques des nitrates sera établie sur deux ans, ce qui nous permettra d'évaluer l'effet de la saisonnalité et les possibles changements de sources d'azote dans l'estuaire.

CHAPITRE I

TWENTIETH CENTURY WARMING IN DEEP WATERS OF THE GULF OF ST. LAWRENCE: A UNIQUE FEATURE OF THE LAST MILLENIUM

Benoît Thibodeau[1,*], Anne de Vernal[1], Claude Hillaire-Marcel[1] and Alfonso Mucci[2]

[1]Geochemistry and Geodynamics Research Center, GEOTOP, Université du Québec à Montréal, Montréal, Québec, H3C 3P8, Canada

[2]Geochemistry and Geodynamics Research Center, GEOTOP, Department of Earth and Planetary Sciences, McGill University, Montréal, Québec, H3A 2A7, Canada

Article publié en 2010 dans la revue *Geophysical Research Letters*

Résumé

Les eaux de fond du chenal laurentien sont issues du mélange des eaux Nord Atlantique centrale (NACW) et des eaux du courant du Labrador (LCW). Dans l'optique d'évaluer la variation de leur température au cours du dernier millénaire, nous avons analysé la composition isotopique des foraminifères benthiques de deux carottes sédimentaires. Les valeurs du $\delta^{18}O$ des assemblages ont diminué de 3.1 à 2.7 ‰ au cours du dernier siècle, ce changement correspond à un réchauffement de 1.6°C depuis 1932 AD. Cette tendance contraste avec les valeurs relativement stables du dernier millénaire (3.09 ‰ ± 0.08), ce qui suggère que l'ensemble de cette période fût plus froide. Nos résultats montrent donc que le réchauffement des eaux du chenal laurentien est régional et qu'il n'y a pas eu d'équivalent durant le dernier millénaire.

Abstract

The impact of human activities on Earth's climate is still subject to debate and the pattern of a sharp recent global temperature increase contrasting with much lesser variable temperatures during preceding centuries has often been challenged, partly due to the lack of unquestionable evidence. In this paper, oxygen isotope compositions of benthic foraminifer shells recovered from sediments of the Lower St. Lawrence Estuary and the Gulf are used to reconstruct temperature changes in a water mass originating from ~ 400 m deep North Atlantic waters. The data demonstrate that the 1.7 ± 0.3°C warming measured during the last century corresponds to a $\delta^{18}O$ shift of 0.4 ± 0.05‰, encompassing the temperature effect and related change in the isotopic composition of the corresponding water mass. In contrast, $\delta^{18}O$ values remained nearly constant over the last millennium, except for a small positive shift which we attribute to the Little Ice Age. We conclude that the 20th century warming of the incoming intermediate North Atlantic water has had no equivalent during the last thousand years.

1. **Introduction**

Dissolved oxygen concentrations [O_2] in bottom waters of the Lower St. Lawrence Estuary (LSLE) have decreased from ~125 to less than 65 μmol L^{-1} over the past 75 years, leading to severe and persistent hypoxia [*Gilbert et al.*, 2005]. An increase in bottom water temperatures, concomitant with the [O_2] decline [*Gilbert et al.*, 2005] may have promoted the remineralisation rate of organic matter in the water column and sediment [*Gillooly et al.*, 2001] and, hence, the magnitude of the oxygen sink. The instrumental records of [O_2] and temperature are discontinuous and postdate 1932 AD. Hence, these fragmentary records make it difficult to quantitatively demonstrate the relationship between temperature and [O_2] and impossible to know if significant variations in bottom water oxygenation occurred prior to this time. In this context, sedimentological records of $\delta^{18}O$ from benthic foraminifera may be useful to document changes in temperature and/or water mass origin beyond the existing instrumental records [*Frew et al.*, 2000].

In this paper, we present oxygen isotope measurements ($\delta^{18}O_c$) in assemblages of the benthic foraminifera *Globobulimina auriculata* extracted from two cores recovered in the LSLE. One spans the last century, the other, the last millennium (Figure 1). Instrumental temperature and salinity records in the ambient water mass are used to assess the temperature and salinity impact on the $\delta^{18}O_c$ record of the last century. Finally, we infer temperature conditions during the last millennium from $\delta^{18}O_c$ data in the longer sedimentary record.

2. Regional Context

The dominant topographic feature of the Estuary and Gulf of St. Lawrence is the Laurentian Channel, a submarine valley 250-500 m deep that extends over 1240 km landward from the continental shelf edge of the Eastern Canadian coast to Tadoussac (Figure 1). The circulation is estuarine and is characterized by three water layers: 1) a thin surface layer (down to 50 m) of low salinity water that flows seaward and originates from mixing of seawater with freshwater runoff from the Great Lakes, St. Lawrence River and Northern Quebec river drainage system, 2) a cold intermediate layer (50-150m), which originates from winter cooling of denser surface waters as tributary flow decreases and ice forms [*Gilbert and Pettigrew*, 1997; *Galbraith*, 2006], and 3) a warmer and saltier deep layer that flows landward and originates from the mixing of the Labrador Current Water (LCW) and the North Atlantic Central Water (NACW) at the shelf edge [*Dickie and Trites*, 1983]. The LCW and NACW have very different temperatures, salinities, and $[O_2]$ but similar densities (supplemental material, table 1) and, thus, mix to form the St. Lawrence Bottom Water (SLBW; *Gilbert et al.*, 2005). Hence, even a small change in the proportion of the two parental water masses may result in variations in the properties of the SLBW. The SLBW is isolated from the atmosphere by a permanent pycnocline situated between 100 and 150 m water depth. Under these conditions, it gradually loses oxygen through respiration and remineralization of organic matter that settles through the water column, as it flows landward from the mouth to the head of the Laurentian Channel, i.e., from Cabot Strait to Tadoussac (Figure 1). At depths greater than 150 m, the oxygen consumed through respiration cannot even be replenished by winter convection [*Petrie et al.*, 1996]. Therefore, the oxygen levels are very sensitive to variations in the properties of the water that enters the Laurentian Channel and the rate of organic matter remineralisation.

3. Methods

Sedimentation rates

The chronostratigraphy of the sediment cores was established based on ^{14}C, $^{210}Pbex$, ^{137}Cs, and isothermal remanent magnetizations measurements [*St-Onge et al.*, 2003; *Thibodeau et al.*, 2006]. Interpretation of these data yields an average sedimentation rate of 0.42 ± 0.04 cm/year for box core CR02-23 which, thus, spans about the last 100 years [*Thibodeau et al.*, 2006]. With a mean sedimentation rate of 0.2 cm/year [*St-Onge et al.*, 2003], the upper 200 cm of piston core MD99-2220 represents the last thousand years. The top 14 cm of sediment in core MD99-2220 was disturbed by the coring process [*St-Onge et al.*, 2003] and was of little use (see supplemental material for detail about sediment recovery). Core COR0503-37BC sedimentation rate was estimated at ~0.15 cm/year [*Genovesi et al.*, 2008].

Isotopic analyses

In order to evaluate the temperature from the isotopic composition of foraminifers ($\delta^{18}O_c$), we used the equation of *Shackleton* [1974]:

$$t = 16.9 - 4.38*(\delta^{18}O_c - \delta^{18}O_w + 0.27) + 0.10*(\delta^{18}O_c - \delta^{18}O_w + 0.27)^2 \quad (1)$$

where t represents the temperature (in °C) of the water from which calcite was precipitated, $\delta^{18}O_c$ is the isotopic composition of the calcite with respect to V-PDB, and $\delta^{18}O_w$ is the isotopic composition of the ambient water versus V-SMOW. The uncertainty on temperature estimates, propagated from the analytical precision, is ± 0.2°C.

We also calculated $\delta^{18}O_w$ from instrumental salinity measurements, since they are strongly correlated in the LSLE and Gulf bottom waters (> 250 m; $\delta^{18}O_w = 0.67*S - 23.1$, $r^2 = 0.86$; see Figure 2 in supplemental material). The standard deviation of $\delta^{18}O_w$ measurements, based on the analysis of duplicate samples, is ± 0.05‰.

4. Results and discussion

$\delta^{18}O_c$ values in core CR02-23 decrease in a stepwise manner from the base (~3.0 ‰ at 45 cm) to the top of core, and reach a minimum value of ~2.7 ‰ in the upper 3 cm (Figure 2 and Figure 1 in the supplemental material). In core MD99-2220, $\delta^{18}O_c$ values below 28 cm depth average 3.09 ± 0.08 ‰ (Figure 3). These values are higher, and are constrained within a far narrower range than those recorded in the upper 28 cm (3.0 to 2.6 ‰) of cores MD99-2220 and CR02-23 (Figure 3). In addition, a set of heavier values averaging 3.15 ± 0.05 ‰. (n = 36) is recorded between 55 and 90 cm in core MD99-2220 (n = 36). This set of values is significantly heavier than those recorded within the 28 to 55 cm interval and below 90 cm (see Figure 3).

Core CR02-23 encompasses the last century, allowing a comparison with historical, instrumental temperature data. $\delta^{18}O_c$ values were converted into temperatures using equation (1), assuming, as a first approximation, a constant isotopic composition of about -0.05 ± 0.04 ‰ for the bottom water mass. This value has been retained as a first estimate, based on seven $\delta^{18}O_w$ measurements carried out in 2007 and 2009, near the study site , which yielded values of -0.04±0.03 (n = 6) and -0.11‰ (n=1), respectively. As illustrated in Figure 2, the calculated and measured temperature curves show very similar patterns but the magnitude of the temporal temperature variation estimated from isotopic data is +1.3 ± 0.2°C (supplemental material figure 1) *vs* +1.7 ± 0.3°C, based on instrumental data [*Gilbert et al.* [2005]. This suggests that part of the temperature-driven shift in $\delta^{18}O_c$-values may have been masked by a small positive shift in $\delta^{18}O_w$-values. In the observed temperature range, one would expect a nearly constant $d\delta_c/dt$ relationship of about -0.3‰/°C (from equation 1). The actual 1.7°C increase in bottom water temperature should thus have induced a shift of about -0.5‰ in the $\delta^{18}O_c$-values of *G. auriculata* shells. The measured shift (-0.3‰) thus suggests a +0.2‰ increase in $\delta^{18}O_w$ values to account for the difference. *Gilbert et al.* [2005] proposed that the recent increase in SLBW

temperature results from the decrease of the proportion of the cold and well oxygenated LCW relative to the warm and less oxygenated NACW in the water mass that feeds the Laurentian Channel. Using temperature and salinity as tracers, *Gilbert et al.* [2005] estimated that the proportion of NACW in the water mass entering the Laurentian Channel trough Cabot Strait increased from 28 to 48 % relative to the LCW between 1930 and 2003 AD. According to recent measurements, the two water masses have $\delta^{18}O_w$-values of about -0.5 (LCW) and +0.5 ‰ (NACW) [*Khatiwala et al.*, 1999]. The $\delta^{18}O_w$ values measured in the LSLE (~ -0.05‰) is consistent with Gilbert et al.'s estimate of the relative contribution (~50:50) of the two water masses to the modern SLBW. The increasing proportion of NACW in this water mass, from ~28% to 48%, since the 1930s, should have resulted in a ~ +0.2‰ shift of the SLBW $\delta^{18}O_w$ values over the same period. This shift in SLBW $\delta^{18}O_w$ value would account for the discrepancy between the temperatures inferred from the measured $\delta^{18}O_c$-record and the instrumental data since the 1930s. This conclusion rests on the assumption that the isotopic compositions of the NADW and LCW have been invariant since 1930. It should also be considered with caution given the small isotopic offsets involved. In order to evaluate the effect of a variation in $\delta^{18}O_w$ on the estimated temperatures, we also calculated a theoretical $\delta^{18}O_c$ from equation 1, using our estimates of $\delta^{18}O_w$ based on salinity measurements and instrumental temperature data (Figure 2 and Figure 2 in supplemental material). The resulting profile is similar to the measured $\delta^{18}O_c$ in CR02-23, suggesting that the $\delta^{18}O_c$ record can be used as a rough paleothermometer in the SLBW. Therefore, irrespective of the offset value, a significant warming (> 1°C) during the course of the last century is indisputable. This is confirmed by a similar trend, with a comparable amplitude, observed at another site of the Laurentian Channel in the Gulf of St. Lawrence (Figure 3; *Genovesi et al.*, 2008). The similarity of $\delta^{18}O_c$ records from the three sites in the Estuary and Gulf of St. Lawrence demonstrates that the warming trend of the last century is a regional feature. In contrast, prior to the last 100 years, the isotopic record from core MD99-2220 is nearly invariant, with a mean $\delta^{18}O_c$ value of 3.09 ± 0.08 ‰ below 28 cm

(Figure 3), i.e., for the time interval spanning from about 1000 to 1900 AD. However, a possible feature of significance is the set of heavier values recorded in the 55 to 95 cm interval (i.e., between ~ 1630 and 1800), peaking at about 70 cm (~ 1740). It suggests a cooling of less than 0.5°C, possibly linked to the Little Ice Age (LIA) (Figure 4). Paradoxically, data from cores collected in the area of the Laurentian fan, at the outlet of the Laurentian Channel in the North Atlantic, indicate sea-surface warming during the LIA [*Keigwin and Pickard* [1999]. This has been interpreted as a northward shift of the slope water current in response to a dominant negative North Atlantic oscillation mode. The hydrography in the area of the Laurentian Fan is complex, as it is located at a front marked by the mixing of three water masses (the Labrador Sea Current, the Labrador Sea Water, and the North Atlantic Drift). Any change in the strength and trajectory of any or several of these water masses may have resulted in changes of surface water characteristics. The hypothesis of *Keigwin and Pickard* [1999] may be correct for surface waters south of 44° but it does not necessarily apply to a water mass collected below 400 m in the NW North Atlantic and carried into the SLBW.

Following the interval which we associate with the LIA, the warming of the SLBW appears to have occurred in two main steps. The first one is tenuous (~ 0.3°C) but, nonetheless significant. It started at the beginning of the 19th Century and is consistent with the Northern Hemisphere compilation of climate changes by Moberg et al. [2005] (Figure 4). This early warming could reflect the recovery from the LIA, although one may argue that it results from anthropogenic forcing. The second warming phase started at the turn of the 20th Century and is more pronounced, > 1°C over the last century. Such a warming is seen in a large array of paleotemperature records (e.g., Crowley, 2000). In the SLBW, the warming likely results from the increased temperature of North Atlantic waters entering the Gulf of St. Lawrence through Cabot Strait. Hence, it would reflect either the change in proportion of parent water masses or the distal effect of heat accumulation in constituent waters masses or both. Whether or not the post-1900 warming is due to anthropogenic forcing is a

matter of debate, which we do not address here. Nonetheless, irrespective of the precise mechanisms responsible for the temperature variations reconstructed from core MD99-2220, it is unquestionable that the last century has been marked there by a warming trend having no equivalent over the last millennium.

5. Conclusion

The isotope records of benthic foraminifer shells in sediment cores recovered from the Laurentian Channel in the Lower Estuary and Gulf of St. Lawrence confirm that the last century was marked by a progressive increase in bottom water temperatures, which could have contributed to the establishment of hypoxia [cf. *Gilbert et a*l., 2005]. A warming trend was previously reported by *Keigwin and Pickard* [1999] for the last 3 or 4 centuries, based on sedimentary time series from the Laurentian Fan on the continental shelf and slope. It appears to be a consistent feature of many proxy climate records of the northern Hemisphere [e.g. *Moberg et al.*, 2005]. This warming might originate from anthropogenic activities but it could also be superimposed on a longer timescale natural oscillation that has not yet been captured in our records. To elucidate the origin of this warming, longer time series of $\delta^{18}O$ in benthic foraminifer shells should be compared, notably, with proxies of overlying water oxygenation, such as the vertical distribution of redox-sensitive metals [e.g., *Sundby et al.*, 2004] and benthic foraminifer assemblages [e.g., *Gooday*, 2003; *Gooday et al.*, 2009]. This would possibly better document the relationship between temperature, bottom water oxygenation, and their linkages with either natural, long-term variations in the North Atlantic thermohaline circulation and surface currents or with the current, anthropogenically-driven global warming.

Acknowledgements

This work was funded by the Natural Sciences and Engineering Research Council of Canada (NSERC) through a Strategic Project Grant. Support from NSERC (Discovery grants to AD, AM, CHM) and the *Fonds Québécois de le Recherche sur la Nature et les Technologies* (infrastructure award to GEOTOP) is also acknowledged.

References

Dickie, L. M., and R. W. Trites (1983), The Gulf of St. Lawrence, *Estuaries and Enclosed Seas*, 403-425.

Edenborn, H. M., A. Mucci, N. Belzile, J. Lebel, N. Silverberg, and B. Sundby (1986), A glove box for the fine-scale subsampling of sediment box cores, *Sedimentology*, *33*(1), 147-150.

Frew, R. D., P. F. Dennis, K. J. Heywood, M. P. Meredith, and S. M. Boswell (2000), The oxygen isotope composition of water masses in the northern North Atlantic, *Deep-Sea Research Part I: Oceanographic Research Papers*, *47*(12), 2265-2286.

Genovesi, L., B. Thibodeau, A. de Vernal, and C. Hillaire-Marcel (2008), Recent changes of bottom water oxygenation and temperature in the Gulf of St. Lawrence: micropaleontological and geochemical evidences, paper presented at Water, Weather, and Climate: Science Informing Decisions, Canadian Meteorological and Oceanographic Society, Kelowna, B.C.

Gilbert, D., B. Sundby, C. Gobeil, A. Mucci, and G. H. Tremblay (2005), A seventy-two-year record of diminishing deep-water oxygen in the St. Lawrence estuary: The northwest Atlantic connection, *Limnology and Oceanography*, *50*(5), 1654-1666.

Gillooly, J. F., J. H. Brown, G. B. West, V. M. Savage, and E. L. Charnov (2001), Effects of size and temperature on metabolic rate, *Science*, *293*(5538), 2248-2251.

Gooday, A. J. (2003), Benthic foraminifera (protista) as tools in deep-water palaeoceanography: Environmental influences on faunal characteristics, in *Advances in Marine Biology*, edited, pp. 1-90.

Gooday, A. J., F. Jorissen, L. A. Levin, J. J. Middelburg, S. W. A. Naqvi, N. N. Rabalais, M. Scranton, and J. Zhang (2009), Historical records of coastal eutrophication-induced hypoxia, *Biogeosciences*, *6*(8), 1707-1745.

Gregory, D. N. (2004), Climate: A database of temperature and salinity observations for the northwest Atlantic, *Canadian Science Advisory Secretariat Research Document 2004/075*.

IPCC (2001), in *Climate Change 2001: The Scientific Basis*, edited by J. Houghton, et al., pp. 99-181, Cambridge University Press, Cambridge.

Keigwin, L. D., and R. S. Pickart (1999), Slope water current over the Laurentian Fan on interannual to millennial time scares, *Science*, *286*(5439), 520-523.

Khatiwala, S. P., R. G. Fairbanks, and R. W. Houghton (1999), Freshwater sources to the coastal ocean off northeastern North America: Evidence from $H_2{}^{18}O/H_2{}^{16}O$, *Journal of Geophysical Research C: Oceans*, *104*(C8), 18241-18255.

Moberg, A., D. M. Sonechkin, K. Holmgren, M. H. Datsenko, and W. Karlén (2005), Highly variable Northern Hemisphere temperatures reconstructed from low- and high-resolution proxy data, *Nature*, *433*(7026), 613-617.

Petrie, B., K. Drinkwater, A. Sandström, R. Pettipas, D. Gregory, D. Gilbert, and P. Sekhon (1996), Temperature, salinity and sigma-t atlas for the Gulf of St. Lawrence, *Can. Tech. Rep. Hydrogr. Ocean Sci.*, *178*, 256.

Shackleton, N. (1974), Attainment of isotopic equilibrium between ocean water and the benthonic foraminifera genus Uvigerina: isotopic changes in the ocean during the last glacial, in *Les méthodes quantitatives d'étude des variations du climat au cours*

du Pléistocène, edited by J. Labeyrie, pp. 203-209, Centre National de la Recherche Scientifique (CNRS), Paris.

St-Onge, G., J. S. Stoner, and C. Hillaire-Marcel (2003), Holocene paleomagnetic records from the St. Lawrence Estuary, eastern Canada: Centennial- to millennial-scale geomagnetic modulation of cosmogenic isotopes, *Earth and Planetary Science Letters*, *209*(1-2), 113-130.

Sundby, B., P. Martinez, and C. Gobeil (2004), Comparative geochemistry of cadmium, rhenium, uranium, and molybdenum in continental margin sediments, *Geochimica et Cosmochimica Acta*, *68*(11), 2485-2493.

Thibodeau, B., A. de Vernal, and A. Mucci (2006), Recent eutrophication and consequent hypoxia in the bottom waters of the Lower St. Lawrence Estuary: Micropaleontological and geochemical evidence, *Marine Geology*, *231*(1-4), 37-50.

Figure caption

Figure 1. Map of the St. Lawrence marine system and the location of coring sites. The contour is the 400 m isobath.

Figure 2. Available instrumental temperature (red), oxygen (green) and salinity (dark blue) records for the St. Lawrence bottom water at a depth > 300m against age (from the CLIMATE database). Theoretical $\delta^{18}O_c$ (dotted light blue) and smoothed theoretical $\delta^{18}O_c$ (solid light blue) were calculated from the relationship between salinity, $\delta^{18}O_w$, and the instrumental temperature in the isotope paleotemperature equation (1) and is plotted beside $\delta^{18}O_c$ measured in core CR02-23 (purple). $\delta^{18}O_c$ measured in core CR02-23 was used to estimate paleotemperature with the equation 1 (black). Error bars report uncertainty for the estimated temperature calculation (± 0.2°C), propagated from the analytical precision of the $\delta^{18}O_c$ measurements (±0.05 ‰), and for the analytical precision itself

Figure 3. $\delta^{18}O_c$ vs. depth in cores MD99-2220, CR02-23 and COR0503-37BC. The dashed line is the +3 ‰ threshold in $\delta^{18}O_c$-values. In core MD2220, the vertical dashed lines represent the mean values for different sections of the core and the shaded zones correspond to the standard deviation (1 sigma). Below 28 cm, 3 sections are defined based on the $\delta^{18}O_c$ values (see supplemental material, section 5). The top 14 cm of sediment in core MD99-2220 is shaded since it was disturbed by the coring process and was of little use [*St-Onge et al.*, 2003].

Figure 4. Top: $\delta^{18}O_c$ in core MD99-2220 vs. age in cal. years BP. Before ca. 1920 AD, 3 sections are defined based on statistically significant $\delta^{18}O_c$-calculated temperature anomalies from the mean pre-15th century value (see supplemental material, section 5). Middle and bottom: Northern Hemisphere atmospheric

temperatures anomalies based on tree ring, ice core, and instrumental records reconstructed by Crowley [2000] and Moberg et al. [2005].

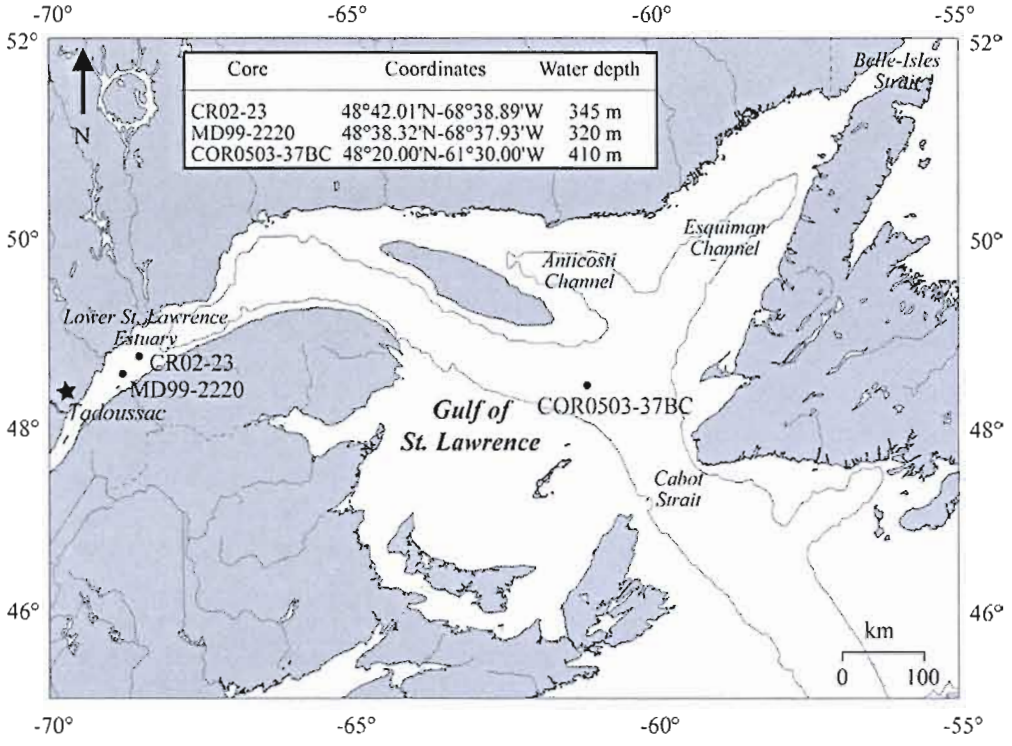

Figure 1.

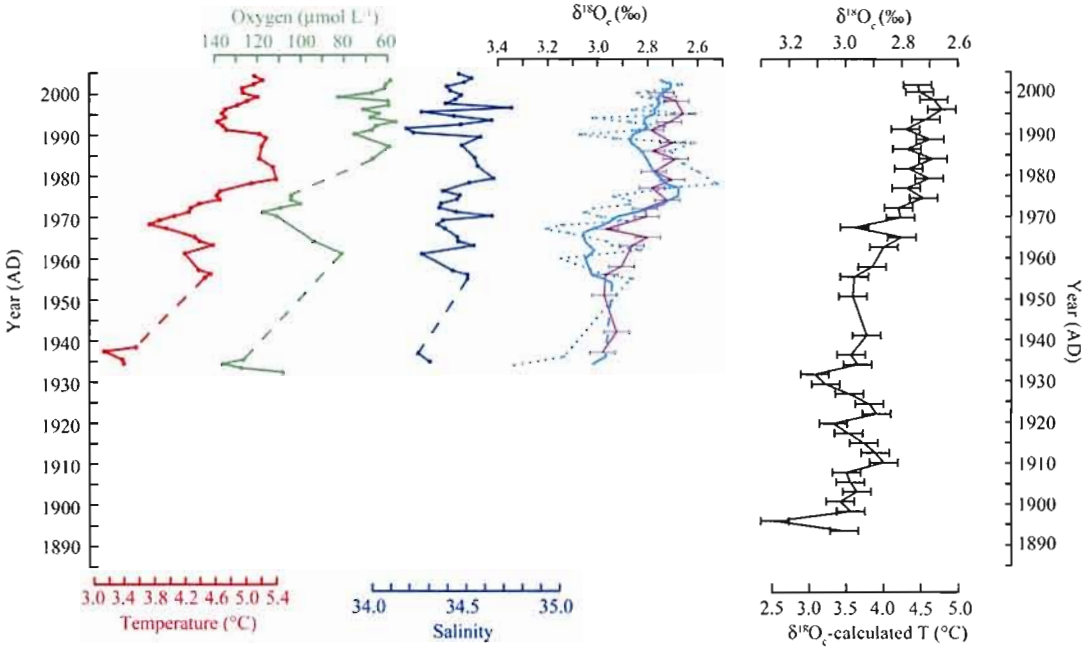

Figure 2.

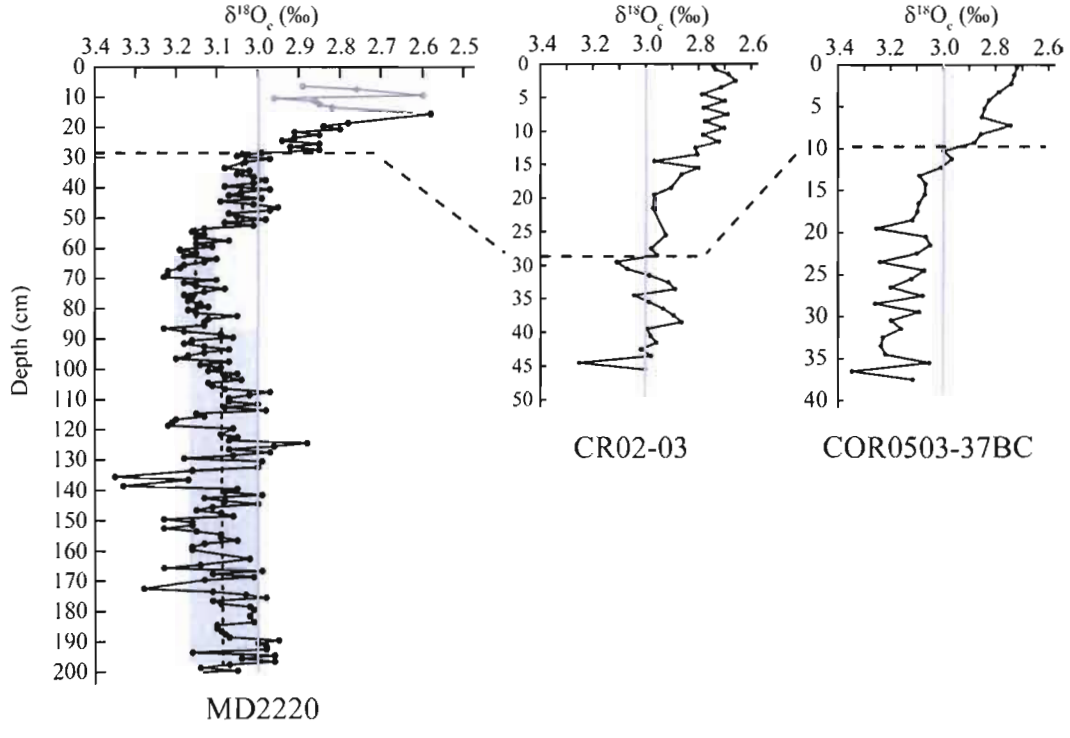

Figure 3.

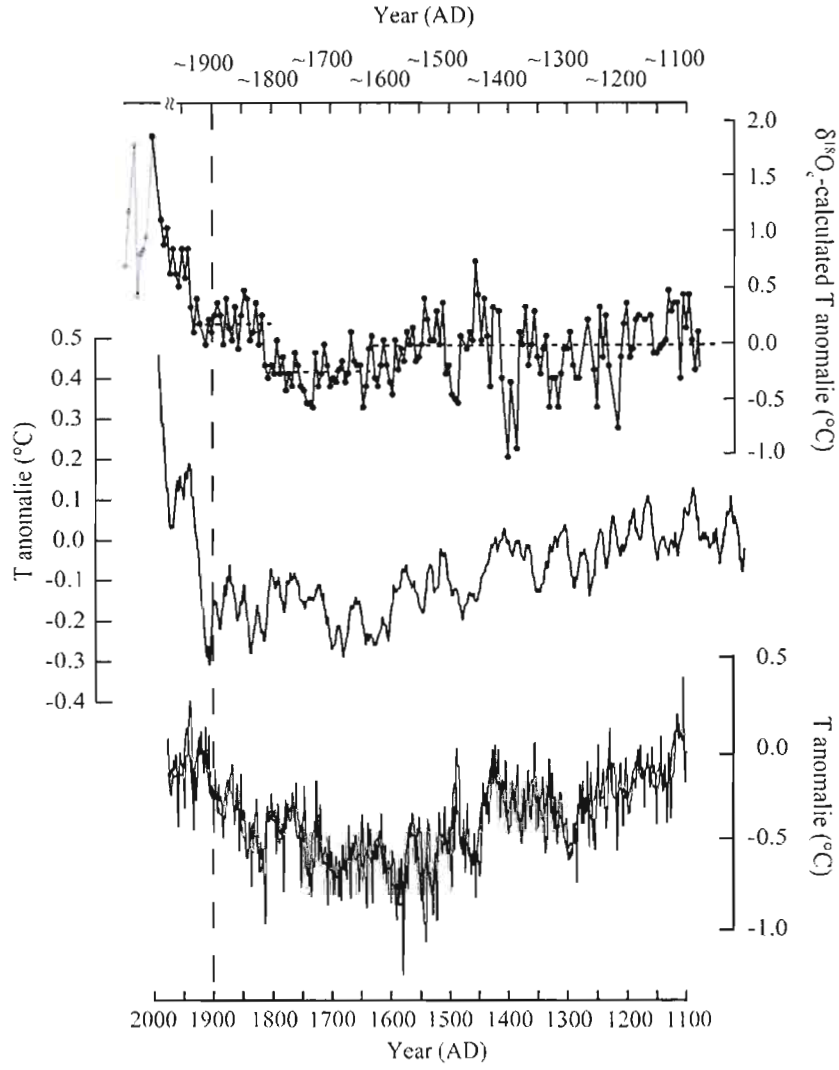
Year (AD)
~1900
~1800
~1700
~1600
~1500
~1400
~1300
~1200
~1100
2.0
1.5
1.0
0.5
0.0
-0.5
-1.0
δ18Oc-calculated T anomalie (°C)
0.5
0.4
0.3
0.2
0.1
0.0
-0.1
-0.2
-0.3
-0.4
T anomalie (°C)
0.5
0.0
-0.5
-1.0
T anomalie (°C)
2000 1900 1800 1700 1600 1500 1400 1300 1200 1100
Year (AD)

Figure 4.

CHAPITRE II

BENTHIC NUTRIENT FLUXES ALONG THE LAURENTIAN CHANNEL: IMPACTS ON THE N-BUDGET OF THE ST. LAWRENCE MARIME SYSTEM

Benoît Thibodeau[1*], Moritz F. Lehmann[2], Jacqueline Kowarzyk[3], Alfonso Mucci[1,4], Yves Gélinas[1,5], Denis Gilbert[6], Roxane Maranger[3], and Mohammad Alkhatib[1]

[1]Geochemistry and Geodynamics Research Center, GEOTOP, Université du Québec à Montréal, Montréal, Québec, H3C 3P8, Canada

[2]Institute for Environmental Geosciences, University of Basel, Bernoullistrasse 30, 4056 Basel, Switzerland

[3]Department of Biological Sciences, Université de Montréal, Montréal, Quebec, H3C 3J7, Canada

[4]Department of Earth and Planetary Sciences, McGill University, Montréal, Québec, H3A 2A7, Canada

[5]Department of Chemistry and Biochemistry, Concordia University, Montréal, Québec, H4B 1R6, Canada

[6]Fisheries and Oceans Canada, Institut Maurice-Lamontagne, Mont-Joli, Québec, G5H 3Z4 Canada

Article publié en 2010 dans la revue *Estuarine, Coastal and Shelf Science.*

Résumé

Des mesures de la concentration dans la colonne d'eau ainsi que des flux sédimentaires des nitrates ont été faites dans le golfe, l'estuaire maritime et l'estuaire moyen du Saint-Laurent dans le but d'établir le bilan de l'azote ainsi que de comprendre le rôle que peut avoir l'hypoxie sur celui-ci. Un déficit en nitrates par rapport au phosphate a été observé aux alentours de la zone hypoxique. Vu que la concentration d'oxygène dissous est supérieure au seuil de 50 μmol L^{-1} partout dans l'estuaire, il est plus probable que la perte d'azote soit via le sédiment, car la perte dans la colonne d'eau requiert une concentration d'oxygène inférieure à 5 μmol L^{-1}. Nous avons donc mesuré les flux sédimentaires diffusifs de nitrates à 8 stations le long des chenaux Laurentien, Esquiman et Anticosti. Ceux-ci varient de 190 μmol m^{-2} d^{-1} dans la zone hypoxique à 100 μmol m^{-2} d^{-1} dans le golfe pour une moyenne de 690 μmol m^{-2} d^{-1} si on y ajoute le flux du au couplage de la nitrification-dénitrification qui compte pour plus de 70% de l'élimination totale des nitrates dans le sédiment. En utilisant les concentrations de la colonne d'eau, nous concluons que le puits sédimentaire d'azote est suffisant pour maintenir un bilan balancé pour le système du Saint-Laurent.

Abstract

Water column concentrations and benthic fluxes of dissolved inorganic nitrogen (DIN) and oxygen (DO) were measured in the Gulf of St. Lawrence and the Upper and Lower St. Lawrence Estuary (USLE and LSLE, respectively) to assess the nitrogen (N) budget in the St. Lawrence (SL) system, as well as to elucidate the impact of bottom water hypoxia on fixed-N removal in the LSLE. A severe nitrate deficit, with respect to ambient phosphate concentrations (N*~-10 μmol L^{-1}), was observed within and in the vicinity of the hypoxic water of the LSLE. Given that DO concentrations in the water column were always >50 μmol L^{-1}, nitrate reduction in suboxic sediments, rather than in the water column, is most likely responsible for the removal of fixed-N from the SL system. Net nitrate fluxes into the sediments, derived from pore water nitrate concentration gradients, ranged from 190 μmol m^{-2} d^{-1} in the hypoxic western LSLE to 100 μmol m^{-2} d^{-1} in the Gulf. The average total benthic nitrate reduction rate for the Laurentian Channel (LC) is on the order of 690 μmol m^{-2} d^{-1}, with coupled nitrification nitrate reduction accounting for more than 70 %. Using average nitrate reduction rates derived from the observed water column nitrate deficit, the annual N elimination within the three main channels of the St. Lawrence was calculated to account to 411 x 10^6 t N, yielding an almost balanced N budget for the SL system.

1. Introduction

Eutrophication is a growing environmental concern in many inhabited marine coastal areas and estuaries (Cloern, 2001). Enhanced local primary productivity results in increased fluxes of organic matter which, upon bacterial respiration, can lead to the depletion of dissolved oxygen (DO) in stratified bottom waters and ultimately to hypoxia or anoxia (Diaz and Rosenberg, 2008). Estuaries are particularly affected by terrestrial organic matter and nutrient inputs (Gearing and Pocklington, 1990) which fuel high organic matter fluxes to the seafloor. As a major bio-limiting nutrient, the availability of fixed (i.e. bio-available) nitrogen is one the most important factors controlling estuarine eutrophication and, thus, the health of coastal marine ecosystems (Nixon et al., 1996; Howarth, 1998; Howarth et al., 2006). Global anthropogenic nitrogen inputs from agricultural and energy production sources to coastal waters increased ten-fold since the late 19^{th} century (Galloway et al., 2004). Understanding how anthropogenic and natural N loading is mitigated by natural N elimination processes is required to establish reliable ecosystem N budgets and, in turn, to develop effective water quality management practices.

Microbial denitrification is the bacterially mediated reduction of nitrate and nitrite to nitric oxide (NO), nitrous oxide (N_2O) and di-nitrogen (N_2) under suboxic conditions (DO < 5-10μmol L^{-1}; Codispoti et al., 2005). Because it results in the release of gaseous forms of N that are lost from the ecosystem and/or mostly unavailable to autotrophic organisms, denitrification is considered an important elimination pathway for fixed N. On regional and global scales, denitrification (or other modes of suboxic N_2 production) is the principal sink of fixed N in the ocean (Middelburg et al., 1996; Gruber and Sarmiento, 1997; Brandes and Devol, 2002).

Denitrification can take place both in the water column and within the sediment. Whereas denitrification in suboxic water is primarily controlled by the availability of organic matter, benthic denitrification rates are largely modulated by redox conditions within the sediments (more specifically the DO penetration depth), a function of bottom water DO concentrations as well as the quantity and reactivity of the organic

matter delivered to the seafloor (Middelburg et al., 1996; Lehmann et al., 2007). In environments where bottom water DO concentration and the flux and sources of organic matter (OM) vary spatially, benthic denitrification rates most likely display significant spatial variability (Lehmann et al., 2005). Elucidating the relationship between N elimination rates, bottom water oxygenation and organic matter availability is critical if basin-scale benthic nitrate reduction rates are to be estimated through the extrapolation of discrete flux measurements.

Recent studies in the Laurentian Channel revealed that approximately 1300 km^2 of the seafloor are now overlain by severely hypoxic waters (<20% saturation) year-round since the mid-1980s (Gilbert et al., 2005). Two-thirds of the historic DO depletion in the LSLE is believed to be caused by changes in ocean circulation patterns in the northwestern Atlantic (Gilbert et al., 2005; Thibodeau et al., In press). Nevertheless, recent elevated autochthonous organic matter fluxes to the seafloor, possibly from eutrophication due to enhanced fertilizer use in the watershed, could have increased the bottom water and sedimentary oxygen demand in the Lower St. Lawrence Estuary (LSLE), contributing to the observed DO depletion (Benoit et al., 2006; Thibodeau et al., 2006; Gilbert et al., 2007). Assessing the impact of external N loading on primary productivity and its respiration in the LSLE, as well as evaluating the SL system's capacity to compensate for the man-made fixed-N sources to the system, requires a detailed knowledge of the N budget, including a quantitative appraisal of external N sources and their fate within the SL system. Previous studies have focused on nutrient distribution and transport in the St. Lawrence (Coote and Yeats, 1979; Yeats, 1988; Savenkoff et al., 2001). To our knowledge, only two studies have addressed benthic denitrification within the SL system, one in the LSLE (Wang et al., 2003) and the other in salt marshes near Rimouski (Poulin et al., 2007), providing very little spatial resolution of this process at the basin scale. Interestingly, rate measurements in both studies, using the isotope pairing technique, revealed that only a small fraction (< 30%) of the nitrate flux into the sediments was ultimately denitrified, suggesting that other NO_3^- dissimilation reactions, such as anaerobic

ammonium oxidation (anammox) and dissimilatory reduction of nitrate to ammonium (DRNA) were active. Detailed information regarding the N budget for the LSLE in general, and the along-channel variability in benthic dissolved inorganic N (DIN) fluxes in particular, is still missing. Consequently, we remain unaware of the extent to which the St. Lawrence system is capable of eliminating fixed N.

Here, we investigate the role of the benthic environment as a sink for fixed N in the SL system (with a focus on the LSLE and the Gulf). Using high-resolution pore water concentration profiles, we estimate the net fluxes of N across the sediment-water interface (SWI) and total denitrification rates at nine stations along the Laurentian, Anticosti and Esquiman Channels (Fig. 1). We briefly examine the sensitivity of nitrate fluxes to spatial variations of bottom water DO and sediment reactivity (i.e., chlorin index, CI), as this topic is presented in greater detail in a companion manuscript by Alkhatib et al. (in revision). The estimated diffusive fluxes are compared to net flux measurements, derived from sediment core incubations, to elucidate the mechanisms responsible for the significant nitrate deficit in the western LSLE. Finally, based on field data and ecosystem denitrification rates, we establish the N budget for the SL marine system.

2. Materials and Methods

2.1. Sampling

Water column samples were collected in the Upper St. Lawrence Estuary (Sta. A to K), the LSLE (Sta. E5 and 24 to 21) and the Gulf (Sta. 20 to 16), including the Anticosti and Esquiman Channels (Sta. CE, TCE, CA and TCA), during the summers of 2005 and 2006 using a 12 x 12-L Niskin bottle/CTD (SeaBird SBE 911) rosette onboard the *R/V Coriolis II* (Fig. 1). Sub-samples were filtered through a 0.45 μm Nylon membrane filter (with polypropylene housing), and stored frozen in acid-washed polyethylene bottles until analysis in the laboratory.

Undisturbed sediment cores were collected at nine stations along the Laurentian Channel (Stations 23 to 16) and at the head of Anticosti and Esquiman Channels

using a Bowers & Connelly Multicorer (10 cm internal diameter, 50 cm long; Barnett et al., 1984) and

Ocean Instruments Mark II box corer (0.06 m^2 x 50 cm long) from water depths ranging from 300 to 450 m. Immediately upon corer recovery, pore water samples were extracted from the Multicorer cores using the whole core squeezing (WCS) method (Martin et al., 1991). Push cores (10 cm internal diameter, 30 cm long) were collected from the box cores, and pore waters were extracted using Rhizon membrane samplers (Seeberg-Elverfeldt et al., 2005). The WCS method provides very fine depth resolution (~5 samples within the first cm) near the sediment-water interface for solutes that are not adversely affected by adsorption (Bender et al., 1987), whereas the membrane sampling method allows the recovery of pore water samples from deeper sediment horizons. All pore water samples were immediately frozen after collection and stored frozen until onshore analyses.

2.2 Dissolved nutrient and N_2 concentration analysis

Dissolved nitrate, nitrite, ammonium, silica and reactive phosphate concentrations were determined at GEOTOP using a Braan and Luebbe autoanalyzer. Detection limits were ~0.1 μmol L^{-1} for nitrate and nitrite, < 0.1 μmol L^{-1} for phosphate and ~0.25 μmol L^{-1} for ammonium and silica (Strickland and Parsons, 1972). Water column DO concentrations were measured on-board using standard Winkler titrations (Grasshoff et al., 1999).

For N_2 concentration measurements, 30 mL of pore water were collected using the WCS with a gas tight syringe, inline with a 0.45μm nylon membrane syringe filter. To minimize atmospheric contamination, samples were filled using an overflow technique in 5 ml glass tubes with ground glass stopper and fixed with 25 μL of a 1 N $HgCl_2$ solution to stop microbial activity. Samples were stored underwater slightly below the in-situ temperature (~5°C) until analyzed in the laboratory. Nitrogen/argon ratios (N_2/Ar) were measured using membrane inlet mass spectrometry (MIMS)

(Kana et al., 1994; Kana et al., 1998). Measured N_2/Ar ratios were calibrated using atmosphere-equilibrated distilled water standards. Running temperature of the pore water samples and standards was maintained at 3°C. N_2 concentrations were calculated by multiplying standard N_2/Ar ratios by the in-situ Ar saturation concentration, taking into consideration the solubility of each gas as a function of salinity, temperature, and pressure, according to the equations of Weiss (1970).

2.3 Isotopic measurements

Stable N isotope analysis of dissolved nitrate was performed using the denitrifier method (Sigman et al., 2001). Briefly, sample nitrate plus nitrite were converted to nitrous oxide (N_2O) by denitrifying bacteria that lack N_2O reductase activity, *Pseudomonas chlororaphis* ATCC #43928. N_2O is stripped from the sample vial using helium carrier gas, purified through a Micromass TraceGas™, and analyzed for its N isotopic composition with a Micromass Isoprime™ universal triple collector isotope ratio mass spectrometer in continuous flow mode. Blank contribution was generally lower than 0.3 nmol (compared to typical values of ~20 nmol in the sample N). Based on replicate measurements of laboratory standards and samples (intra- and inter-run), the reproducibility of $\delta^{15}N$ analyses was estimated at better than ±0.3‰ (1σ). Isotope values were calibrated using IAEA-N3, an international KNO_3 reference material with an assigned $\delta^{15}N$ value of +4.7‰ relative to atmospheric N_2 (Gonfiantini et al., 1995).

An N-isotope enrichment experiment was conducted to provide information on the microbial pathways of nitrate reduction within the sediments. ^{15}N-labeled KNO_3 was added to the overlying water of an undisturbed Multicorer core recovered from Sta. 18 and incubated for 48 hours. Pore water was then extracted by the WCS method and the mole percent of ^{15}N-labelled NH_4^+ was determined using high performance liquid chromatography (Gardner et al., 1995) to determine the depth and degree of label transfer to NH_4^+.

2.4. Benthic flux calculations

Net nutrient fluxes across the sediment-water interface were calculated from high-resolution nitrate profiles using Fick's first law of diffusion (Boudreau, 1996; Schulz, 2006). The diffusive flux was calculated as follows:

$F = D_{sed} \bullet \Delta C/\Delta z$

where D_{sed} is the diffusion coefficient of the target solute (e.g., nitrate, ammonium, O_2), corrected for temperature and sediment porosity (Boudreau, 1996), and $\Delta C/\Delta z$ is the vertical solute concentration gradient across the sediment-water interface (SWI). $\Delta C/\Delta z$ was calculated from the first derivative of best-fit curves of the linear portion of the target solute concentration profiles just below the sediment-water interface. Bottom water temperatures ranged from 3 to 5°C, and the porosity of the surface sediments generally decreased from 95% to 75% within the top 5 cm.

In addition, ex-situ incubation experiments were conducted on intact Multicorer cores to independently assess the net benthic oxygen and nitrate exchange across the SWI. A detailed decription of the procedure can be found in Katsev et al. (2007). Briefly, incubations were carried out for 48h to 60h. During the incubations, the overlying water was continuously stirred by a rotating paddle, and up to 6 samples were withdrawn at distinct time intervals. Overlying waters were replaced upon each sub-sampling with an equivalent volume of bottom water to maintain the DO concentration nearly invariant throughout the incubations. Fluxes were calculated by multiplying the volume of overlying bottom water by the change in solute concentration, divided by the incubation time.

3. Results

3.1. Water column measurements

Nitrate concentrations were highest (~30 μmol L^{-1}) in the freshwater of the St. Lawrence River (Sta. A) and at the head of the Upper St. Lawrence Estuary (USLE, Sta. B-G). They gradually decreased (to 15 μmol L^{-1}) downstream throughout the USLE and the salinity-transition zone (Sta. H to E5) (Fig. 2a). For $S < 25$, there was a

significant negative linear correlation between salinity and nitrate concentrations in the surface waters (not shown, $R^2 = 0.73$). The nitrate vertical profiles in the LSLE and the Gulf were consistent with nitrate assimilation by phytoplankton in the photic zone: low surface water [NO_3^-] (< 5 μmol L^{-1}) and regeneration in subsurface and deep waters. The distribution pattern of soluble reactive phosphate (SRP) is similar to that of nitrate (Fig. 2b), except for the USLE, where SRP concentrations were only slightly higher than in the surface water of the Gulf (< 1 μmol L^{-1}).

During the assimilation-remineralization cycle, fixed nitrogen and phosphates are generally consumed and released at a fixed stoichiometry, resulting in a linear N:P molar relationship of approximately 16:1 for ocean waters (Redfield, 1958). Deviations from this relationship, denoted as N* (with N* (μmol L^{-1}) = [NO_3^-] - 16[PO_4^-] + 2.9 μmol L^{-1}, where the residual of 2.9 μmol $L^{-1}$was originally added to obtain a global oceanic mean N* of zero) can be used to identify and quantify fixed-N sources and sinks in marine reservoirs (Gruber and Sarmiento, 1997; Deutsch et al., 2001; Bourbonnais et al., 2009). Excess N (e.g., through external N-loading or N_2 fixation) is indicated by a positive N* whereas a negative N* generally reflects a net loss of nitrate, most likely via denitrification.

In the SL system, positive N* values (in excess of 15 μmol L^{-1}) were observed in the USLE (Fig. 2c), suggesting nutrient loading with elevated N:P ratios in the St. Lawrence River. In contrast, in the western part of the LSLE, mid-depth and bottom waters were characterized by a severe nitrate deficit, with N* values as low as -11 μmol L^{-1}, suggesting that the deep waters of the LSLE are a sink for fixed N.

With the exception of the USLE where the water column is well mixed, DO concentrations decreased with depth at all stations, with minor variations below ~200 m (Fig. 2d). DO concentrations in the deep waters (>150-200m) progressively decreased landward from Sta.16 to Sta. 23, as DO is consumed through respiration of organic matter settling through the water column and at the seafloor (Gilbert et al., 2005; Benoit et al., 2006; Lehmann et al., 2009). The oxygen minimum or hypoxic

zone in the vicinity of Sta. 23, at the western end of the LSLE, nearly coincided with the N*-minimum zone. The lowest DO concentrations measured in the Estuary and the Gulf ($\geq$ 55 μmol L^{-1}) should not allow for water column denitrification since denitrification is limited to suboxic and anoxic environments (with less than 5 μmol L^{-1}). Further evidence to support this claim is that the $\delta^{15}N\text{-}NO_3$ in the water column is essentially invariant below the photic zone (Fig. 3) and does not show significant ^{15}N-enrichment associated with nitrate removal from the water column. A detailed dataset and discussion of ^{15}N in the water column of the St. Lawrence system will be provided in a subsequent paper.

3.2. Pore water nutrient concentrations and calculated benthic fluxes

Voltammetric microelectrode dissolved oxygen measurements in sediment, previously recovered with the Multicorer from the LSLE, indicate that the O_2 penetration depth is about 0.5 to 1 cm (Katsev et al., 2007). Hence, suboxic and anoxic conditions allowing denitrification are found below that depth. With the exception of Sta. 16, where a positive nitrate gradient was observed immediately below the SWI, all other nitrate pore water profiles are characterized by sharp negative concentration gradients from the SWI down to ~1 to 2 cm depth, where $[NO_3^-]$ is generally below the detection limit (Fig. 4). These profiles indicate that in most of the LC, nitrate consumption through benthic nitrate reduction exceeds benthic production through nitrification. Hence, with the exception of Sta. 16, the net nitrate flux was always from the water column to the sediments. Sta. 16 is located in the southeastern part of the LC, closest to Cabot Strait, where the highest bottom water DO concentrations and lowest organic carbon fluxes (Smith and Schafer, 1999) are observed. At most sampled stations, nitrite concentrations were mostly below the detection limit near the SWI and reached a maximum (up to 2-3 μmol L^{-1}) 1 to 3 cm below the SWI.

The pore water ammonium profiles display progressively increasing concentrations with depth reaching in excess of 50 μmol L^{-1} at the bottom of the cores (Fig. 4). At most stations, dissolved ammonium was absent at or directly above the oxic-suboxic transition zone and, presumably, oxidized (i.e., nitrified) as it diffuses from below. Nevertheless, in some instances (e.g., Sta. 21 and 20), nitrification within the thin oxic sediment layer was not complete, and may result in a small diffusive flux of NH_4^+ to the overlying water. Like ammonium, SRP concentrations increased progressively with depth, consistent with the release of phosphate from the sediments to the pore waters (Fig. 4), in response to OM remineralization and reductive dissolution of iron oxide carrier phases. Pore water silica concentrations increased rapidly with depth (presumably in response to the dissolution of diatoms) before levelling off at the bottom of the core (Fig. 4). N_2 is produced by denitrification and anammox in the sediment and, therefore, its concentration is highest below the oxic layer. Porewater profiles of N_2 showed clear accumulation in the sediment (Fig. 5), although there was a slight increase in N_2 in the overlying waters that may have resulted from the potential warming of the overlying waters and N_2 flux out of the sediment during initial handling. However, we also observed a very strong negative correspondence between N_2 concentration and NO_3 concentration in the porewater (R^2=0.68, n=49), supporting N_2 flux from the sediment to the overlying water as a function of a concentration gradient. N_2 concentration gradients yielded flux values of 130 to 210 μmol m^{-2} d^{-1} without any significant trend between different stations (Table 1). The highest estimated diffusive nitrate fluxes into the sediments (130-190 μmol m^{-2} d^{-1}) (Table 1) were found in the LSLE, where we also observed the lowest DO concentrations and N* in the water column. Conversely, the lowest nitrate fluxes into the sediment were observed in the Gulf (95-110 μmol m^{-2} d^{-1}), at stations where both DO concentrations and N* in the water column were higher than in the LSLE, and the apparent sediment reactivity was lower, as indicated by the higher chlorin index (CI) (Alkhatib et al. in revision; Fig. 6 and caption for definition and methodology of the CI). Intermediate nitrate fluxes (120-130 μmol m^{-2} d^{-1}) were observed

at the head of both Anticosti (Sta. TCA) and Esquiman (Sta. TCE) Channels, where DO concentrations were low (< 30% saturation) and both the nitrate deficiency and sedimentary organic matter reactivity were slightly greater than in the Gulf (Figs. 2 and 6). Overall, the nitrate fluxes are well correlated to the bottom-water DO (R^2 = 0.77), N* (R^2 = 0.69) and the CI (R^2 = 0.76) (Fig. 6).

In the LC, no obvious relationship exists between NH_4^+ fluxes and bottom water DO concentrations or CI. Overlying water DO concentrations and sedimentary OM reactivity control the fluxes of NH_4^+ across the SWI, as they determine the rates and loci of NH_4^+ consumption and production, respectively. The inverse correlation (R^2 = 0.76; Fig 6c) between the nitrate fluxes, a function of the overlying water DO, and CI in the LSLE and the Gulf indicates that they may counteract each other so that net NH_4^+ fluxes are spatially invariant. Silica and SRP fluxes were always out of the sediment but no consistent along-channel variation could be discerned.

3.3. *Ex-situ* incubations

In all on-board core incubations, we observed a decline in both DO and NO_3^- concentrations during the first 24 hours, consistent with oxic respiration and denitrification within the sediments. Net fluxes of nitrate and DO derived from the incubation experiments are reported in Table 2. The calculated DO fluxes display large spatial variability, with the highest fluxes at Sta. 24 (6490 μmol m^{-2} d^{-1}) and the lowest ones at the head of the Esquiman Channel (2310 μmol m^{-2} d^{-1}). Net nitrate fluxes estimated from the incubation experiments were 2- to 4-fold larger than those determined from pore water nitrate concentration gradients in the LSLE, but were only 30-40% higher in the Gulf. This suggests that nitrate exchange at the sediment-water interface is enhanced by non-diffusive transport processes (i.e., bioirrigation), particularly in sediments of the hypoxic LSLE, which display higher densities of total and surface-traces of biological activity than the normoxic stations (Belley et al., 2010). Despite the difference in absolute rates, incubation-derived fluxes of nitrate

show the same spatial trend as diffusive fluxes estimated from concentration gradients, with a seaward decrease in net nitrate fluxes (Table 1).

4. Discussion

4.1. Origin of the N-deficiency in the Lower St. Lawrence Estuary

When reliable constraints on ocean circulation and water residence times are available, N* can be used as a valuable integrative tracer for net nitrogen loss from the ocean, at the ocean-basin scale (Gruber and Sarmiento, 1997; Deutsch et al., 2001) or for individual basins (Sigman et al., 2003; Lehmann et al., 2005). On the other hand, N* does not yield absolute rates of fixed-N elimination, nor does it provide information on the mechanisms responsible for the observed nitrate deficits (e.g., benthic vs. water column denitrification). The low N* values (Fig. 2c) in the LSLE do not necessarily reflect nitrate loss *per se*; they indicate a N deficiency with respect to phosphate in response to phosphate addition or nitrate removal. The 1.1 μmol L^{-1} increase in SRP concentrations in the deep waters (> 150m) of the Laurentian Channel (LC) between Sta. 16 and Sta. 23 corresponds to a 132 μmol L^{-1} decrease in DO. This value is consistent with the stoichiometry of OM respiration by oxygen according to the Redfield ratio (O_2:P = 138:1: Redfield et al., 1958). Hence, whereas the increase in deep water SRP concentrations along the E-W transect is concomitant with cumulative O_2 consumption, nitrate concentrations are lower than expected. One possible interpretation is that as the deep waters of the LC travel landward, N is eliminated through nitrate reduction, causing the N* minimum at Sta. 23.

Although the observed DO concentrations (> 50 μmol L^{-1}) are too high to expect active nitrate reduction within the water column, aerobic conditions *per se* do not preclude nitrate reduction (Lloyd, 1993; Yoshinari and Koike, 1994) as it can take place within micro-environments of the hypoxic water column such as in suspended particles and marine snow (Alldredge and Cohen, 1987). Irrespective of the exact

mechanisms at work, denitrification within the water column should result in elevated water column nitrate $\delta^{15}N$ signatures (Cline and Kaplan, 1975; Brandes et al., 1998; Sigman et al., 2003; Lehmann et al., 2005). In the deep waters of the LSLE, nitrate $\delta^{15}N$ values (~6.3‰) (Fig. 3) are only slightly higher than those observed in the water entering the LC at Sta. 16 (~5.6‰). In contrast to nitrate reduction in the water column, benthic nitrate reduction does not produce significant ^{15}N enrichment in water column nitrate (Brandes and Devol, 1997; Lehmann et al., 2007). Hence, the lack of nitrate ^{15}N-isotope enrichment in the nitrate deficient deep waters of the LSLE most likely reflects sedimentary nitrate reduction.

4.2. Pathways and rates of N elimination in the Laurentian Channel

Nitrate fluxes can be estimated either from pore water nitrate concentration profiles or incubation experiments. The pore water concentration gradient is used to calculate the benthic nitrate reduction rates sustained by the diffusive flux of nitrate from the overlying water into the sediments, but not by nitrate produced through the coupled remineralization of organic N to ammonium and its subsequent oxidation. Some of the nitrate, produced in the oxic layer though ammonium oxidation, diffuses down into the suboxic zone where denitrification is active and adds to the total amount of denitrified nitrate. Since the zones of nitrification and denitrification are close to one another in coastal and continental shelf sediment (Christensen et al., 1987b), the products of nitrification may be quickly denitrified without measurable accumulation in the pore water (Jenkins and Kemp, 1984). Hence, estimated nitrate fluxes across the SWI underestimate benthic nitrate reduction rates (Christensen et al., 1987a).

The rate of nitrate production by remineralization/nitrification (liberating fixed N that is then eliminated by denitrification) was derived from the stoichiometric relationship between O_2 consumption and N remineralization ($O_2/N = 8.6$) proposed by Froelich (1979). We assume that all O_2 is consumed by OM oxidation and that all fixed N produced by remineralization is ultimately denitrified. This allows us to roughly

estimate coupled nitrification-denitrification rates through O_2 fluxes. The nitrate production rate through the coupled nitrification-denitrification pathway was then added to the diffusive flux of nitrate across the sediment-water interface (SWI) to yield estimates of the total sediment nitrate reduction rates (Table 2). The latter were 2 to 7 times larger than the diffusive nitrate fluxes (380 to 950 μmol m^{-2} d^{-1}; Table 1). Our results indicate that coupled nitrification-denitrification is a major contributor (70% to 90%) to the overall nitrate reduction rate, a finding that is consistent with observations by Poulin et al. (2007) who measured denitrification rates in a salt marsh of the LSLE and found that more than 80% of the denitrified nitrate originates from nitrification. Despite uncertainties associated with the stoichiometric approach used in this study, the overall nitrate reduction rates are in good agreement with previous estimates of N-loss determined by LSLE sediment incubations (~460 μmol N m^{-2} d^{-1} by Anschutz et al., 2000; ~600 μmol N m^{-2} d^{-1} by Wang et al., 2003; ~570 μmol N m^{-2} d^{-1} by Katsev et al., 2007).

The end-product of most nitrate reduction pathways is N_2. Hence, measuring N_2 fluxes across the SWI provides a means of evaluating the combined suboxic N_2 production, including denitrification, coupled nitrification-denitrification and anammox. N_2 fluxes were calculated from pore water concentration profiles measured at stations in the LSLE and the Gulf (Figure 5). They are up to 2 times larger than the nitrate diffusive fluxes (Table 1) but significantly lower than our net nitrate reduction rate estimates (Table 2). This discrepancy may in part be methodological, for example the shortcoming of flux estimates assuming Fickian diffusion (not considering bioirrigation) or some loss of N_2 gas during sampling. Precaution was taken to prevent atmospheric gas exchange, but N_2 losses during sampling could explain the lower fluxes. From a more mechanistic point of view, the discrepancy between the N fluxes may be explained by the fact that a significant fraction of DO consumption (used to estimate the coupled nitrification-denitrification rate) is not consumed to re-mineralize organic matter but for the oxidation of reduced pore water solutes (e.g., NH_4^+, Mn^{2+}, Fe^{2+}, HS^-). Alternatively, nitrate reduction pathways that

do not produce N_2 may account for the difference between nitrate reduction rates based on N_2 fluxes and nitrate (and DO) fluxes. Using the isotope pairing technique, Wang et al. (2003) found a large discrepancy between the diffusive flux of labeled ^{15}N-nitrate into the sediments and the production rate of $^{15}N_2$ at Sta. 23, with the latter being an order of magnitude lower. The authors concluded that pathways of nitrate reduction to N_2, other than denitrification or anammox, must also be at work. Nitrate reduction can occur through dissimilatory reduction of nitrate to ammonium (DRNA) and via the assimilation of DIN by benthic microorganisms. In coastal marine sediments, rates of DRNA have been reported to be as important as canonical denitrification (Bonin et al., 1998; Rysgaard et al., 1998; An and Gardner, 2002). Nevertheless, denitrifiers are generally more efficient than DRNA bacteria (Seitzinger and Kroeze, 1998), and it is unlikely that most of the pore water nitrate is reduced to ammonium rather than N_2 gas. The progressive increase in pore water ammonium concentration with depth (with no apparent NH_4^+ maximum; Fig. 4) suggests that little or none of the downward diffusing nitrate is reduced to ammonium, although ammonium could also be directly consumed as it is produced (Anschutz et al., 2000).

We used ^{15}N labeled nitrate in *ex-situ* core incubations (48h) to determine if it is reduced to ammonium in LSLE sediments (Fig. 7). ^{15}N-ammonium was found in the overlying water and down to ~ 1.3 cm below the SWI, suggesting that ^{15}N labeled nitrate is transferred to the ammonium pool at Sta. 18. However, this does not allow for a more quantitative assessment of this N transfer, nor does it provide conclusive evidence as to the actual pathway of nitrate reduction to ammonium. The ^{15}N-nitrate shuttling into the ammonium pool could result from DRNA, but it could also reflect benthic assimilation of the nitrate and the subsequent remineralization of the *in-situ* synthesized organic N to ammonium (Blackburn et al., 1996; Cook et al., 2004). Regardless, total nitrate reduction cannot currently explain the discrepancy between N_2 fluxes and total denitrification rates estimated using our stoichiometric approach. The relative importance of alternate benthic nitrate reduction pathways (assimilatory

or dissimilatory), other than denitrification, in the SL sediments remains to be confirmed.

4.3 Environmental controls on sediment-water nitrate exchange

Organic matter remineralization proceeds through a well-established sequence of redox reactions (Froelich, 1979). Nitrate is reduced to gaseous forms (i.e., N_2, N_2O) under suboxic conditions, and is produced mostly through the aerobic oxidation of ammonium originating from OM remineralization. Accordingly, one of the factors that govern the balance of nitrate consumption and supply within the sediments is the oxygen penetration depth (OPD). The OPD determines the depth at which nitrate production and consumption occur, and will modulate the magnitude and direction of the nitrate diffusive flux at the SWI. For example, a relatively shallow denitrification zone will yield steep nitrate concentration gradients and, thus, potentially high nitrate fluxes to the sediment. The OPD is determined by the bottom water DO concentration, sediment porosity and biological oxygen demand of the sediment, in turn a function of the supply and reactivity of OM and temperature (Katsev et al., 2007). On the other hand, high OM supply/reactivity not only drives shallow-sediment DO depletion and high denitrification rates, it also stimulates high remineralization/nitrification rates which can dampen or even reverse net fluxes of nitrate into the sediments.

In the SL system, nitrate diffusive fluxes into the sediment decrease from the LSLE to the Gulf, where bottom water DO levels are higher (Fig. 6). Likewise, net nitrate fluxes, derived from the incubation experiments, which capture the advective component of the nitrate flux due to bioirrigation, were smaller in the Gulf than in the LSLE. Hence, both net and diffusive flux estimates confirm the inverse relationship between nitrate fluxes and bottom water DO. The observed in-shore/off-shore trend may also be linked to the spatial variability of sedimentary OM reactivity. Alkhatib et al. (in revision) determined the chlorin-based degradation index CI (Schubert et al., 2005) for sedimentary OM in the Laurentian Channel, which provides indications on

the freshness or reactivity of sedimentary organic matter (Fig. 6). They argue that the apparent higher OM reactivity in the Estuary results from a progressive degradation of organic particles with exposure time in an increasingly oxygenated water column seaward from the hypoxic LSLE. Irrespective of the exact mechanism(s) that yield the observed trends in sediment characteristics, a significant positive correlation exists between the apparent sediment OM reactivity and nitrate fluxes (Fig. 6).

4.4. Water column constraints on benthic N elimination

Whereas the landward increasing N deficit in bottom water is clearly related to benthic reduction, the location of the maximum N deficit is not necessarily the expression of maximum N-reduction in the LSLE but rather of the cumulative sedimentary N-reduction along the LC. Water column nitrate concentrations or N* measurements integrate nitrate reduction processes over large spatial and temporal scales and, thus, provided water residence time and basin geometry are well constrained, afford a more robust estimate of the mean estuarine N elimination rate than direct, punctual flux measurements. The averaged N* at Sta. 23 (from 100 to 350 m water depth) is 9.2 μmol L^{-1} lower than for the same isopycnals at Sta. 16. Assuming a cross-channel average advection velocity of 0.5 cm s^{-1} (Bugden, 1988) to 1 cm s^{-1} (Gilbert, 2004), the travel time of the deep water mass from Sta.16 to Sta. 23 would be between 2 and 4 years. Using the 300 m bathymetric contour (with an estimated sediment surface to water volume ratio of 1:280 m^{-1}) and the two bottom water advection velocity estimates, we calculate that an average sediment denitrification rate between 1770 and 3540 μmol m^{-2} d^{-1} in the LC is required to generate the observed nitrate deficit in the deep water of the LSLE. These rates are significantly higher than the average rates calculated from both diffusive fluxes and incubations experiments, but our area estimate for sediment below the 300 m bathymetric contour line likely underestimates the total sediment surface area, as it neglects denitrification on the channel side walls and, thus, overestimates

denitrification per m^2. Extrapolation of the N*-based nitrate fluxes to the sediment surface area of the Laurentian Channel between Sta. 23 and 16 (~35700 km^2) reveals that between 325 and 650 x 10^6 t of fixed N are lost annually to the LC sediments. The same calculations were applied to the other channels and yield N-loss rates of 690 to 1380 and 570 to 1140 μmol m^{-2} d^{-1} (here, the minimum denitrification rates are closer to our measured field rates, possibly because of the smaller uncertainties regarding the surface sediment areas), or 37 to 74 and 51 to 102 x 10^6 t N for the Anticosti and Esquiman Channels, respectively.

Savenkoff et al. (2001) estimated the net N input to the St. Lawrence, through riverine discharge and net N exchange with continental shelf waters at Cabot and Belle-Isle Straits, at 445 x 10^6 t N yr^{-1} (using an advection rate of 0.5 cm s^{-1}; Bugden et al., 1991). Atmospheric deposition over the St-Lawrence system was estimated at 9 x 10^6 t N (from Prospero et al., 1996). N burial is believed to be minor (~ 1 x 10^6 t N yr^{-1}; Savenkoff et al., 2001) but may have been underestimated given that quantitative nitrate assimilation and the subsequent storage of N into benthic bacterial biomass have been neglected so far. Uncertainties aside, our lower estimate of N*-based, annual benthic nitrate elimination in the three main channels of the St. Lawrence system, (413 x 10^6 t N; using the same advection rate of 0.5 cm s^{-1} as Savenkoff et al. (2001)) is close to the net input of N (454 x 10^6 t N yr^{-1}) to the SL system, suggesting that benthic nitrate reduction in the St. Lawrence Channel sediments is highly efficient (93% of the N inputs). This result demonstrates the importance of benthic N-elimination as a natural regulator of N inputs in this particular coastal estuarine environment.

5. Summary and Concluding Remarks

The combination of water column nutrient concentration and nitrate N-isotope data with *ex-situ* estimates of benthic nitrate fluxes provides new constraints on the nitrate deficit in the deep waters of the LSLE. Several complementary approaches were used

to evaluate the strength of sedimentary fixed-N elimination processes. The average flux-based, total benthic nitrate reduction rate in the LSLE and the Gulf of St. Lawrence was 690 μmol m^{-2} d^{-1}, 70% of which is fueled by nitrification of remineralized OM. This estimate is significantly lower than the ecosystem scale estimate for benthic nitrate reduction derived from the water column nitrate deficit, suggesting that processes not captured by our direct measurements are at work. For example, bioirrigation can enhance solute transport across the SWI (Katsev et al., 2007) and, thus, the diffusive nitrate fluxes estimated from pore water profiles likely underestimate the sediment-water exchange rate. Furthermore, pore water-based estimates of the total benthic denitrification may be biased by high spatial heterogeneity, limiting their utility for extrapolation to the whole LC ecosystem. In contrast, water column N* integrates biogeochemical processes over a large spatial and temporal scale and, thus, provides a more comprehensive, albeit indirect, estimate of the system-wide nitrate reduction. Nevertheless, fixed-N elimination rates, estimated from N*, may carry large uncertainties given uncertainties on the water residence time in the SL system and basin geometry (surface sediment-to-water volume ratio).

We demonstrated that the diffusive nitrate fluxes, but not necessarily the total nitrate reduction rates, are correlated with bottom water DO concentration and the chlorin index, highlighting the sensitivity of benthic N-transformations and DIN fluxes at the sediment-water interface to bottom water oxygenation and sediment oxygen demand. The discrepancy between nitrate fluxes estimated from field measurements and the N* approach may highlight an incomplete understanding of the benthic nitrogen cycle in the SL system. Future investigations into benthic N-consumption processes in and along the LC should include *in situ* incubations and isotope pairing experiments to better constrain the contribution of various nitrate reducing metabolic pathways and identify their role in the N cycle of the SL system.

Irrespectively of the uncertainties associated with both approaches, our data show that benthic denitrification rates in the LC are high enough to maintain a nitrate deficit in

the LSLE, despite relatively short water renewal times. We conclude that N elimination in SL sediments nearly balances the present-day fixed-N inputs to the SL system. Enhanced N fertilization in the SL watershed over the last decades may have promoted primary productivity locally, close to the mouth of the St. Lawrence River and in the LSLE (Thibodeau et al., 2006) but does not appear to extend to the Gulf of St. Lawrence and the Esquiman Channel (Genovesi et al., 2008) at this time. This suggests that N is effectively eliminated in the LSLE and that present-day enhanced anthropogenic N-inputs have not created an imbalance in the N-budget of the whole SL ecosystem, although they may be contributing to increased respiration and O_2 losses in the bottom waters.

Acknowledgements

We thank the captain and crew of the R/V Coriolis II for their assistance during sample collection, G. Chaillou and S. Xiu Phuong for their technical assistance during onboard incubations and laboratory measurements, respectively, and W. Gardner and M. McCarthy for HPLC ammonium isotope analyses and helpful discussions. Furthermore, discussions with G. Chaillou and B. Williams and three anonymous reviewers helped to improve the manuscript. Figure 1 was prepared using Online Map Creation (OMC) by M. Weinelt. Figure 2 was prepared using Ocean Data View Software (Schlitzer, 2009).

This work was funded by the Natural Sciences and Engineering Research Council of Canada (NSERC) through a Strategic Research Grant, Ship-Time Allocation Grants to MFL, YG and AM, and Discovery Grants to MFL and AM.

References

Alkhatib, M., Lehmann, M.F., del Giorgio, P., Schubert, C.J. and Y. Gélinas, 2010. Organic matter reactivity and amino acid biogeochemistry in St. Lawrence Estuary sediments; in revision; Geochimica et Cosmochimica Acta.

Alldredge, A.L. and Cohen, Y., 1987. Can microscale chemical patches persist in the sea? Microelectrode study of marine snow, fecal pellets. Science, 235(4789): 689-691.

An, S. and Gardner, W.S., 2002. Dissimilatory nitrate reduction to ammonium (DNRA) as a nitrogen link, versus denitrification as a sink in a shallow estuary (Laguna Madre/Baffin Bay, Texas). Marine Ecology Progress Series, 237: 41-50.

Anschutz, P., Sundby, B., Lefrançois, L., Luther III, G.W. and Mucci, A., 2000. Interactions between metal oxides and species of nitrogen and iodine in bioturbated marine sediments. Geochimica et Cosmochimica Acta, 64(16): 2751-2763.

Barnett, P.R.O., Watson, J. and Connelly, D., 1984. A multiple corer for taking virtually undisturbed samples from shelf, bathyal and abyssal sediments. Oceanologica acta, 7(4): 399-408.

Bender, M., Martin, W., Hess, J., Sayles, F., Ball, L. and Lambert, C., 1987. A whole-core squeezer for interfacial pore-water sampling. Limnology & Oceanography, 32(6): 1214-1225.

Benoit, P., Gratton, Y. and Mucci, A., 2006. Modeling of dissolved oxygen levels in the bottom waters of the Lower St. Lawrence Estuary: coupling of benthic and pelagic processes. Marine Chemistry, 102: 13-32.

Blackburn, T.H., Hall, P.O.J., Hulth, S. and Landén, A., 1996. Organic-N loss by efflux and burial associated with a low efflux of inorganic N and with nitrate assimilation in Arctic sediments (Svalbard, Norway). Marine Ecology Progress Series, 141(1-3): 283-293.

Bonin, P., Omnes, P. and Chalamet, A., 1998. Simultaneous occurrence of denitrification and nitrate ammonification in sediments of the French Mediterranean Coast. Hydrobiologia, 389(1-3): 169-182.

Boudreau, B.P., 1996. Diagenetic models and their implementation: modelling transport and reactions in aquatic sediments. Diagenetic models and their implementation: modelling transport and reactions in aquatic sediments. Springer-Verlag, New York.

Bourbonnais, A., Lehmann, M.F., Waniek, J.J. and Schulz-Bull, D.E., 2009. Nitrate isotope anomalies reflect N2 fixation in the Azores Front region (subtropical N-E Atlantic). Journal of Geophysical Research, 114: C03003, doi:10.1029/2007JC004617.

Brandes, J.A., Boctor, N.Z., Cody, G.D., Cooper, B.A., Hazen, R.M. and Yoder Jr, H.S., 1998. Abiotic nitrogen reduction on the early Earth. Nature, 395: 365-367.

Brandes, J.A. and Devol, A.H., 1997. Isotopic fractionation of oxygen and nitrogen in coastal marine sediments. Geochimica et Cosmochimica Acta, 61(9): 1793-1801.

Brandes, J.A. and Devol, A.H., 2002. A global marine-fixed nitrogen isotopic budget: Implications for Holocene nitrogen cycling. Global Biogeochemical Cycles, 16(4): 67-1.

Bugden, G.L., 1988. Oceanographic conditions in the deeper waters of the Gulf of St. Lawrence in relation to local and oceanic forcing. NAFO SCR Document 88/87.

Christensen, J.P., Murray, J.W., Devol, A.H. and Codispoti, L.A., 1987a. Denitrification in continental shelf sediments has major impact on the oceanic nitrogen budget. Global Biogeochem. Cycles, 1(2): 97-116.

Christensen, J.P., Smethie Jr, W.M. and Devol, A.H., 1987b. Benthic nutrient regeneration and denitrification on the Washington continental shelf. Deep Sea Research Part A, Oceanographic Research Papers, 34(5-6): 1027-1047.

Cline, J.D. and Kaplan, I.R., 1975. Isotopic fractionation of dissolved nitrate during denitrification in the eastern tropical north pacific ocean. Marine Chemistry, 3(4): 271-299.

Cloern, J.E., 2001. Our evolving conceptual model of the coastal eutrophication problem. Marine Ecology Progress Series, 210: 223-253.

Codispoti, L., Yoshinari, T. and Devol, A., 2005. Suboxic respiration in the oceanic water column. In: P.A. del Giorgio and P.J. Le B Williams (Editors), Respiration in Aquatic Ecosystems. Oxford University Press, Oxford, pp. 225–247.

Cook, P.L.M., Eyre, B.D., Leeming, R. and Butler, E.C.V., 2004. Benthic fluxes of nitrogen in the tidal reaches of a turbid, high-nitrate sub-tropical river. Estuarine, Coastal and Shelf Science, 59(4): 675-685.

Coote, A.R. and Yeats, P.A., 1979. Distribution of nutrients in the Gulf of St. Lawrence. Journal of the Fisheries Research Board of Canada, 36: 122-131.

Deutsch, C., Gruber, N., Key, R.M., Sarmiento, J.L. and Ganachaud, A., 2001. Denitrification and N_2 fixation in the Pacific Ocean. Global Biogeochemical Cycles, 15(2): 483-506.

Diaz, R.J. and Rosenberg, R., 2008. Spreading dead zones and consequences for marine ecosystems. Science, 321(5891): 926-929.

Froelich, P.N., 1979. Early oxidation of organic matter in pelagic sediments of the eastern equatorial Atlantic: suboxic diagenesis. Geochimica et Cosmochimica Acta, 43(7): 1075-1090.

Galloway, J.N., Dentener, F.J., Capone, D.G., Boyer, E.W., Howarth, R.W., Seitzinger, S.P., Asner, G.P., Cleveland, C.C., Green, P.A., Holland, E.A., Karl, D.M., Michaels, A.F., Porter, J.H., Townsend, A.R. and Vöosmarty, C.J., 2004. Nitrogen Cycles: Past, Present, and Future. Biogeochemistry, 70(2): 153-226.

Gardner, W.S., Bootsma, H.A., Evans, C. and St John, P.A., 1995. Improved chromatographic analysis of ^{15}N:^{14}N ratios in ammonium or nitrate for isotope addition experiments. Marine Chemistry, 48(3-4): 271-282.

Gearing, J.N. and Pocklington, R., 1990. Organic geochemical studies in the St. Lawrence Estuary. In: M.I. El-Sabh and N. Silverberg (Editors), Oceanography of a large-scale estuarine system, the St.-Lawrence Coastal and estuarine studies Springer-Verlag, New York, pp. 170–201.

Genovesi, L., Thibodeau, B., de Vernal, A. and Hillaire-Marcel, C., 2008. Recent changes of bottom water oxygenation and temperature in the Gulf of St. Lawrence: micropaleontological and geochemical evidences, Water, Weather, and Climate: Science Informing Decisions. Canadian Meteorological and Oceanographic Society, Kelowna, B.C., pp. 17-18.

Gilbert, D., Sundby, B., Gobeil, C., Mucci, A. and Tremblay, G.H., 2005. A seventy-two-year record of diminishing deep-water oxygen in the St. Lawrence estuary: The northwest Atlantic connection. Limnology and Oceanography, 50(5): 1654-1666.

Gonfiantini, R., Stichler, W. and Rozanski, K., 1995. Standards and intercomparison materials distributed by the International Atomic Energy Agency for stable isotope measurements., Proceedings of a consultants meeting International Atomic Energy Agency, Vienna, Austria, pp. 13–29.

Grasshoff, K., Kremling, K. and Ehrhardt, M., 1999. Methods of seawater analysis, Weinheim, Toronto, 600 pp.

Gruber, N. and Sarmiento, J.L., 1997. Global patterns of marine nitrogen fixation and denitrification. Global Biogeochemical Cycles, 11(2): 235-266.

Hedges, J.I., Baldock, J.A., Gélinas, Y., Lee, C., Peterson, M.L. and Wakeham, S.G., 2002. The biochemical and elemental compositions of marine plankton: A NMR perspective. Marine Chemistry, 78(1): 47-63.

Howarth, R.W., 1998. An assessment of human influences on fluxes of nitrogen from the terrestrial landscape to the estuaries and continental shelves of the North Atlantic Ocean. Nutrient Cycling in Agroecosystems, 52(2-3): 213-223.

Howarth, R.W., Swaney, D.P., Boyer, E.W., Marino, R., Jaworski, N. and Goodale, C., 2006. The influence of climate on average nitrogen export from large watersheds in the Northeastern United States. Biogeochemistry, 79(1-2): 163-186.

Jenkins, M.C. and Kemp, W.M., 1984. The coupling of nitrification and denitrification in two estuarine sediments. Limnology & Oceanography, 29(3): 609-619.

Kana, T.M., Darkangelo, C., Oldham, J.B., Bennett, G.E. and Cornwell, J.C., 1994. Membrane inlet mass spectrometer for rapid high-precision determination of N_2, O_2, and Ar in environmental water samples. Analytical Chemistry, 66(23): 4166-4170.

Kana, T.M., Sullivan, M.B., Cornwell, J.C. and Groszkowski, K.M., 1998. Denitrification in estuarine sediments determined by membrane inlet mass spectrometry. Limnology and Oceanography, 43(2): 334-339.

Katsev, S., Chaillou, G., Sundby, B. and Mucci, A., 2007. Effects of progressive oxygen depletion on sediment diagenesis and fluxes: A model for the lower St. Lawrence River Estuary. Limnology and Oceanography, 52(6): 2555-2568.

Lehmann, M.F., Barnett, B., Géinas, Y., Gilbert, D., Maranger, R.J., Mucci, A., Sundby, B. and Thibodeau, B., 2009. Aerobic respiration and hypoxia in the lower st. lawrence estuary: Stable isotope ratios of dissolved oxygen constrain oxygen sink partitioning. Limnology and Oceanography, 54(6): 2157-2169.

Lehmann, M.F., Sigman, D.M., McCorkle, D.C., Brunelle, B.G., Hoffmann, S., Kienast, M., Cane, G. and Clement, J., 2005. Origin of the deep Bering Sea nitrate deficit: Constraints from the nitrogen and oxygen isotopic composition

of water column nitrate and benthic nitrate fluxes. Global Biogeochemical Cycles, 19(4).

Lehmann, M.F., Sigman, D.M., McCorkle, D.C., Granger, J., Hoffmann, S., Cane, G. and Brunelle, B.G., 2007. The distribution of nitrate $^{15}N/^{14}N$ in marine sediments and the impact of benthic nitrogen loss on the isotopic composition of oceanic nitrate. Geochimica et Cosmochimica Acta, 71(22): 5384-5404.

Lloyd, D., 1993. Aerobic denitrification in soils and sediments: From fallacies to facts. Trends in Ecology and Evolution, 8(10): 352-356.

Martin, W.R., Bender, M., Leinen, M. and Orchardo, J., 1991. Benthic organic carbon degradation and biogenic silica dissolution in the central equatorial Pacific. Deep Sea Research Part A, Oceanographic Research Papers, 38(12): 1481-1516.

Middelburg, J.J., Soetaert, K., Herman, P.M.J. and Heip, C.H.R., 1996. Denitrification in marine sediments: A model study. Global Biogeochemical Cycles, 10(4): 661-673.

Nixon, S.W., Ammerman, J.W., Atkinson, L.P., Berounsky, V.M., Billen, G., Boicourt, W.C., Boynton, W.R., Church, T.M., Ditoro, D.M., Elmgren, R., Garber, J.H., Giblin, A.E., Jahnke, R.A., Owens, N.J.P., Pilson, M.E.Q. and Seitzinger, S.P., 1996. The fate of nitrogen and phosphorus at the land-sea margin of the North Atlantic Ocean. Biogeochemistry, 35(1): 141-180.

Poulin, P., Pelletier, E. and Saint-Louis, R., 2007. Seasonal variability of denitrification efficiency in northern salt marshes: An example from the St. Lawrence Estuary. Marine Environmental Research, 63(5): 490-505.

Prospero, J.M., Barrett, K., Church, T., Dentener, F., Duce, R.A., Galloway, J.N., Levy Ii, H., Moody, J. and Quinn, P., 1996. Atmospheric deposition of nutrients to the North Atlantic Basin. Biogeochemistry, 35(1): 27-73.

Redfield, A.C., 1958. The biological control of chemical factors in the environment. American Scientist, 46: 205-221.

Rysgaard, S., Thamdrup, B., Risgaard-Petersen, N., Fossing, H., Berg, P., Christensen, P.B. and Dalsgaard, T., 1998. Seasonal carbon and nutrient mineralization in a high-Arctic coastal marine sediment, Young Sound, Northeast Greenland. Marine Ecology Progress Series, 175: 261-276.

Savenkoff, C., Vézina, A.F., Smith, P.C. and Han, G., 2001. Summer transports of nutrients in the Gulf of St. Lawrence estimated by inverse modelling. Estuarine, Coastal and Shelf Science, 52(5): 565-587.

Schubert, C.J., Niggemann, J., Klockgether, G. and Ferdelman, T.G., 2005. Chlorin Index: A new parameter for organic matter freshness in sediments. Geochemistry Geophysics Geosystems, 6: Q03005.10.1029/2004GC000837.

Schulz, H., 2006. Quantification of Early Diagenesis: Dissolved Constituents in Pore Water and Signals in the Solid Phase, Marine Geochemistry. Springer-Verlag, pp. 73-124.

Seeberg-Elverfeldt, J., Schlüter, M., Kölling, M. and Feseker, T., 2005. Rhizon - an excellent pore water sampler for low maintenance collection and filtration of small volume samples, EGU General Assembly, Vienna, Austria.

Seitzinger, S.P. and Kroeze, C., 1998. Global distribution of nitrous oxide production and N inputs in freshwater and coastal marine ecosystems. Global Biogeochemical Cycles, 12(1): 93-113.

Sigman, D.M., Casciotti, K.L., Andreani, M., Barford, C., Galanter, M. and Böhlke, J.K., 2001. A bacterial method for the nitrogen isotopic analysis of nitrate in seawater and freshwater. Analytical Chemistry, 73(17): 4145-4153.

Sigman, D.M., Robinson, R., Knapp, A.N., van Geen, A., McCorkle, D.C., Brandes, J.A. and Thunell, R.C., 2003. Distinguishing between water column and sedimentary denitrification in the Santa Barbara Basin using the stable isotopes of nitrate. Geochemistry Geophysics Geosystems, 4(5): 1040.

Smith, J.N. and Schafer, C.T., 1999. Sedimentation, bioturbation, and Hg uptake in the sediments of the estuary and Gulf of St. Lawrence. Limnology and Oceanography, 44(1): 207-219.

Strickland, J.D.H. and Parsons, T.R., 1972. A pratical handbook of seawater analysis. Bulletin Fisheries Research Board of Canada, 167: 207-211.

Thibodeau, B., de Vernal, A. and Mucci, A., 2006. Recent eutrophication and consequent hypoxia in the bottom waters of the Lower St. Lawrence Estuary: Micropaleontological and geochemical evidence. Marine Geology, 231(1-4): 37-50.

Wang, F., Juniper, S.K., Pelegrí, S.P. and Macko, S.A., 2003. Denitrification in sediments of the Laurentian Trough, St. Lawrence Estuary, Québec, Canada. Estuarine, Coastal and Shelf Science, 57(3): 515-522.

Weiss, R.F., 1970. The solubility of nitrogen, oxygen and argon in water and seawater. Deep-Sea Research and Oceanographic Abstracts, 17(4): 721-735.

Yeats, P.A., 1988. Nutrients. Canadian Bulletin of Fisheries and Aquatic Sciences, 220: 29-48.

Yoshinari, T. and Koike, I., 1994. The use of stable isotopes for the study of gaseous nitrogen species in marine environments. In: K. Lajtha and R. Michener (Editors), Stable Isotopes in Ecology and Environmental Science. Blackwell Science, Norwell, MA, pp. 114-137.

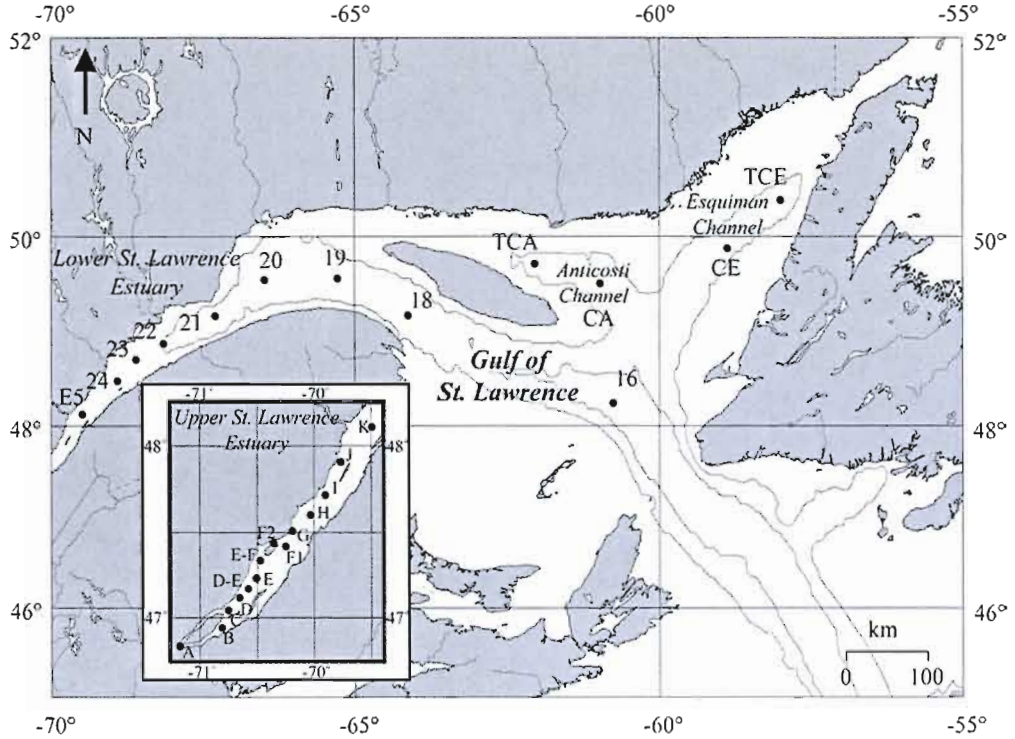

Figure 1. Map of the St. Lawrence Estuary and Gulf with sampling locations. Bathymetric contours outlining the Laurentian, Esquiman and Anticosti Channels along the 300 and 400 m isobaths.

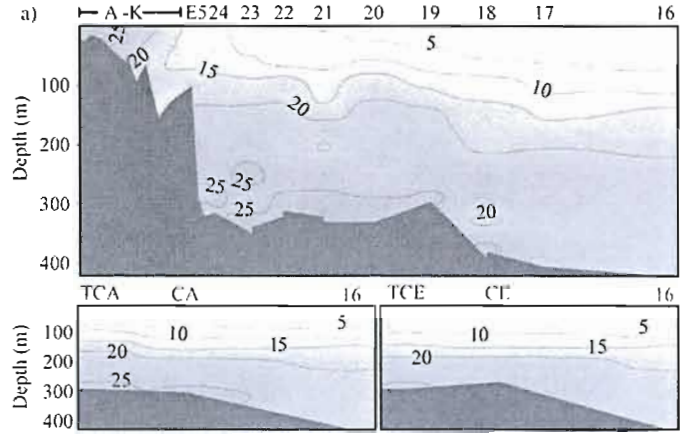
a)
A -K
E524 23 22 21 20 19 18 17 16
Depth (m)
100
200
300
400
5
10
15
20
25
TCA
CA
TCE
CE

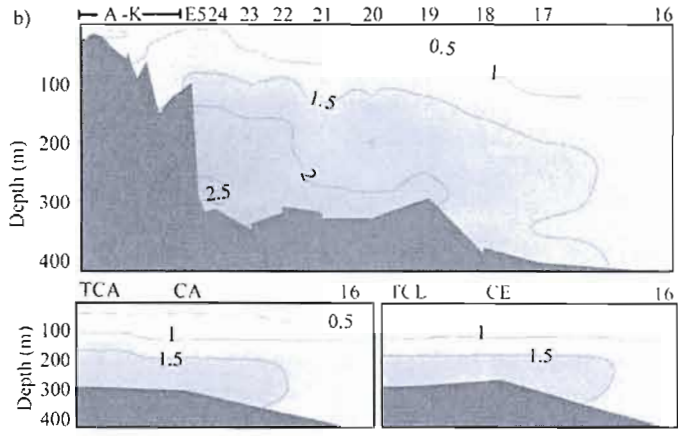
b)
A -K
E524 23 22 21 20 19 18 17 16
Depth (m)
0.5
1
1.5
2
2.5
TCA
CA
TCE
CE

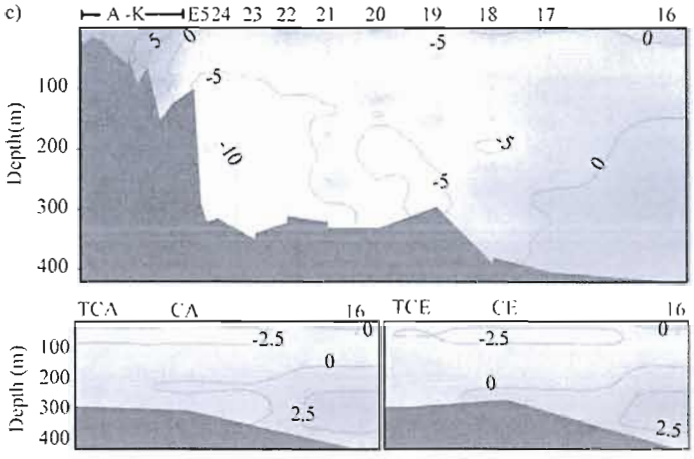
c)
A -K
E524 23 22 21 20 19 18 17 16
Depth(m)
5
0
-5
-10
TCA
CA
TCE
CE
-2.5
2.5

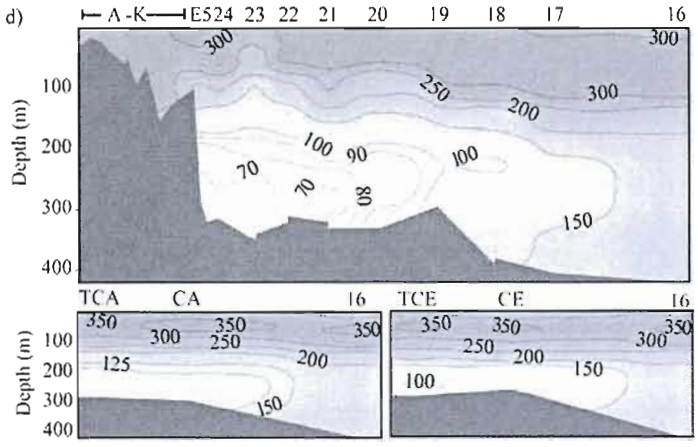

Figure 2. Dissolved (a) Nitrate + nitrite, (b) phosphate, (c) N*, and (d) oxygen concentrations along the Upper and Lower St. Lawrence Estuary, the Gulf of St. Lawrence and the Anticosti and Esquiman Channels. Stations numbers are indicated on the *x*-axis.

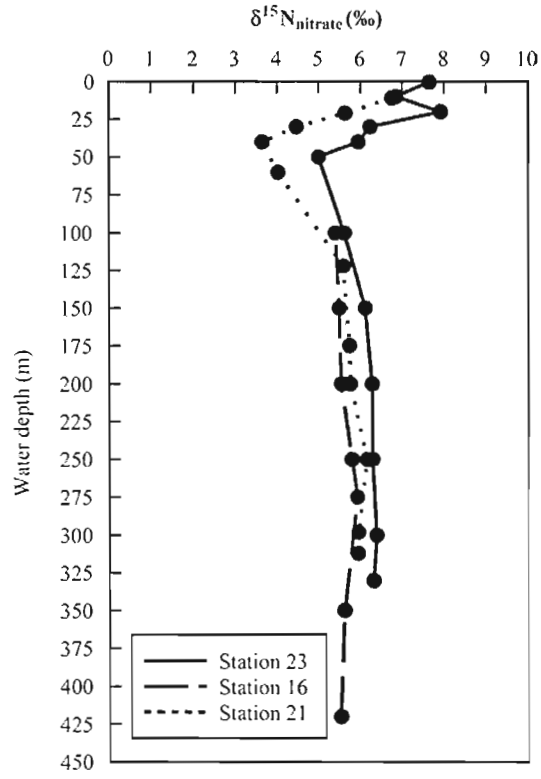

Figure 3. Water column $\delta^{15}N$ in nitrate at Stations 23, 21, and 16.

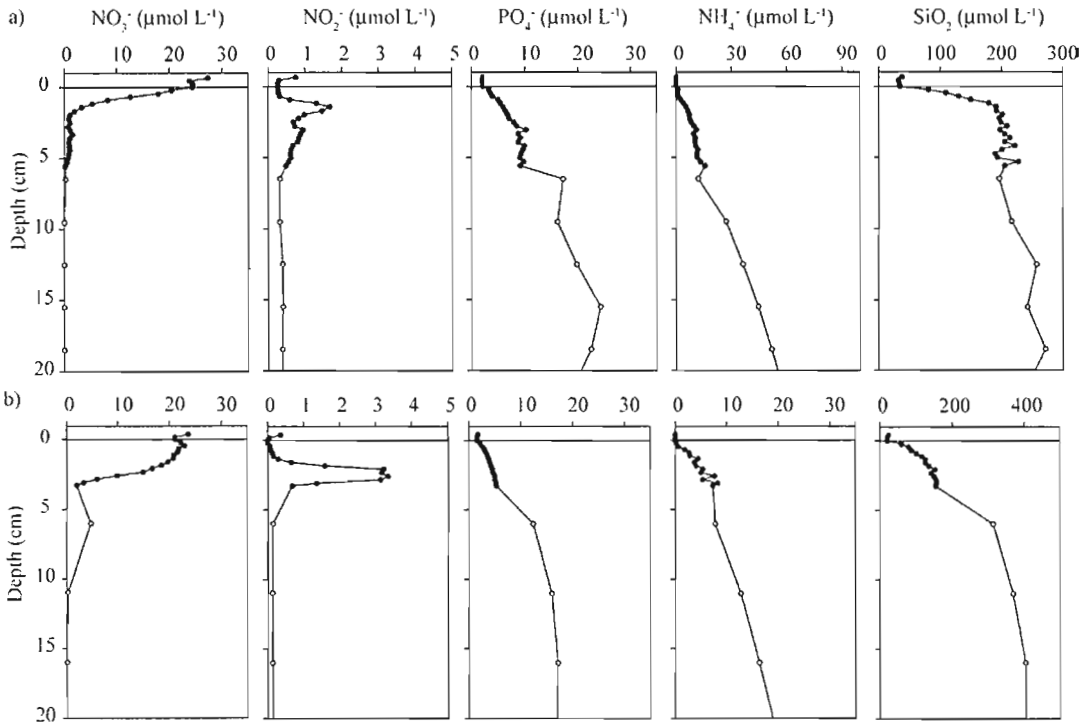

Figure 4. Representative pore water profiles for nitrate, nitrite, reactive phosphate, ammonium and silica where we observed sediment uptake of nitrate (Sta. 20) (a), and sediment release of nitrate (Sta. 16) (b) to the overlying waters. Closed symbols represent pore water samples extracted by WCS, open symbols represent pore waters extracted with Rhizon membrane samplers.

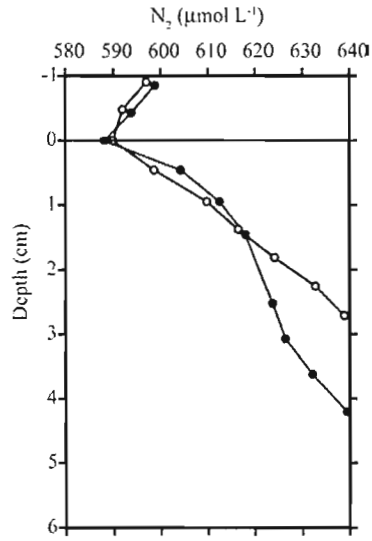

Figure 5. Representative pore water profiles of di-nitrogen in the St. Lawrence Estuary at Sta 21 (filled) and in the Gulf at Sta. 20 (empty).

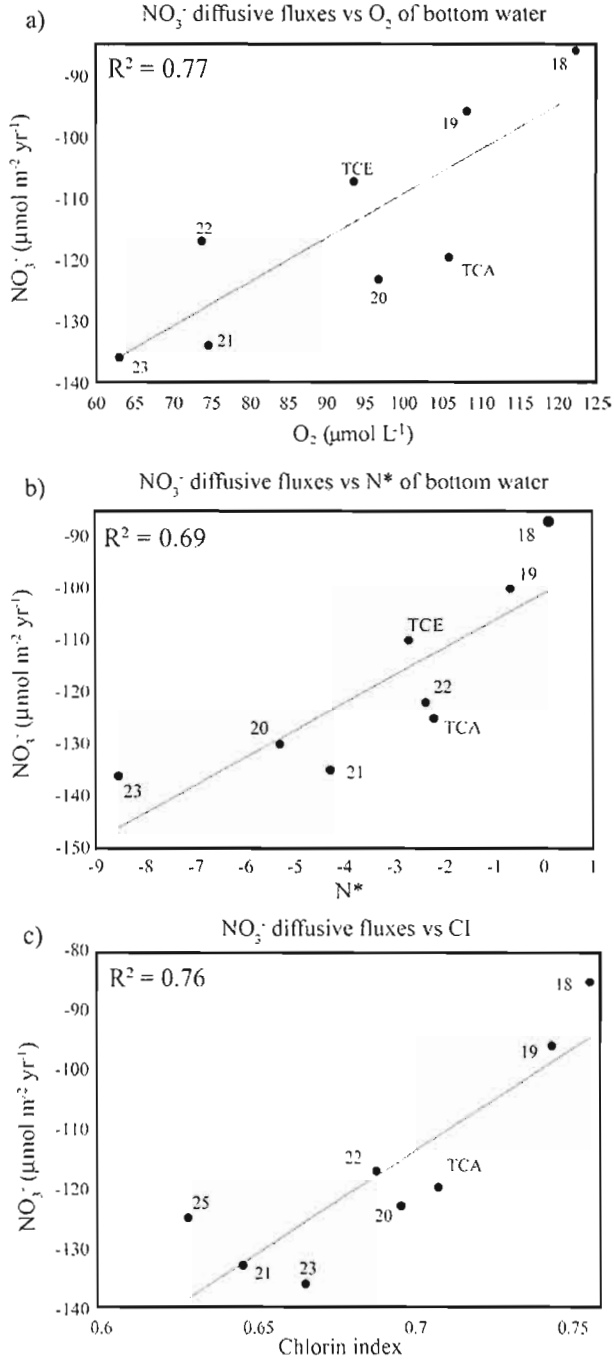

Figure 6. Relationships between nitrate diffusive fluxes and (a) DO in the overlying water, (b) N*, and (c) chlorin index (CI) for LC sediments. CI data are taken from Alkhatib et al. (2010). The chlorin index (CI) is calculated as the ratio of the

fluorescence of the acidified chlorin extract (acetone sediment extract of chlorophyll and its degradation products) and the fluorescence of the original chlorin extract. The CI scale ranges from 0.2 for pure chlorophyll (high reactivity) to approximately 1 for highly degraded organic matter, i.e., low-reactivity sediments (Schubert et al., 2005).

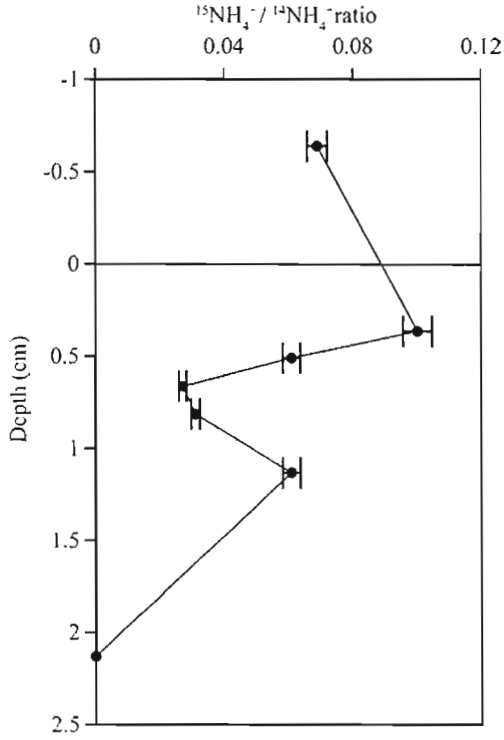

Figure 7. Profile showing ^{15}N label in pore water ammonium in a core taken at Sta. 18, 48h after the addition of ^{15}N-labelled nitrate to the overlying water.

	----------Diffusive fluxes (μmol m^{-2} d^{-1})----------					Conc. (μmol L^{-1})	
Station	NO_3^-	PO_4^{3-}	NH_4^+	SiO_2	N_2	NO_3^-	O_2
E5	-130	-	-	250	n.d	29	65
24	-190	7	-	230	n.d	29	65
23	-140	8	-	470	n.d	29	65
22	-140	3	-	500	132	26	70
21	-140	7	14	330	210	29	75
20	-130	5	20	480	153	26	97
19	-110	5	-	470	180	26	108
18	-100	4	-	540	168	26	122
16	25	4	-	300	n.d	22	197
TCA	-130	3	-	510	n.d	26	106
TCE	-120	6	-	300	n.d	26	94

Table 1: Benthic diffusive fluxes of nitrate, phosphate, ammonium, silica and di-nitrogen estimated from pore water concentration gradients, and bottom water nitrate and dissolved oxygen concentrations. Negative signs for flux rates indicate fluxes into the sediment.

Station	Nitrate flux (from conc. gradient) (μmol m^{-2} d^{-1})	Nitrate flux (from incubations) (μmol m^{-2} d^{-1})	O_2 flux (from incubations) (μmol m^{-2} d^{-1})	Total denitrification (estimated) (μmol m^{-2} d^{-1})
E5	-130	-450	-6410[1]	-870
24	-190	-630	-6490[1]	-950
23	-140	-580	-4300[1]	-640
22	-140	n.d	n.d	n.d
21	-140	-250	-3220	-510
20	-130	n.d	n.d	n.d
19	-110	n.d	-3750	-540
18	-100	-130	-4950	-660
16	25	n.d	n.d	n.d
TCA	-130	n.d	-4360	-630
TCE	-120	n.d	-2310	-380

Table 2: Benthic nitrate fluxes (estimated from pore water concentrations gradients and from core incubations), benthic O_2 fluxes (from core incubations), and total denitrification rates (see text for details). Negative fluxes point into the sediments.
[1]Data from Katsev et al. (2007).

CHAPITRE III

SEASONAL VARIATIONS OF NITROGEN SOURCES AND CYLING IN THE ST. LAWRENCE RIVER

Benoît Thibodeau[1], Moritz F. Lehmann[2], Jean-François Hélie[1] and Éric Rosa[1]

[1]Geochemistry and Geodynamics Research Center, GEOTOP, Université du Québec à Montréal, Montréal, Québec, H3C 3P8, Canada

[2]Institute for Environmental Geosciences, University of Basel, Bernoullistrasse 30, 4056 Basel, Switzerland

Résumé

Dans le contexte de l'hypoxie observée dans l'estuaire maritime, nous avons mesuré la composition isotopique des nitrates dans le fleuve Saint-Laurent dans le but d'identifier leurs sources et d'évaluer l'importance du recyclage interne. L'échantillonnage couvre la période de juin 2006 à juillet 2008, à raison d'une à deux fois par mois à la hauteur de la Ville de Québec. La concentration en nitrates est caractérisée par un fort signal saisonnier, avec des valeurs minimums en automne (< 15 μmol L^{-1}) et maximum au printemps et en hiver (> 30 μmol L^{-1}). Les valeurs de $\delta^{18}O\text{-}NO_3^-$ diminuent aussi pendant l'été et atteignent leur minimum en automne (≤ 3 ‰) pour, par la suite, augmenter pendant l'hiver pour atteindre leurs maximums en avril (> 6 ‰). Les valeurs de $\delta^{15}N\text{-}NO_3^-$ suivent un patron opposé, avec des valeurs maximums à la fin de l'été (> 7 ‰), qui persistent jusqu'à décembre et diminuent avec l'arrivée du printemps (< 4.5 ‰). Le $\delta^{18}O\text{-}NO_3^-$ et le $\delta^{15}N\text{-}NO_3^-$ sont négativement corrélés (R^2= 0.62) avec une pente de -1. La même relation existe entre la composition isotopique des nitrates pour chaque saison prise individuellement, exceptée pour l'automne, où aucune relation n'est observée. La corrélation négative entre le $\delta^{18}O\text{-}NO_3^-$ et le $\delta^{15}N\text{-}NO_3^-$ suggère que le fractionnement isotopique associé avec le processus de réduction des nitrates n'est pas le principal facteur influençant la composition isotopique des nitrates dans le fleuve Saint-Laurent. De plus, l'absence de relation entre la valeur modélisée de $\delta^{18}O\text{-}NO_3^-$ et celle mesurée suggère que la signature isotopique des nitrates est fortement influencée par la signature des sources non nitrifiées, et donc, possiblement les apports atmosphériques. Nous concluons donc que la signature isotopique des nitrates est fortement influencée par la saisonnalité. Par contre, pour être en mesure de mieux contraindre l'estimation des différentes sources et leur flux nous aurions besoin d'un échantillonnage simultané des différents tributaires qui amènent les nitrates ainsi que les précipitations touchant le bassin versant.

Abstract

In the context of the observed hypoxia in the Lower St. Lawrence Estuary we measured the isotopic composition of nitrate in the St. Lawrence in order to identify nitrate sources and estimate the importance of in-stream cycling. We sampled biweekly from June 2006 to July 2008 in Quebec City. Nitrate concentrations of water samples are characterized by a strong annual cycle, with minimal values (< 15 μmol L^{-1}) in the fall and maximal values (> 30 μmol L^{-1}) in winter/spring. The $\delta^{18}O$-NO_3^- values also decrease over the summer to reach a minimum in the fall (3 ‰) and then increase over the winter to reach a maximum in April (> 6 ‰). $\delta^{15}N$-NO_3^- values follow the opposite pattern, with maximum values (> 7 ‰) at the end of the summer (August) which persist through December, and minimum values (< 4.5 ‰) in April. The anti-correlation between $\delta^{15}N$-NO_3^- and $\delta^{18}O$-NO_3^- suggests that the isotopic fractionation associated with removal processes is not the principal factor influencing the isotopic composition of nitrates in the St. Lawrence River. Also, the absence of relationship between modelled $\delta^{18}O$- NO_3^- and measured $\delta^{18}O$-NO_3^- suggests that nitrates isotopic signature in the St. Lawrence River system is heavily influenced by the signature of non-nitrified sources and thus, most probably from atmospheric inputs. We thus conclude that seasonal cycles are of major influence on the isotopic signature of nitrate in the St. Lawrence River. Also, in order to be able to better constraint the different nitrates sources and their respective fluxes we would need a synchronous sampling of the different tributaries that bring load of nitrates and of the precipitations in the watershed.

1. Introduction

Riverine transport of and processing of terrestrial nitrogen (N) is one of the major links between the terrestrial and marine/estuarine nitrogen cycles and exerts a strong influence on the productivity and biodiversity of the coastal marine ecosystem (Miyajima et al., 2009). Estuaries are particularly sensitive to terrestrial organic matter and nutrient inputs (Gearing & Pocklington, 1990), which can lead to high primary productivity, high organic matter (OM) deposition, and thus high OM remineralization rates. As a major nutrient, fixed (i.e. bio-available) N is responsible for most of estuarine eutrophication, and thus for the health of coastal marine ecosystems (Nixon et al., 1996; Howarth, 1998; Howarth et al., 2006). Anthropogenic N inputs from agricultural and fossil fuel burning sources increased ten-fold globally since the late 19^{th} century, adding an enormous amount of fertilizing N to coastal waters (Galloway et al., 2004).

Recent studies in the Laurentian Channel have shown that approximately 1300 km^2 of the bottom sediments are now permanently exposed to hypoxic waters (Gilbert et al., 2005). Climate driven changes in ocean circulation patterns, which determine the partitioning of water masses that enter the Gulf of St. Lawrence from the North-Atlantic through Cabot Strait may have contributed to the historic decline in dissolved oxygen (DO) Lower St. Lawrence estuary (LSLE) during the last decades (Gilbert et al. 2005; Thibodeau et al., GRL, submitted). However, estuarine eutrophication, enhancing surface water primary productivity and organic particle fluxes, has also cause recent changes in the St. Lawrence estuarine DO budget

(Benoit et al., 2006; Thibodeau et al., 2006). The observed eutrophication-driven decline in oxygen content in the LSLE bottom waters appears to be directly related to a 70% increase in the amount of fertilizers sold in the St. Lawrence watershed between 1970 and 1988 (Thibodeau et al., 2006). Hence, it is reasonable to assume that anthropogenic inputs of N, besides climatic/oceanographic constraints, play an important role in the generation and maintenance of hypoxic conditions in the LSLE. While we know that the major sources of nitrate in large catchments are generally from agricultural areas (artificial fertilizer and manure), soils, and atmospheric precipitation, the importance of the various N contamination sources to the St. Lawrence system is poorly constrained, and the relative contribution of those sources can be expected to vary with time. Efficient measures to preserve water quality of an aquatic system such as the St. Lawrence River and Estuary require the identification of the main fixed nitrogen sources and the fate of nitrogen within this system (i.e, in-stream cycling through assimilation, denitrification, remineralization and nitrification).

Nitrate N isotopes ($\delta^{15}N\text{-}NO_3^-$), and more recently nitrate O isotopes ($\delta^{18}O\text{-}NO_3^-$) have proven to be excellent tracers of nitrate sources. The "dual isotope approach" is based on the fact the nitrate from commercial fertilizers, from manure, from soils, or from atmospheric precipitation has distinct isotopic signatures that characterize the different origins (see Kendall et al., 2007 for a review). For example, inorganic fertilizers show significantly higher $\delta^{18}O$ values as compared to most other

nitrate sources, whereas its $\delta^{15}N$ value is generally much lower than the $\delta^{15}N$ of nitrate derived from organic sources (Amberger and Schmidt, 1987). The $\delta^{18}O$ and $\delta^{15}N$ values for riverine nitrate are, however, not only modulated by the isotopic composition of the nitrate loading. In addition it depends on the isotope fractionation during (1) in-stream removal processes such as denitrification and assimilation, and (2) in-stream nitrification (i.e. production of nitrates with a different isotopic signature than pre-formed nitrates) (Figure 1) (Miyajima et al., 2009). The combined N and O isotope analysis of nitrate allows the assessment of co-occurring processes such as nitrification and denitrification that may have a cancelling effect on the nitrate concentration and $\delta^{15}N\text{-}NO_3^-$ alone (Burns & Kendall, 2002; Mayer et al., 2002; Kendall et al., 2007; Burns et al., 2009). Nitrification results in newly produced nitrate with a $\delta^{18}O$ that is modulated by the ambient water isotopic composition (Casciotti et al. 2002; 2007; Sigman 2009). Seasonally-driven variation in the $\delta^{18}O$ of river water should hence leave its imprint in the $\delta^{18}O$ of the nitrate that has been regenerated in-stream.

Here we present 42 measurements of dual nitrate isotopes from the St. Lawrence River at its outlet (Quebec City) from June 2006 to July 2008. We use the data to identify nitrate sources to the LSLE and to evaluate the role of in-stream nitrate cycling. We compare the nitrate-$\delta^{18}O$ with a $\delta^{18}O\text{-}H_2O$ dataset obtained from the same location during the same time interval, in order to assess to which extent natural $\delta^{18}O$ variations of the stream water can modulate variations in the isotopic

composition of the riverine nitrate pool, and how, in turn, information on in-stream-nitrate regeneration can be gained from these observations.

2. Methods

Dissolved nitrate concentrations were determined at GEOTOP using a Braan and Luebbe autoanalyzer, with a detection limit of ~0.1 μmol L^{-1} (Strickland & Parsons, 1972). Stable N and O isotope ratios of dissolved nitrates ($\delta^{15}N$, $\delta^{18}O$) were measured using the denitrifier method (Sigman et al., 2001; Casciotti et al., 2002). Here, sample nitrate (and nitrite) is converted to nitrous oxide (N_2O) by denitrifying bacteria that lack N_2O reductase activity (*Pseudomonas chlororaphis* ATCC #43928 or ATCC #13985). The N_2O is then stripped from the sample vial with helium as carrier gas, cryo-concentrated, purified using a Micromass TraceGas™ and analyzed for its N and O isotopic composition with a Micromass Isoprime™ universal triple collector isotope ratio mass spectrometer in continuous flow mode. Blank contribution was generally lower than 0.3 nmol (~1.5% of sample). For $\delta^{18}O$ isotope analyses, only *P. chloroaphis* ATCC #13985 was used. O-isotope exchange with the ambient water during N_2O production leads to an $d^{18}O$-scale compression, which we corrected for according to Casciotti et al. 2002. O-isotope exchange was never higher than 5%. Based on replicate measurements of laboratory standards and samples (intra- and inter-run), the reproducibility of $\delta^{15}N$ and $\delta^{18}O$ was better than ±0.3‰ (1σ) and ±0.5‰ (1σ), respectively. Isotopic values were calibrated using

IAEA-N3, an international KNO_3 reference material with an assigned $\delta^{15}N$ value of +4.7‰ relative to atmospheric N_2 (Gonfiantini et al., 1995) and a $\delta^{18}O$ value of +25.6‰ relative to V-SMOW (Bohlke et al., 2003). All isotope measurements are reported in the delta notation in permil (‰), relative to atmospheric N2 (AIR) for $\delta^{15}N$ and V-SMOW for $\delta^{18}O$.

Water was analyzed for its ^{18}O content at the GEOTOP research centre on water sampled in 60 ml plastic bottles entirely filled and stored at 4°C. 100 µl of unfiltered water were equilibrated with 50 to 100 µl of CO2 gas at 40°C in vials previously purged with He gas. Equilibration time ranged from 12 to 24 hours. Equilibrated CO_2 gas was then sampled and diverted through the isotope ratio mass spectrometer. The resulting isotopic values were corrected for any apparent drift and corrected to their absolute values using international standards (V-SMOW and SLAP) and/or with internal lab standards calibrated against international standards. Data were also temperature corrected and equilibration isotope effect was taken into account. Every water sample was equilibrated in three different vials and the mean isotopic value was calculated. The overall analytical uncertainty was ± 0.1 ‰.

3. Regional settings

All samples were taken from a pumping facility of a water filtration plant on the south shore of the St. Lawrence River (SLR) at its outlet to the upper SLE (see Hélie & Hillaire-Marcel, 2006 for methods). Here, the SLR water represents a mixture of various water sources originating from the Great Lakes and down-stream tributaries, such as the Ottawa River (Figure 2). The discharge from Lake Ontario

does not display significant seasonal variations. In contrast, discharge from the tributaries is strongly modulated by seasonal hydrological cycle. During spring snowmelt, outflow rates are three times higher compared to the mean annual discharge (Environment Canada, unpublished data). Hence, the contribution from Great Lake water to the total discharge at Quebec City varies from > 70 % in summer to < 55 % in spring (Environment Canada, unpublished data). Baseflow conditions can be assumed for the summer months. The watershed is composed of different eco- and land use zones, i.e., boreal and mixed forests, as well as agricultural and urban areas (Figure 2).

4. Results

Nitrate variations display a strong annual cyclicity, with minimal concentrations (< 15 μmol L^{-1}) in fall and maximum concentrations (> 30 μmol L^{-1}) in winter/spring (Figure 3). The $\delta^{15}N\text{-}NO_3^-$ values increase over the summer to reach a maximum in the fall (> 7 ‰) and decrease during the winter months to reach a minimum in April (< 4.5 ‰; Figure 3). $\delta^{18}O\text{-}NO_3^-$ values follow an opposite pattern, with minimum values (< 3 ‰) at the end of the summer (August), which persist through December, and highest values (> 6 ‰) in April (Figure 3). As a consequence, $\delta^{18}O\text{-}NO_3^-$ and $\delta^{15}N\text{-}NO_3^-$ show a clear negative correlation (R^2= 0.62; Figure 4), with and anti-proportionality factor of -1. The observed co-variance between $\delta^{18}O\text{-}NO_3^-$ and $\delta^{15}N\text{-}NO_3^-$ is similar for every season (individual plots not shown) except in fall,

when no apparent relationship between N and O isotope ratios can be discerned. Strong intra seasonal variability is observed in the spring but seems to be of less importance during other seasons (Table 1). Except for spring and winter, mean [NO_3^-], $\delta^{15}N\text{-}NO_3^-$ and $\delta^{18}O\text{-}NO_3^-$ show distinct, discernible isotope signatures.

5. Discussion

5.1 In-stream removal processes

Denitrification refers to the dissimilatory reduction of NO_3^- to gaseous products (N_2, N_2O, or NO) and usually occurs only where O_2 concentrations are less than 20 μM (Kendall et al., 2007). Denitrification causes the $\delta^{15}N$ and $\delta^{18}O$ values of the residual nitrate pool to increase exponentially as nitrate concentrations decreases (Kendall et al., 2007). Measured enrichment factors are variable and range from 10 to 40 ‰ with a $\delta^{18}O/\delta^{15}N$ ratio of 0.5 to 1 (Böttcher et al., 1990; Cey et al., 1999; Granger et al., 2004a; Panno et al., 2006). The extent of measured fractionation will depend on the environmental conditions, while the full fractionation linked to water column denitrification is expressed in the isotopic composition of residual NO_3^-, the sedimentary denitrification expression is limited (to 0-3 ‰) by sedimentary diffusion processes (Lehmann et al., 2004; Sigman et al., 2005; Lehmann et al., 2007). While denitrification in the water column should not play a role in the St. Lawrence, closed system conditions are often prevalent in anaerobic soil compartments, along the groundwater flow path in aquifers and riparian zones, and occasionally in river

sediments (Kellman & Hillaire-Marcel, 1998; Sebilo et al., 2003). Nitrate that has undergone partial denitrification in these watershed compartments should, therefore, have elevated $\delta^{15}N$ and $\delta^{18}O$ values and lowered concentrations compared to input values.

The present dataset is characterized by a significant negative correlation between $\delta^{15}N\text{-}NO_3^-$ and $\delta^{18}O\text{-}NO_3^-$, and both $\delta^{15}N\text{-}NO_3^-$ and $\delta^{18}O\text{-}NO_3^-$ are not correlated with nitrate concentrations which, suggest that observed isotopic variations throughout the year cannot be attributed to removal processes but rather to mixing. Although denitrification within the system cannot be excluded, the $\delta^{18}O\text{-}NO_3^-$ and $\delta^{15}N\text{-}NO_3^-$ data presented here do not carry the isotopic signature of such process. It cannot per se be argued, that denitrification is not significant in the St. Lawrence River. Rather, the isotopic fractionation linked to those processes may be overprinted by stronger signals, possibly due to external N loading. The missing anti-correlation between nitrate concentration and isotope ratios could also be due to denitrification occurring under limited diffusion conditions (i.e. in the sediment), which would limit the expression of the isotopic fractionation (Lehmann et al., 2007).

Another removal process that is known to discriminates between nitrogen isotopes is the assimilation of inorganic nitrogen compounds into organic form during biosynthesis by living organisms (Altabet et al., 1999). It can produce a large range of N fractionation (0-30 ‰) with a strongly coupled ratio of 1:1 between N and O fractionation (Granger et al., 2004b). Thus again, the anti-correlation between $\delta^{18}O$-

NO_3^- and $\delta^{15}N\text{-}NO_3^-$ data suggest that either assimilation is not present, or is overprinted by other fractionating processes. Hélie and Hillaire-Marcel (2006) demonstrated that particulate organic carbon at the sampling station was mainly of autochthonous origin, which confirm the importance of primary productivity which, in turn, implies assimilation of nitrate by algae being important. We thus conclude that the isotopic signal of assimilation is overprinted by a stronger signal of source mixing or by the remineralization cycle signature.

5.2 In-stream production of nitrate

During production of nitrate by nitrification the $\delta^{15}N$ and $\delta^{18}O$ of new nitrate are affected in different ways (Bourbonnais et al., 2009). The N–isotopic composition of nitrates produced in-stream by nitrification is principally constrained by the $\delta^{15}N$ of the organic matter subject to remineralization (Miyajima et al., 2009). The aerobic mineralization of organic matter is usually accompanied by small isotope fractionation, and results in ammonium with a 0-4 ‰ lower $\delta^{15}N$ than the bulk original organic matter (Lehmann et al., 2002; Dijkstra et al., 2008). Nitrification of ammonium to nitrate is associated with large isotopic discriminations (14-38‰; Casciotti et al., 2003), although this process may be difficult to observe in river systems when remineralization and nitrification proceed nearly at steady state and to completion (i.e. with no ammonium accumulation) (Miyajima et al., 2009), which should be the case in the SLR. Thus, we can expect that nitrate from nitrification will

have a $\delta^{15}N$ lower or equal (of about 0-4 ‰) to the $\delta^{15}N$ of the particulate organic matter (Table 2). While it is still a matter of debate as to what exactly controls the $\delta^{18}O$ of nitrate from nitrification (see Kendall et al., 2007 for a review), it was recently assumed that the $\delta^{18}O$ value of newly nitrified nitrate in marine environment is enriched of ~2‰, compared to the $\delta^{18}O$ of ambient water, which imply that the $\delta^{18}O$ of dissolved O_2 have almost no effect on the $\delta^{18}O$ of the resulting nitrate (Casciotti et al., 2002; Wankel et al., 2006; Wankel et al., 2007; Knapp et al., 2008; Bourbonnais et al., 2009). This contrasts with the previous conception that $\delta^{18}O\text{-}NO_3^-$ could be view as the results of a mixture of two oxygen atoms from H_2O and one from dissolved O_2 (Hollocher, 1984; Böttcher et al., 1990; Kendall, 1998).

Values of $\delta^{18}O\text{-}H_2O$ at Quebec City are characterized by a clear seasonal cycle, with ^{18}O-depleted values during the spring due to snowmelt and more ^{18}O enriched values in the fall (Myre, 2006). This seasonal pattern is driven by seasonal variations observed in the $\delta^{18}O\text{-}H_2O$ of precipitation which is due to the temperature-dependent fractionation occurring during condensation of water in air masses (Dansgaard, 1964). Snowmelt events thus represent an input of the ^{18}O-depleted precipitation that was stocked on land during winter. Since we have access to both $\delta^{18}O\text{-}O_2$ (collected in 2000-2001 by Hélie, unpublished results) and $\delta^{18}O\text{-}H_2O$ measurements we can model the theoretical isotopic composition of nitrate produced by nitrification, for both $\delta^{18}O$ hypothesis. $\delta^{18}O\text{-}O_2$ values were mostly constant throughout the year (22.0 ± 0.9 ‰) they were thus considered constant in the

equation (1) which allowed us to model nitrate produced by nitrification considering an effect from the $\delta^{18}O\text{-}O_2$.

$$\delta^{18}O\text{-}NO_3^- = 2/3(\delta^{18}O\text{-}H_2O) + 1/3(\delta^{18}O\text{-}O_2) \quad (1)$$

This calculation was applied to the 7 samples for which we measured $\delta^{15}N$ on particulate organic matter (Table 2). The mean difference between measured and modelled $\delta^{18}O\text{-}NO_3^-$ for those 7 samples is 2.8 ± 1.5 ‰ (Figure 6), with maximum difference in winter and spring (> 2.7) and minimum in summer and fall (2.0). To test the second hypothesis we simply added 2 ‰ to the $\delta^{18}O\text{-}H_2O$ values of each samples (Table 2). This yielded much lower modelled $\delta^{18}O\text{-}NO_3^-$ than equation (1), as illustrated by the mean difference of 11.1 ± 1.9 ‰ between measured and modelled $\delta^{18}O\text{-}NO_3^-$ (Figure 6). On the other hand, the difference is still higher in winter and spring (> 11.4) compared to summer and fall (10.4). The maximum difference in winter and spring could indicate that either there are major inputs of heavy $\delta^{18}O\text{-}NO_3^-$ in those seasons or that removal processes like assimilation are more active during those period of the year. But as discussed previously, removal processes do not seems to be the major influence on the nitrate isotopic composition as shown by the anti-correlation between $\delta^{18}O\text{-}NO_3^-$ and $\delta^{15}N\text{-}NO_3^-$, thus leaving the sources signal as the most probable driver of the observed variations in nitrate isotopic composition.

5.3 Inputs of nitrate

There are various potential sources of nitrates in riverine systems, including i) nitrates derived from natural N_2 fixation followed by remineralization and nitrification in the watershed soils, ii) nitrates derived from atmospheric deposition of nitrogen oxides in the watershed and iii) anthropogenic nitrates derived from manure, inorganic fertilizers, septic and animal wastes, and domestic and industrial wastewaters. Each pool of nitrate is characterized by specific values of $\delta^{15}N$ and $\delta^{18}O$ values (Kendall et al., 2007). Nitrates derived from manure, septic and animal waste, as well as domestic waste typically display high $\delta^{15}N$ (+10 ‰ or higher; McClelland & Valiela, 1998; Bedard-Haughn et al., 2003). Since nitrates from these sources are produced via nitrification, the resulting $\delta^{18}O$ should follow the same trend that the measured $\delta^{18}O$-H_2O, since in both model the $\delta^{18}O$-NO_3^- produced by nitrification is mostly constrained by it (Miyajima et al., 2009), which we do not observe. Synthetic fertilizers are characterized by low $\delta^{15}N$-NO_3^- (0-5‰). The $\delta^{18}O$-NO_3^- derives from artificial N fertilizers will depend on whether they are applied in reduced form (ammonium) or directly as nitrate, since the subsequent nitrification of ammonium will lead to a $\delta^{18}O$-NO_3^- dependant to that of ambient water, while fertilizer under nitrate form will carry a $\delta^{18}O$-NO_3^- that is in general significantly higher (~20‰). Thus, the high $\delta^{18}O$-NO_3^- observed in the spring could come from an increased contribution of the nitrate fertilizers, Nevertheless, this type of fertilizer is the less

used by farmers in Quebec (Agriculture and Agri-Food Canada, 2002). Nitrates from atmospheric depositions are heavily enriched in ^{18}O ($\delta^{18}O > 60$ ‰; Kendall et al., 2007). In the area surrounding the Great Lakes and the St. Lawrence River watershed, Kendall (2007) has measured $\delta^{15}N\text{-}NO_3^-$ in precipitation ranging from -3.4 to +0.6 ‰. Hence, nitrates from precipitation yield higher $\delta^{18}O\text{-}NO_3^-$ and lower $\delta^{15}N\text{-}NO_3^-$ than the nitrates values observed in the SLR on average. Yet, it is possible that the increase in $\delta^{18}O\text{-}NO_3^-$ concomitant with $\delta^{15}N\text{-}NO_3^-$ decrease is due to an elevated contribution of N from atmospheric precipitation due to the spring snowmelt.

6. Conclusion

The anti-correlation between $\delta^{15}N\text{-}NO_3^-$ and $\delta^{18}O\text{-}NO_3^-$ suggests that the isotopic fractionation associated with removal processes is not the principal factor influencing the isotopic composition of nitrates in the St. Lawrence River. Also, the absence of relationship between measured $\delta^{18}O\text{-}H_2O$ and measured $\delta^{18}O\text{-}NO_3^-$ suggests that nitrates isotopic signature in the St. Lawrence River system is heavily influenced by the signature of non-nitrified sources. Both models we used to calculate theoretical value of $\delta^{18}O\text{-}NO_3^-$ produced by nitrification highlight this absence of relationship. This suggests that the observed variations in nitrate isotopic composition could be due to variations in the origin and the mixing of the sources of nitrate. The temporal variation in the difference between modelled and measured $\delta^{18}O\text{-}NO_3^-$ suggests that spring is the season when the St. Lawrence receive a greatest proportion

of a source characterized by high $\delta^{18}O\text{-}NO_3^-$ and low $\delta^{15}N\text{-}NO_3^-$. Spring is characterized by intense snowmelt, thus atmospheric nitrates stocked in snowpack are added to the riverine nitrate pool, which might be one of the cause of the elevated $\delta^{18}O\text{-}NO_3^-$ and low $\delta^{15}N\text{-}NO_3^-$. $\delta^{15}N\text{-}NO_3^-$ and $\delta^{18}O\text{-}NO_3^-$ observed in the summer (baseflow conditions) are characterized by the isotopic signature of soil nitrates (or a mix of manure, sewage, etc.) and value closer to what should be the $\delta^{18}O\text{-}NO_3^-$ value of nitrate produced in-stream. We thus conclude that seasonal cycles are of major influence on the isotopic signature of nitrate in the St. Lawrence River. Also, isotopic signature of nitrate in baseflow condition could be the results of a mixing of different sources of nitrates, thus in order to be able to better constrain the different nitrates sources and their respective fluxes, we would need a synchronous sampling of the different tributaries that bring load of nitrates and of the precipitations in the watershed. Also, a better coverage of the time-series with $\delta^{15}N$ of particulate organic matter would allow us to better constrain the exact importance of nitrate production in-stream.

References

Agriculture and AgriFood Canada (2002) Canadian Fertilizer Consumption, Shipments and Trade 2001-2002.

Altabet MA, Pilskaln C, Thunell R, Pride C, Sigman D, Chavez F & Francois R (1999) The nitrogen isotope biogeochemistry of sinking particles from the margin of the eastern North Pacific. Deep-Sea Research Part I: Oceanographic Research Papers 46: 655-679

Bedard-Haughn A, van Groenigen JW & van Kessel C (2003) Tracing ^{15}N through landscapes: potential uses and precautions. Journal of Hydrology 272: 175-190
Benoit P, Gratton Y & Mucci A (2006) Modeling of dissolved oxygen levels in the bottom waters of the Lower St. Lawrence Estuary: coupling of benthic and pelagic processes. Marine Chemistry 102: 13-32

Bohlke JK, Mroczkowski SJ & Coplen TB (2003) Oxygen isotopes in nitrate: New reference materials for ^{18}O:^{17}O:^{16}O measurements and observations on nitrate-water equilibration. Rapid Communications in Mass Spectrometry 17: 1835-1846

Böttcher J, Strebel O, Voerkelius S & Schmidt HL (1990) Using isotope fractionation of nitrate-nitrogen and nitrate-oxygen for evaluation of microbial denitrification in a sandy aquifer. Journal of Hydrology 114: 413-424

Bourbonnais A, Lehmann MF, Waniek JJ & Schulz-Bull DE (2009) Nitrate isotope anomalies reflect N_2 fixation in the Azores Front region (subtropical N-E Atlantic). Journal of Geophysical Research 114: C03003, doi:03010.01029/02007JC004617

Burns DA, Boyer EW, Elliott EM & Kendall C (2009) Sources and transformations of nitrate from streams draining varying land uses: Evidence from dual isotope analysis. Journal of Environmental Quality 38: 1149-1159

Burns DA & Kendall C (2002) Analysis of $\delta^{15}N$ and $\delta^{18}O$ to differentiate NO_3^- sources in runoff at two watersheds in the Catskill Mountains of New York. Water Resources Research 38: 91-912

Casciotti KL, Sigman DM, Hastings MG, Böhlke JK & Hilkert A (2002) Measurement of the oxygen isotopic composition of nitrate in seawater and freshwater using the denitrifier method. Analytical Chemistry 74: 4905-4912

Casciotti KL, Sigman DM & Ward BB (2003) Linking diversity and stable isotope fractionation in ammonia-oxidizing bacteria. Geomicrobiology Journal 20: 335-353

Cey EE, Rudolph DL, Aravena R & Parkin G (1999) Role of the riparian zone in controlling the distribution and fate of agricultural nitrogen near a small stream in southern Ontario. Journal of Contaminant Hydrology 37: 45-67

Dansgaard W (1964) Stable isotopes in precipitation. Tellus 16: 436-468

Dijkstra P, Laviolette CM, Coyle JS, Doucett RR, Schwartz E, Hart SC & Hungate BA (2008) ^{15}N enrichment as an integrator of the effects of C and N on microbial metabolism and ecosystem function. Ecology Letters 11: 389-397

Galloway JN, Dentener FJ, Capone DG, Boyer EW, Howarth RW, Seitzinger SP, Asner GP, Cleveland CC, Green PA, Holland EA, Karl DM, Michaels AF, Porter JH, Townsend AR & Vöosmarty CJ (2004) Nitrogen Cycles: Past, Present, and Future. Biogeochemistry 70: 153-226

Gearing JN & Pocklington R (1990) Organic geochemical studies in the St. Lawrence Estuary. In: El-Sabh MI & Silverberg N (Eds) Oceanography of a large-scale estuarine system, the St.-Lawrence Coastal and estuarine studies pp 170–201). Springer-Verlag, New York

Gilbert D, Sundby B, Gobeil C, Mucci A & Tremblay GH (2005) A seventy-two-year record of diminishing deep-water oxygen in the St. Lawrence estuary: The northwest Atlantic connection. Limnology and Oceanography 50: 1654-1666

Gonfiantini R, Stichler W & Rozanski K (1995) Standards and intercomparison materials distributed by the International Atomic Energy Agency for stable isotope measurements. Proceedings of a consultants meeting pp 13–29). International Atomic Energy Agency, Vienna, Austria

Granger J, Sigman DM, Lehmann MF & Tortell PD (2004a) Nitrogen and oxygen isotope effects associated with nitrate assimilation and denitrification by laboratory cultures of marine plankton. Eos Trans. AGU 85

Granger J, Sigman DM, Needoba JA & Harrison PJ (2004b) Coupled nitrogen and oxygen isotope fractionation of nitrate during assimilation by cultures of marine phytoplankton. Limnology and Oceanography 49: 1763-1773

Hélie JF & Hillaire-Marcel C (2006) Sources of particulate and dissolved organic carbon in the St Lawrence River: Isotopic approach. Hydrological Processes 20: 1945-1959

Hollocher TC (1984) Source of the oxygen atoms of nitrate in the oxidation of nitrite by Nitrobacter agilis and evidence against a PON anhydride mechanism in oxidative phosphorylation. Archives of Biochemistry and Biophysics 233: 721-727

Howarth RW (1998) An assessment of human influences on fluxes of nitrogen from the terrestrial landscape to the estuaries and continental shelves of the North Atlantic Ocean. Nutrient Cycling in Agroecosystems 52: 213-223

Howarth RW, Swaney DP, Boyer EW, Marino R, Jaworski N & Goodale C (2006) The influence of climate on average nitrogen export from large watersheds in the Northeastern United States. Biogeochemistry 79: 163-186

Kellman L & Hillaire-Marcel C (1998) Nitrate cycling in streams: Using natural abundances of NO_3^- $\delta^{15}N$ to measure in-situ denitrification. Biogeochemistry 43: 273-292

Kendall C (1998) Tracing nitrogen sources and cycling in catchments. Isotope Tracers in Catchment Hydrology: 519-576

Kendall C, Elliott EM & Wankel SD (2007) Tracing anthropogenic inputs of nitrogen to ecosystems. Stable Isotopes in Ecology and Environmental Science: 375-449

Knapp AN, DiFiore PJ, Deutsch C, Sigman DM & Lipschultz F (2008) Nitrate isotopic composition between Bermuda and Puerto Rico: Implications for N_2 fixation in the Atlantic Ocean. Global Biogeochemical Cycles 22: art. no. GB3014

Lehmann MF, Bernasconi SM, Barbieri A & McKenzie JA (2002) Preservation of organic matter and alteration of its carbon and nitrogen isotope composition during simulated and in situ early sedimentary diagenesis. Geochimica et Cosmochimica Acta 66: 3573-3584

Lehmann MF, Sigman DM & Berelson WM (2004) Coupling the $^{15}N/^{14}N$ and $^{18}O/^{16}O$ of nitrate as a constraint on benthic nitrogen cycling. Marine Chemistry 88: 1-20

Lehmann MF, Sigman DM, McCorkle DC, Granger J, Hoffmann S, Cane G & Brunelle BG (2007) The distribution of nitrate $^{15}N/^{14}N$ in marine sediments and the impact of benthic nitrogen loss on the isotopic composition of oceanic nitrate. Geochimica et Cosmochimica Acta 71: 5384-5404

Mayer B, Boyer EW, Goodale C, Jaworski NA, Van Breemen N, Howarth RW, Seitzinger S, Billen G, Lajtha K, Nadelhoffer K, Van Dam D, Hetling LJ, Nosal M &

Paustian K (2002) Sources of nitrate in rivers draining sixteen watersheds in the northeastern U.S.: Isotopic constraints. Biogeochemistry 57-58: 171-197

McClelland JW & Valiela I (1998) Linking nitrogen in estuarine producers to land-derived sources. Limnology and Oceanography 43: 577-585

Miyajima T, Yoshimizu C, Tsuboi Y, Tanaka Y, Tayasu I, Nagata T & Koike I (2009) Longitudinal distribution of nitrate $\delta^{15}N$ and $\delta^{18}O$ in two contrasting tropical rivers: implications for instream nitrogen cycling. Biogeochemistry: 1-18

Myre A (2006) Isotopic monitoring (^{2}H and ^{18}O) of the St. Lawrence and Ottawa rivers from 1997 to 2003 - Linkages with seasonal and interannual hydroclimatc variability. (p 81). Université du Québec à Montréal, Montreal

Nixon SW, Ammerman JW, Atkinson LP, Berounsky VM, Billen G, Boicourt WC, Boynton WR, Church TM, Ditoro DM, Elmgren R, Garber JH, Giblin AE, Jahnke RA, Owens NJP, Pilson MEQ & Seitzinger SP (1996) The fate of nitrogen and phosphorus at the land-sea margin of the North Atlantic Ocean. Biogeochemistry 35: 141-180

Panno SV, Hackley KC, Kelly WR & Hwang HH (2006) Isotopic evidence of nitrate sources and denitrification in the Mississippi River, Illinois. Journal of Environmental Quality 35: 495-504

Sebilo M, Billen G, Grably M & Mariotti A (2003) Isotopic composition of nitrate-nitrogen as a marker of riparian and benthic denitrification at the scale of the whole Seine River system. Biogeochemistry 63: 35-51

Sigman DM, Casciotti KL, Andreani M, Barford C, Galanter M & Böhlke JK (2001) A bacterial method for the nitrogen isotopic analysis of nitrate in seawater and freshwater. Analytical Chemistry 73: 4145-4153

Sigman DM, Granger J, DiFiore PJ, Lehmann MM, Ho R, Cane G & van Geen A (2005) Coupled nitrogen and oxygen isotope measurements of nitrate along the eastern North Pacific margin. Global Biogeochemical Cycles 19: GB4022.doi:4010.1029/2005GB002458

Silva SR, Ging PB, Lee RW, Ebbert JC, Tesoriero AJ & Inkpen EL (2002) Forensic Applications of Nitrogen and Oxygen Isotopes in Tracing Nitrate Sources in Urban Environments. Environmental Forensics 3: 125-130

Strickland JDH & Parsons TR (1972) A pratical handbook of seawater analysis. Bulletin Fisheries Research Board of Canada 167: 207-211

Thibodeau B, de Vernal A & Mucci A (2006) Recent eutrophication and consequent hypoxia in the bottom waters of the Lower St. Lawrence Estuary: Micropaleontological and geochemical evidence. Marine Geology 231: 37-50

Wankel SD, Kendall C, Francis CA & Paytan A (2006) Nitrogen sources and cycling in the San Francisco Bay estuary: A nitrate dual isotopic composition approach. Limnology and Oceanography 51: 1654-1664

Wankel SD, Kendall C, Pennington JT, Chavez FP & Paytan A (2007) Nitrification in the euphotic zone as evidenced by nitrate dual isotopic composition: Observations from Monterey Bay, California. Global Biogeochemical Cycles 21

Figure captions

Figure 1. Conceptual model of nitrate inputs and outputs in the St. Lawrence River at its outlet to the estuary. Dashed line represents reactions with isotopic fractionation. Isotopic values are in permil vs. air for $\delta^{15}N$ and vs. V-SMOW for $\delta^{18}O$. (inspired from Miyajima et al., 2009)

Figure 2. Map representing the land use in the Great lakes and St. Lawrence watershed.

Figure 3. a) Nitrate concentrations and b) nitrate isotope ratios ($\delta^{15}N$: solid line; $\delta^{18}O$: dashed line) from June 2006 to July 2008.

Figure 4. Plot of nitrate $\delta^{15}N$ vs. $\delta^{18}O$ for all the samples collected.

Figure 5. Measurements of nitrate $\delta^{18}O$ with modelled nitrate $\delta^{18}O$ with equation (1) (triangles) and without considering O_2 effect (dots).

Figure 6. Plot of nitrates $\delta^{15}N$ and $\delta^{18}O$ (in permil) for all samples and typical values for the different possible end-members. The dashed line represents the average modelled nitrates $\delta^{18}O$ from nitrification using equation (1). $\delta^{18}O$ value range for reduced-N fertilizers, soil organic N and sewage and manures are base on the average modelled nitrates $\delta^{18}O$ from nitrification.

Table captions

Table 1. Average nitrate concentrations (in μmol L^{-1}), $\delta^{18}O\text{-}NO_3^-$ and $\delta^{15}N\text{-}NO_3^-$ values by seasons with the standard deviation associated with each term.

Table 2. Measurements of $\delta^{15}N$ on the particulate organic matter (POM) for 7 dates. Also nitrate isotopic composition and $\delta^{18}O$ of the water for the same samples and modelled $\delta^{18}O$ value of nitrate with equation (1)[a] and with the addition of 2 ‰ to the $\delta^{18}O$ of the water[b].

*Data from the 07-03-2008, ** Data from the 02-07-2008.

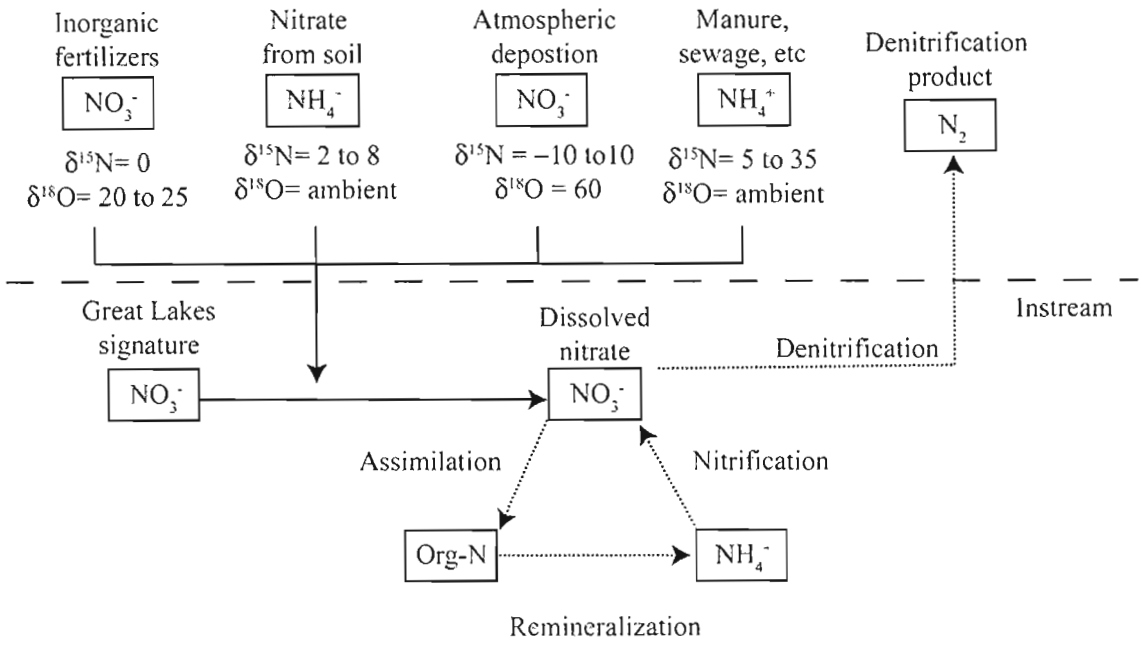
Inorganic fertilizers
NO3-
δ15N= 0
δ18O= 20 to 25
Nitrate from soil
NH4-
δ15N= 2 to 8
δ18O= ambient
Atmospheric depostion
NO3-
δ15N = −10 to10
δ18O = 60
Manure, sewage, etc
NH4+
δ15N= 5 to 35
δ18O= ambient
Denitrification product
N2
Great Lakes signature
NO3-
Dissolved nitrate
NO3-
Denitrification
Instream
Assimilation
Nitrification
Org-N
NH4-
Remineralization

Figure 1.

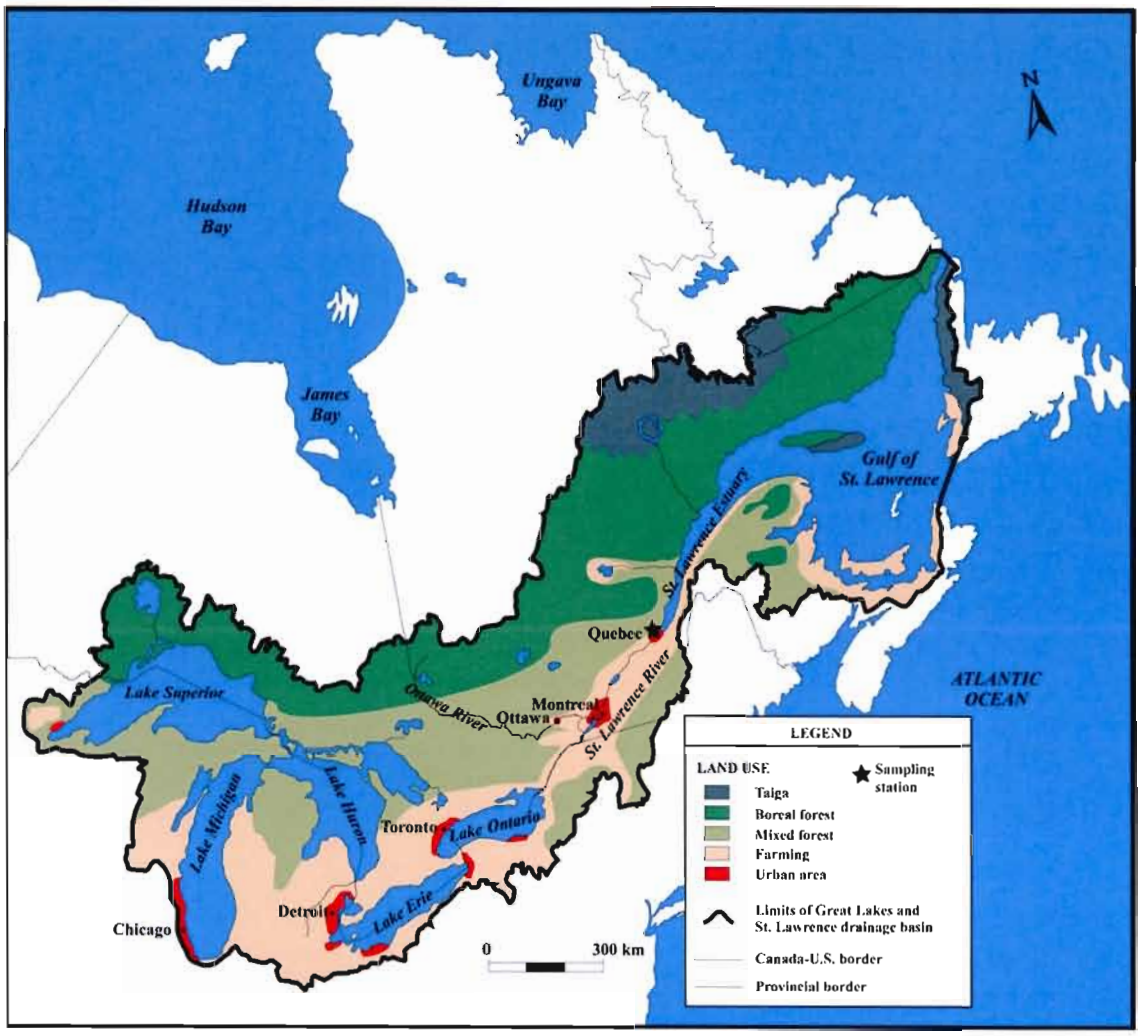
Ungava Bay
Hudson Bay
James Bay
Gulf of St. Lawrence
St. Lawrence Estuary
Quebec
ATLANTIC OCEAN
Lake Superior
Ottawa River
Montreal
Ottawa
St. Lawrence River
Lake Michigan
Lake Huron
Toronto
Lake Ontario
Detroit
Lake Erie
Chicago
0
300 km
N
LEGEND
LAND USE
Sampling station
Taiga
Boreal forest
Mixed forest
Farming
Urban area
Limits of Great Lakes and St. Lawrence drainage basin
Canada-U.S. border
Provincial border

Figure 2.

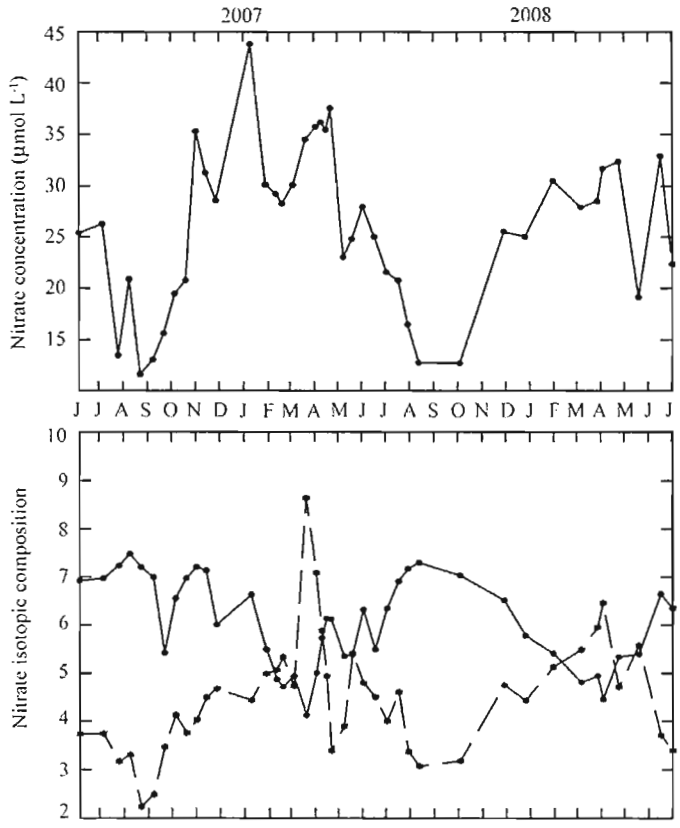
2007
2008
Nitrate concentration (µmol L-1)
45
40
35
30
25
20
15
J J A S O N D J F M A M J J A S O N D J F M A M J J
Nitrate isotopic composition
10
9
8
7
6
5
4
3
2

Figure 3.

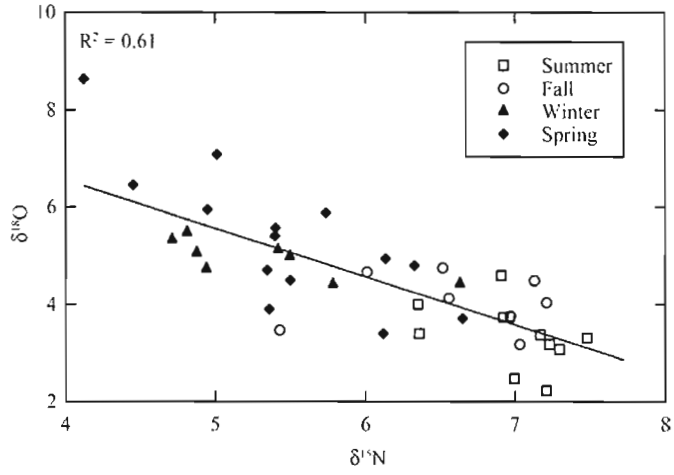

Figure 4.

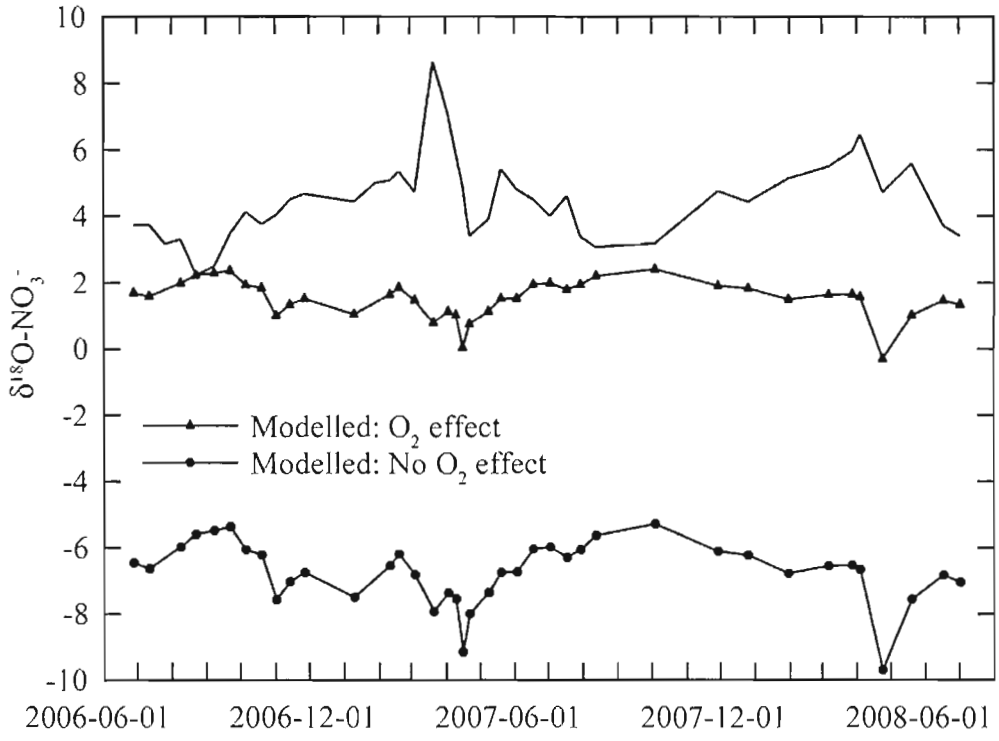
10
8
6
4
2
0
-2
-4
-6
-8
-10
$\delta^{18}O\text{-}NO_3^-$
Modelled: O_2 effect
Modelled: No O_2 effect
2006-06-01
2006-12-01
2007-06-01
2007-12-01
2008-06-01

Figure 5.

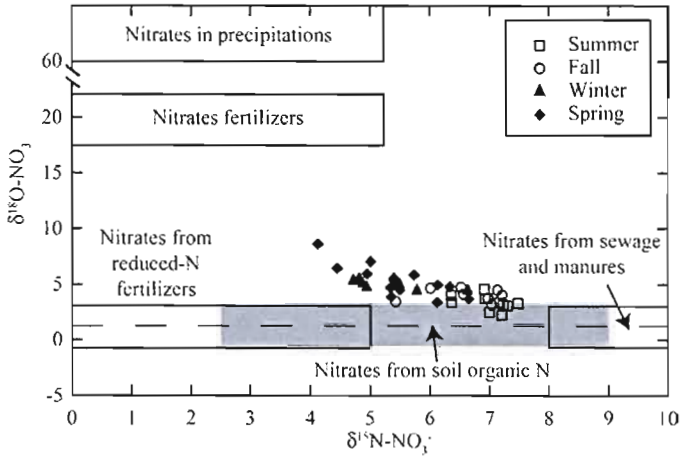
Nitrates in precipitations
Nitrates fertilizers
Nitrates from reduced-N fertilizers
Nitrates from sewage and manures
Nitrates from soil organic N
Summer
Fall
Winter
Spring
60
20
15
10
5
0
-5
0
1
2
3
4
5
6
7
8
9
10
δ18O-NO3
δ15N-NO3

Figure 6.

Season	NO_3^- concentration ($\mu mol\ L^{-1}$)	SD	$\delta^{15}N\text{-}NO_3^-$ (‰)	SD	$\delta^{18}O\text{-}NO_3^-$ (‰)	SD
Spring	30.4	5.7	5.5	0.7	5.4	1.4
Winter	30.6	5.6	5.3	0.6	5.0	0.4
Fall	23.7	7.9	6.6	0.6	4.1	0.6
Summer	18.6	5.3	7.0	0.4	3.4	0.7

Table 1. Average nitrate concentrations (in $\mu mol\ L^{-1}$), $\delta^{18}O\text{-}NO_3^-$ and $\delta^{15}N\text{-}NO_3^-$ values

by seasons with the standard deviation associated with each term.

Date	$\delta^{15}N$-POM (‰)	$\delta^{15}N$-NO_3^- (‰)	$\delta^{18}O$-NO_3^- (‰)	$\delta^{18}O$-H_2O (‰)	$^a\delta^{18}O$-NO_3^- (‰)	$^b\delta^{18}O$-NO_3^- (‰)
05-03-2007	2.9	4.9	4.7	-8.8	1.4	-6.8
23-04-2007	3.4	6.1	3.4	-10.0	0.7	-8.0
30-07-2007	3.9	7.2	3.4	-8.1	1.9	-6.1
19-10-2007	4.5	7.0	3.2	-7.3	2.4	-5.3
28-02-2008	1.5	4.8*	5.5*	-8.6	1.6	-6.6
24-04-2008	2.9	5.3	4.7	-11.7	-0.5	-9.7
16-07-2008	3.9	6.4**	3.4**	-9.0	1.3	-7.0

Table 2. Measurements of $\delta^{15}N$ on the particulate organic matter (POM) for 7 dates. Also nitrate isotopic composition and $\delta^{18}O$ of the water for the same samples and modelled $\delta^{18}O$ value of nitrate with equation (1)[a] and with the addition of 2 ‰ to the $\delta^{18}O$ of the water[b].

*Data from the 07-03-2008, ** Data from the 02-07-2008.

CONCLUSION

Les résultats présentés dans cette thèse s'articulent autour du développement récent de l'hypoxie dans l'estuaire maritime du Saint-Laurent (Gilbert et al., 2005) qui risque de constituer un problème majeur pour l'écosystème. Déjà l'influence d'une diminution du taux d'oxygénation sur les communautés benthiques a été mise en évidence dans l'estuaire et le golfe (Belley et al., 2010) et une diminution de la diversité de ces communautés a été observée depuis quelques décennies (Bourque et al., 2009). De plus, des conséquences sur les pêcheries sont probables, notamment en raison de l'effet migratoire engendré par la présence de la zone hypoxie. Par exemple, cela pourrait avoir joué un rôle important dans le déclin de la morue et du sébaste observé par Sirois et al. (2009) dans le fjord du Saguenay. Aussi, les espèces redox sensibles piégées dans le sédiment, dont certaines sont toxiques, peuvent être relâchées par le sédiment lorsque la concentration d'oxygène dissous diminue. Par exemple, des résultats préliminaires suggèrent que le flux d'arsenic provenant du sédiment a augmenté avec le déclin des concentrations d'oxygène dissous dans l'estuaire maritime du Saint-Laurent (Lefort, com. Pers.). Dans ce contexte, ce projet de doctorat avait pour objectifs d'améliorer notre compréhension des phénomènes ayant contribué à la diminution en oxygène dissous afin de mieux prévoir quelle sera l'évolution de l'écosystème en fonction de l'évolution des causes externes comme l'apport en azote et le réchauffement des eaux profondes ainsi que des mécanismes internes comme le devenir de l'azote une fois introduit dans le système. Pour mieux comprendre le rôle de ces paramètres dans le développement de l'hypoxie, nous avons examiné avec attention 3 aspects: 1) les changements de circulation océanique et le réchauffement de la masse d'eau profonde qui jouent un rôle déterminant sur l'oxygénation de la masse d'eau entrante (Gilbert et al., 2005) et sur l'intensité de l'activité bactérienne (Gillooly et al., 2001), 2) l'équilibre interne des espèces azotées qui affectent fortement la productivité et les flux de carbone dont la décomposition s'accompagne d'une consommation d'O_2 notamment dans les milieux estuariens

(Cloern, 2001; Diaz and Rosenberg, 2008; Gilbert et al., 2009; Rabalais et al., 2010) et 3) la caractérisation des sources d'apport azoté et l'identification des processus de recyclage internes qui sont primordiales dans l'optique de prévoir les conséquences de futures mesures de remédiation (Wankel et al., 2006; Kendall et al., 2007; Wankel et al., 2009). Cette thèse aborde d'abord la problématique sous un angle paléocéanographique nous permettant de mieux identifier le rôle qu'a pu jouer la température dans la diminution des concentrations d'O_2 au cours du dernier siècle, voire du dernier millénaire. Pour la première fois, l'hypothèse d'un changement dans la proportion des masses d'eaux entrantes est confrontée à des données paléocéanographiques. Les chapitres portant sur le cycle de l'azote sont, pour leur part, des études portant sur la situation actuelle de l'azote dans le système du Saint-Laurent. L'utilisation d'une approche intégratrice pour estimer le taux d'élimination de l'azote est une première pour le Saint-Laurent et une des rares études de ce type en milieu côtier (Lehmann et al., 2005), elle nous permet de calculer approximativement, pour la première fois, le bilan régional de l'azote dans la partie maritime du Saint-Laurent et donc de mieux comprendre le réel impact des apports azotés. L'utilisation des isotopes des nitrates sur une série temporelle couvrant deux années est aussi une première dans le fleuve Saint-Laurent. Cela nous apporte des informations sur l'importance de certaines sources, jusqu'ici peu mentionnées, comme les apports atmosphériques.

Tous les enregistrements sédimentaires examinés dans cette étude, de l'estuaire au golfe du Saint-Laurent, sont caractérisés par une même tendance, à savoir une augmentation de la température des masses d'eau profondes depuis environ un siècle. L'augmentation de la température est en phase avec la diminution de l'oxygène dissous mesurée au cours des 70 dernières années. Une hausse de la température peut faire diminuer la concentration d'O_2 dissous par son effet positif sur l'activité métabolique des organismes dégradant la matière organique (Gillooly et al., 2001) qui consomme de ce fait plus d'O_2. La concentration en oxygène dissous dans

les eaux marines est en outre influencée par la stratification et la ventilation. Or, il s'agit de facteurs étroitement liés aux conditions climatiques et de circulation dans les océans (Slowey and Curry, 1992; Doney and Jenkins, 1994; Paillet and Arhan, 1996; Druffel, 1997; Paillet and Mercier, 1997). Puisque les eaux de fond du Saint-Laurent proviennent d'un mélange de masses d'eau de l'Atlantique et du Labrador, certaines de leurs caractéristiques, comme la température et leur teneur en oxygène dissous, sont héritées de celle des masses d'eau parentes. Dans ce contexte, le réchauffement observé dans l'estuaire et le golfe du Saint-Laurent reflèterait la proportion du mélange des eaux entrant dans le golfe du Saint-Laurent par le détroit de Cabot (Gilbert et al., 2005). Une augmentation dans la proportion d'eau atlantique s'accompagnerait d'une augmentation de la composition isotopique de l'eau. La différence d'environ 0,25 ‰ enregistrée entre la valeur $\delta^{18}O$ mesurée et la valeur théorique peut être expliquée par une augmentation de 20 % de la masse d'eau atlantique, ce qui concorde avec l'hypothèse de Gilbert et al. (2005). Notre évaluation repose cependant sur l'hypothèse que la composition isotopique des masses d'eau atlantique et de la mer du Labrador n'a pas changée au cours de ce laps de temps, ce qui ne peut être démontré au vu de la faible amplitude des variations isotopiques. Quoi qu'il en soit, nos résultats illustrent un réchauffement des masses d'eau contenues dans le chenal laurentien de 1.6°C depuis un siècle. Un tel réchauffement n'a pas d'équivalent à l'échelle du dernier millénaire. Il est ainsi possible qu'il s'agisse d'un phénomène récent résultant des activités anthropiques (Bopp et al., 2002; Keeling and Garcia, 2002; Plattner et al., 2002; Meehl, 2007). Toutefois, une variabilité naturelle de la circulation océanique selon des échelles de temps décennales, séculaires ou millénaires ne peut être exclue (Keigwin and Pickart, 1999; DeMenocal et al., 2000; Greene and Pershing, 2003; Frölicher et al., 2009; Ito and Deutsch, 2010). Par contre, ce réchauffement ne peut, à lui seul, expliquer que 50 à 67% de la diminution d'O_2 observée dans l'estuaire maritime (Gilbert et al., 2005). Il

est donc important d'explorer d'autres pistes, notamment celle de l'augmentation de la productivité primaire due aux apports azotés.

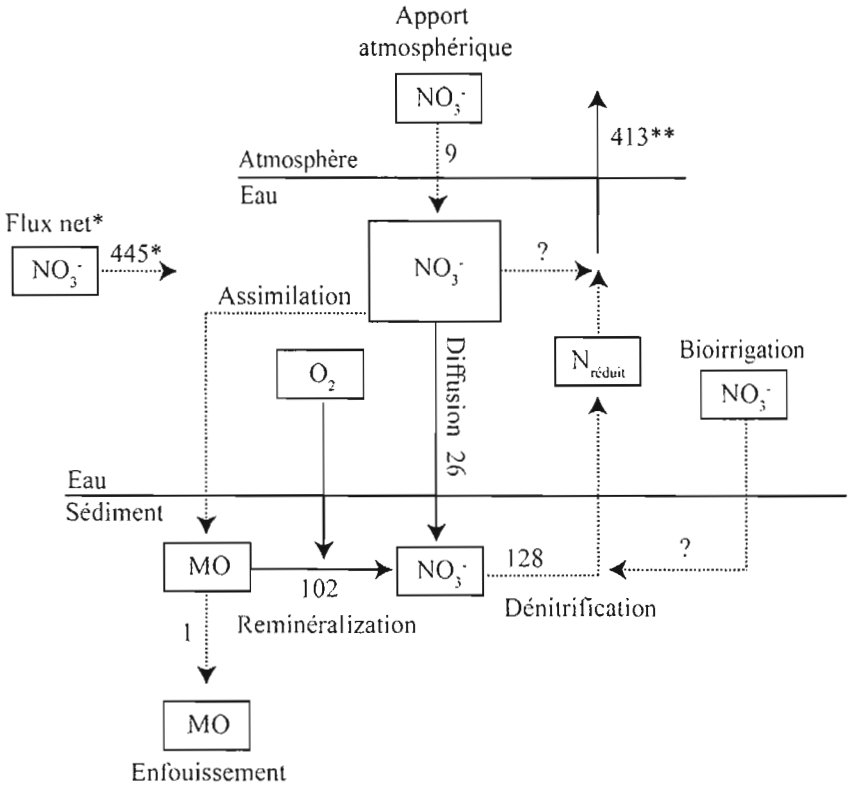

Figure 1. Bilan de l'azote pour le système marin du Saint-Laurent, en 10^6 t N par année. Les flèches pleines représentent les flux calculés dans cette étude et les flèches pointillées proviennent de la littérature (Savenkoff et al., 2001). Le flux net (*) représente la différence des flux entrants et sortants par le fleuve Saint-Laurent, le détroit de Cabot et le détroit de Belle-Isle. L'estimation de l'élimination totale d'azote du système (**) est la valeur dérivée du déficit d'azote observé.

Pour examiner l'hypothèse de changement de productivité à l'origine de l'hypoxie, nous nous sommes concentrés sur l'établissement d'un bilan régional de l'azote pour le système marin du Saint-Laurent (figure 1). Un tel bilan est en effet nécessaire à la compréhension de l'impact des apports continentaux de nitrate sur la

fertilisation possible des eaux de surface. Nos mesures directes des taux de dénitrification benthique ne sont pas les premières (Anschutz et al., 2000; Wang et al., 2003; Katsev et al., 2007). Elles couvrent cependant une superficie beaucoup plus large, ce qui nous permet d'estimer un taux de dénitrification moyen à l'échelle des chenaux de l'estuaire et du golfe. Nos mesures directes révèlent des valeurs légèrement plus élevées que celles déjà publiées (Katsev et al., 2007), mais du même ordre de grandeur (690 ± 90 μmol m^{-2} d^{-1} vs ~550 μmol m^{-2} d^{-1}). Par contre, lorsque l'on extrapole le taux de dénitrification à l'ensemble des sédiments, le bilan de l'azote est en déséquilibre lorsque l'on considère les apports mesurés par Savenkoff et al. (2001) qui sont de 454 x 10^6 t N yr^{-1} pour moins de 200 x 10^6 t N yr^{-1} dénitrifié. Même en considérant la marge d'incertitude liée à l'interpolation des données nous arrivons à la conclusion que le déséquilibre est significatif. Plusieurs études ont fait état d'une possible augmentation de la productivité primaire des eaux de surface de l'estuaire due à un apport accru de nitrate (Gilbert et al., 2005; Benoit et al., 2006; Thibodeau et al., 2006). Un surplus d'azote pourrait donc avoir déjà fait augmenter la concentration d'azote dans l'estuaire. Le déséquilibre observée entre les mesures directes et indirectes peut en effet être dû au fait que les mesures directes ne peuvent tenir compte des variations ponctuelles comme la biorrigation et la bioturbation, deux phénomènes qui seraient déterminants dans l'environnement du chenal laurentien (Katsev et al., 2007). Les taux d'élimination de l'azote calculés à partir des concentrations en nitrates mesurées dans la colonne d'eau sont donc une alternative valable, puisque intégrateur de l'ensemble des phénomènes éliminant l'azote. En considérant ces valeurs, le bilan du système marin du Saint-Laurent peut être évalué comme étant à l'équilibre (apport de 454 x 10^6 t N yr^{-1} pour ~411 x 10^6 t N yr^{-1} éliminé). Cette conclusion est extrêmement importante pour la compréhension de la dynamique des nutriments une fois qu'ils atteignent l'estuaire. Un des effets les plus néfastes est un apport accru de nitrate appelé *effet cascade* (Galloway et al., 2004), c'est-à-dire qu'après un effet initial de fertilisation, l'azote est recyclé *in situ* sans être éliminé vers l'atmosphère (par transformation en N_2). Une même molécule de nitrate

peut donc re-fertiliser plusieurs fois la même zone. Si, comme nous le suggérons, le système marin du Saint-Laurent est proche de l'équilibre en terme d'azote, cela impliquerait que *l'effet cascade* des apports continentaux est minime, voire nul, car le taux d'élimination d'azote est égal aux flux entrants. Cette hypothèse expliquerait pourquoi l'estuaire maritime semble caractérisé par une augmentation de la productivité primaire depuis les 50 dernières années (Thibodeau et al., 2006), mais pas les régions plus éloignées du golfe (Genovesi et al., 2008) ou du chenal Esquiman (appendice D). Les apports d'azote sont entièrement consommés dès leur arrivée dans les eaux pauvres en nitrates de l'estuaire et sont ensuite soustraites du système dans le sédiment, sans re-fertiliser les eaux de surface. L'augmentation de la productivité primaire due aux apports continentaux est donc limitée à la région de l'estuaire qui jouxte le fleuve, ce qui suggère que d'autres phénomènes, liés à la température par exemple, sont responsables des variations de concentration en oxygène dissous dans le golfe et les autres chenaux éloignés des apports continentaux.

Afin de mieux comprendre le devenir des apports continentaux d'azote, il est important de déterminer leur origine et d'identifier les mécanismes de transformation actifs dans l'écosystème. La corrélation négative entre le $\delta^{18}O$ et $\delta^{15}N$ des nitrates dissous échantillonnés au cours de deux années consécutives à la station de Lévis suggère que la signature isotopique des nitrates est influencée principalement par la signature des sources, à l'opposé des activités biologiques (assimilation, dénitrification) qui résultent en un fractionnement $\delta^{18}O$ et $\delta^{15}N$ proportionnels. Une corrélation négative entre $\delta^{18}O$ et $\delta^{15}N$ est rare, mais a été observée à Austin, Texas, où la signature isotopique des nitrates varie en relation avec les tornades qui apportent une grande quantité de nitrate atmosphérique (Silva et al., 2002). La corrélation négative observée entre le $\delta^{18}O$ et le $\delta^{15}N$ des nitrates dissous dans le système du Saint-Laurent pourrait aussi s'expliquer par des variations d'apports atmosphériques.

Dans les séries analysées, nous n'avons pas observé de relation entre le $\delta^{18}O$ des nitrates et le $\delta^{18}O$ de l'eau. Cela implique que les nitrates mesurés ne sont pas

produits principalement par nitrification *in situ* (Kendall et al., 2007) et donc, ne proviennent pas des engrais ammoniaqués majoritairement utilisés au Québec. La différence entre le $\delta^{18}O$ des nitrates et le $\delta^{18}O$ de l'eau est élevée au printemps, saison caractérisée par la fonte des neiges et conséquemment par un apport d'eau contenant des nitrates d'origine atmosphérique. Comme dans le cas du site d'Austin (Silva et al., 2002), le $\delta^{18}O$ très élevé des nitrates pourraient s'expliquer par la forte saisonnalité du signal dans le Saint-Laurent. Par contre, vu les conditions hydrographiques du Saint-Laurent, les variations isotopiques saisonnières observées pourraient aussi correspondre aux changements de proportion des eaux provenant des grands lacs et des tributaires du nord. Pour vérifier cette hypothèse, nous suggérons d'effectuer le même type d'analyses sur les échantillons pris aux stations d'échantillonnages de Montréal et de Carillon durant la même période.

Cette thèse apporte ainsi des éléments importants dans la compréhension générale du développement de l'hypoxie et nous permet d'établir des champs prioritaires pour la poursuite des études sur l'hypoxie à une échelle régionale. Bien que nous fassions l'hypothèse que le réchauffement de la masse d'eau profonde joue un rôle dans l'appauvrissement en O_2, nous ne savons pas encore exactement quels processus sont mis en œuvre. Une étude sur les taux de minéralisation au cours du dernier siècle à l'aide du $\delta^{13}C$ des foraminifères endobenthiques pourrait nous aider à quantifier la proportion de la baisse en O_2 due à l'augmentation de l'activité métabolique reliée à la hausse de température. Des mesures isotopiques sur les foraminifères d'une carotte prise dans le détroit de Cabot pourraient aussi nous permettre de mieux circonscrire les changements de composition des masses d'eau entrantes. De plus, notre conclusion sur le cycle régional de l'azote nous permet d'émettre l'hypothèse qu'une réduction des apports azotés dans le bassin versant du Saint-Laurent n'aurait d'influence que sur la productivité dans la partie amont de l'estuaire maritime. Enfin, l'impossibilité de bien discerner la signature isotopique

des nitrates d'origine anthropique à la station de Québec nous incite à redoubler de prudence avant de conclure sur l'impact des activités humaines sur le cycle de l'azote dans le Saint-Laurent. Dans l'optique d'identifier les sources et de prédire le devenir de l'azote dans le fleuve, nous suggérons de mieux caractériser du point de vue isotopique chaque source (ainsi que leur lixiviat) ainsi que d'évaluer l'importance de l'élimination de l'azote dans le fleuve. Finalement, comme l'impact des apports azotés semble restreint à l'estuaire moyen et maritime, la simple conservation de milieu naturel reconnue comme puits d'azote, tel les marais (Poulin et al., 2007), pourrait avoir un impact significatif sur le maintien de l'équilibre du cycle de l'azote.

APPENDICE A

DONNÉES PRÉSENTÉES DANS LE CHAPITRE I

Tableau A.1

Oxygène dissous, température et salinité à 350 m de profondeur dans l'estuaire maritime entre 1971 à 2004

Année	O_2 ($\mu mol\ l^{-1}$)	T (°C)	Salinité
2004		5,12	34,47
2003	58,65	5,22	34,53
2002	60,62	5,11	34,49
2001	61,43	4,96	34,40
2000	66,93	4,97	34,42
1999	82,65	5,16	34,48
1998	59,69	5,02	34,45
1997	59,38	4,90	34,40
1996	71,10	4,73	34,75
1995	63,99	4,69	34,27
1994	67,68	4,74	34,44
1993	56,11	4,63	34,64
1992	65,28	4,70	34,48
1991	67,12	4,75	34,19
1990	75,14	5,18	34,23
1989		5,27	34,58
1988			
1987	59,09	5,21	34,48
1986			
1985			
1984	66,73	5,18	34,55
1983			
1982		5,36	34,57
1981			
1980			
1979		5,40	34,65
1978		5,08	34,52
1977			
1976		4,66	34,38
1975	104,37	4,62	34,47
1974	104,50	4,66	34,46
1973	100,33	4,39	34,37
1972	109,42	4,28	34,36
1971	117,50	4,26	34,45

Tableau A.2
Oxygène dissous, température et salinité à 350 m de profondeur dans l'estuaire maritime entre 1932 à 1960

Année	O_2 ($\mu mol\ l^{-1}$)	T (°C)	Salinité	T lissé 7 (°C)
1970	111,16	4,06	34,64	4,08
1969		3,88	34,38	4,03
1968		3,74	34,35	4,04
1967		3,96	34,39	4,06
1966				4,14
1965		4,33	34,46	4,20
1964	94,00	4,39	34,46	4,29
1963		4,57	34,54	4,37
1962				4,37
1961	81,00	4,20	34,27	4,39
1960				4,38
1959				4,37
1958				4,40
1957		4,38	34,43	4,46
1956		4,54	34,51	4,46
1955		4,46	34,51	4,46
1954				
1953				
1952				
1951				
1950				
1949				
1948				
1947				
1946				
1945				
1944				
1943				
1942				
1941				
1940				
1939				
1938		3,56	34,02	3,36
1937		3,14	34,25	3,37
1936				3,37
1935	126,56	3,38	34,31	3,37
1934	136,16	3,40	33,57	3,31
1933	127,53			
1932	108,48			

Tableau A.3

Température calculée à partir du $\delta^{18}O$ de *Globobulimina auriculata* (foraminifère benthique) dans la carotte CR02-23 (0-30 cm)

CR02-23				
Profondeur (cm)	$\delta^{18}O$ (‰)	$\delta^{18}O_w$ (‰)	A (‰)	T (°C)
0,25	2,74	-0,03	-0,3	4,49
0,75	2,74	-0,03	-0,3	4,52
1,5	2,69	-0,03	-0,3	4,71
2,5	2,66	-0,03	-0,3	4,82
3,5	2,71	-0,03	-0,3	4,60
4,5	2,79	-0,03	-0,3	4,33
5,5	2,70	-0,03	-0,3	4,66
6,5	2,78	-0,03	-0,3	4,35
7,5	2,69	-0,03	-0,3	4,70
8,5	2,78	-0,03	-0,3	4,37
9,5	2,70	-0,03	-0,3	4,65
10,5	2,78	-0,03	-0,3	4,34
11,5	2,72	-0,03	-0,3	4,57
12,5	2,81	-0,03	-0,3	4,24
13,5	2,81	-0,03	-0,3	4,26
14,5	2,97	-0,03	-0,3	3,65
15,5	2,80	-0,03	-0,3	4,28
16,5	2,86	-0,03	-0,3	4,04
17,5		-0,03	-0,3	
18,5	2,91	-0,03	-0,3	3,89
19,5	2,97	-0,03	-0,3	3,65
20,5		-0,03	-0,3	
21,5	2,97	-0,03	-0,3	3,63
22,5		-0,03	-0,3	
23,5		-0,03	-0,3	
24,5		-0,03	-0,3	
25,5	2,92	-0,03	-0,3	3,82
26,5		-0,03	-0,3	
27,5	2,98	-0,03	-0,3	3,61
28,5	2,96	-0,03	-0,3	3,69
29,5	3,11	-0,03	-0,3	3,13

Tableau A.4

Température calculée à partir du $\delta^{18}O$ de *Globobulimina auriculata* (foraminifère benthique) dans la carotte CR02-23 (30-46 cm)

	CR02-23			
Profondeur (cm)	$\delta^{18}O$ (‰)	$\delta^{18}O_w$ (‰)	A (‰)	T (°C)
30,5	3,07	-0,03	-0,3	3,27
31,5	2,99	-0,03	-0,3	3,58
32,5	2,92	-0,03	-0,3	3,85
33,5	2,89	-0,03	-0,3	3,95
34,5	3,04	-0,03	-0,3	3,37
35,5	2,99	-0,03	-0,3	3,57
36,5	2,94	-0,03	-0,3	3,78
37,5	2,90	-0,03	-0,3	3,93
38,5	2,86	-0,03	-0,3	4,04
39,5	3,00	-0,03	-0,3	3,55
40,5	2,98	-0,03	-0,3	3,60
41,5	2,96	-0,03	-0,3	3,68
42,5	3,02	-0,03	-0,3	3,46
43,5	2,98	-0,03	-0,3	3,60
44,5	3,25	-0,03	-0,3	2,60
45,5	3,01	-0,03	-0,3	3,51

Tableau A.5

$\delta^{18}O$ et $\delta^{13}C$ de *Globobulimina auriculata* (foraminifère benthique) dans la carotte MD99-2220 (0-30 cm)

Profondeur (cm)	$\delta^{18}O$ (‰)	$\delta^{13}C$ (‰)
0,5		
1,5		
2,5		
3,5		
4,5		
5,5		
6,5	2,89	-1,75
7,5	2,76	-1,66
8,5		
9,5	2,6	-2,15
10,5	2,96	-1,53
11,5	2,86	-2,01
12,5	2,85	-2,03
13,5	2,82	-1,53
14,5		
15,5	2,58	-2,89
16,5		
17,5		
18,5	2,78	-2,1
19,5	2,84	-1,76
20,5	2,8	-1,61
21,5	2,91	-1,98
22,5	2,85	-2,61
23,5	2,91	-2,04
24,5	2,94	-1,81
25,5	2,85	-2,29
26,5	2,92	-1,79
27,5	2,85	-2,18
28,5	2,99	-2,05
29,5	3,05	-2,54

Tableau A.6

$\delta^{18}O$ et $\delta^{13}C$ de *Globobulimina auriculata* (foraminifère benthique) dans la carotte MD99-2220 (30-60 cm)

Profondeur (cm)	$\delta^{18}O$ (‰)	$\delta^{13}C$ (‰)
30,5	2,97	-2,51
31,5	3,03	-2,41
32,5		
33,5	3,08	-2,26
34,5	3,02	-2,34
35,5	3,05	-2,55
36,5	3,01	-2,53
37,5	2,98	-2,84
38,5	3,01	-2,84
39,5	3,08	-2,23
40,5	2,97	-2,34
41,5	3,04	-2,1
42,5	3,07	-2,1
43,5	2,99	-1,88
44,5	3,09	-2,39
45,5	3,01	-2,57
46,5	2,95	-2,42
47,5	2,97	-2,49
48,5	3,07	-1,93
49,5	3,05	-1,75
50,5	2,98	-1,94
51,5	3,08	-1,78
52,5	3,01	-2,19
53,5	3,13	-2,26
54,5	3,16	-2,05
55,5	3,13	-1,82
56,5	3,15	-1,86
57,5	3,07	-2,27
58,5	3,15	-2,18
59,5	3,11	-2,12

Tableau A.7

$\delta^{18}O$ et $\delta^{13}C$ de *Globobulimina auriculata* (foraminifère benthique) dans la carotte MD99-2220 (60-90 cm)

Profondeur (cm)	$\delta^{18}O$ (‰)	$\delta^{13}C$ (‰)
60,5	3,19	-2,18
61,5	3,15	-2,32
62,5	3,18	-1,98
63,5	3,1	-1,98
64,5	3,13	-1,49
65,5	3,18	-1,73
66,5	3,19	-1,63
67,5	3,22	-1,76
68,5	3,22	-1,5
69,5	3,23	-2,03
70,5	3,1	-1,82
71,5	3,18	-2,22
72,5	3,15	-2,34
73,5	3,08	-2,45
74,5	3,13	-2,08
75,5	3,18	-2,41
76,5	3,16	-2,18
77,5	3,17	-2,22
78,5	3,14	-2,41
79,5	3,12	-2,15
80,5	3,17	-2,08
81,5	3,15	-2,01
82,5	3,05	-2,35
83,5	3,12	-2,04
84,5	3,13	-2,22
85,5	3,13	-2,22
86,5	3,23	-1,92
87,5	3,18	-1,89
88,5	3,09	-2,04
89,5	3,06	-2,34

Tableau A.8

$\delta^{18}O$ et $\delta^{13}C$ de *Globobulimina auriculata* (foraminifère benthique) dans la carotte MD99-2220 (90-120 cm)

Profondeur (cm)	$\delta^{18}O$ (‰)	$\delta^{13}C$ (‰)
90,5	3,16	-1,84
91,5	3,18	-2,12
92,5	3,13	-1,91
93,5	3,07	-2,59
94,5	3,13	-1,88
95,5	3,17	-2,04
96,5	3,2	-1,91
97,5	3,07	-2,08
98,5	3,14	-2,18
99,5	3,09	-2,17
100,5	3,12	-2,37
101,5	3,05	-2,27
102,5	3,08	-2,19
103,5	3,04	-2,42
104,5	3,12	-2,11
105,5	3,11	-2,15
106,5	3,08	-2,24
107,5	2,97	-2,1
108,5	3,02	-1,7
109,5	3,07	-1,94
110,5	3,07	-1,83
111,5	3,00	-2,31
112,5	3,08	-2,09
113,5	2,98	-2,3
114,5	3,15	-2,1
115,5	3,13	-2,26
116,5	3,2	-2,1
117,5	3,21	-2,34
118,5	3,22	-1,52
119,5	3,06	-2,03

Tableau A.9

$\delta^{18}O$ et $\delta^{13}C$ de *Globobulimina auriculata* (foraminifère benthique) dans la carotte MD99-2220 (120-150 cm)

Profondeur (cm)	$\delta^{18}O$ (‰)	$\delta^{13}C$ (‰)
120,5		
121,5	3,09	-2,05
122,5	3,05	-2,01
123,5	3,07	-2,6
124,5	2,88	-2,36
125,5	2,96	-1,79
126,5	3,07	-2,32
127,5	2,97	-2,34
128,5	3,06	-2,24
129,5	3,18	-2,15
130,5	2,99	-2,21
131,5		
132,5	3,00	-2,12
133,5	3,16	-1,77
134,5		
135,5	3,35	-1,6
136,5	3,17	-1,92
137,5		
138,5	3,33	-2,72
139,5	3,05	-2,1
140,5	3,08	-2,15
141,5	2,99	-2,27
142,5	3,13	-2,03
143,5	3,08	-1,78
144,5	3,00	-2,78
145,5	3,11	-2,38
146,5	3,15	-2,12
147,5	3,09	-1,95
148,5	3,06	-2,22
149,5	3,23	-2,71

Tableau A.10

$\delta^{18}O$ et $\delta^{13}C$ de *Globobulimina auriculata* (foraminifère benthique) dans la carotte MD99-2220 (150-180 cm)

Profondeur (cm)	$\delta^{18}O$ (‰)	$\delta^{13}C$ (‰)
150,5	3,16	-2,11
151,5	3,16	-2,11
152,5	3,23	-2,16
153,5	3,15	-1,93
154,5	3,09	-2,01
155,5	3,09	-2,24
156,5	3,05	-2,58
157,5	3,13	-2,17
158,5	3,16	-2,02
159,5	3,16	-2,13
160,5		
161,5		
162,5	3,02	-1,53
163,5		
164,5	3,14	-1,56
165,5	3,23	-1,36
166,5	2,99	-2,88
167,5	3,11	-1,9
168,5	3,01	-2,4
169,5	3,13	-2,37
170,5		
171,5		
172,5	3,28	-1,05
173,5	3,11	-1,99
174,5	3,03	-2,17
175,5	2,98	-1,49
176,5	3,11	-1,68
177,5	3,09	-1,73
178,5	3,02	-2,21
179,5	3,01	-1,48

Tableau A.11

$\delta^{18}O$ et $\delta^{13}C$ de *Globobulimina auriculata* (foraminifère benthique) dans la carotte MD99-2220 (180-200 cm)

Profondeur (cm)	$\delta^{18}O$ (‰)	$\delta^{13}C$ (‰)
180,5		
181,5	3,02	-1,91
182,5		
183,5	3,01	-2,33
184,5	3,1	-2,26
185,5	3,1	-1,94
186,5	3,09	-2,15
187,5	3,08	-1,86
188,5	3,07	-2,11
189,5	2,95	-2,19
190,5	3,00	-2,46
191,5	2,98	-2,37
192,5	2,98	-2,83
193,5	3,16	-2,4
194,5	2,96	-2,74
195,5	3,04	-2,62
196,5	2,96	-2,93
197,5	3,07	-2,69
198,5	3,14	-3,07
199,5	3,05	-2,71

APPENDICE B

DONNÉES PRÉSENTÉES DANS LE CHAPITRE II

Tableau B.1

Concentration de NO_x^-, PO_4^- et SiO_2 dans la colonne d'eau à la station 23

Station	Date mois/jour/an	Lon (°E)	Lat (°N)	Profondeur (m)	NO_x^- ($\mu mol\ l^{-1}$)	PO_4^- ($\mu mol\ l^{-1}$)	SiO_2 ($\mu mol\ l^{-1}$)
23	08/20/2005	-68,65	48,70	327	27,63	2,62	47,14
23	08/20/2005	-68,65	48,70	300	17,58	1,65	19,57
23	08/20/2005	-68,65	48,70	250	26,27	2,45	43,68
23	08/20/2005	-68,65	48,70	200	24,32	2,21	32,43
23	08/20/2005	-68,65	48,70	150	21,90	2,06	26,71
23	08/20/2005	-68,65	48,70	100	16,69	1,60	15,48
23	08/20/2005	-68,65	48,70	050	12,00	1,25	7,39
23	08/20/2005	-68,65	48,70	040	10,66	1,19	4,43
23	08/20/2005	-68,65	48,70	030	8,21	1,08	2,56
23	08/20/2005	-68,65	48,70	020	10,02	1,09	4,61
23	08/20/2005	-68,65	48,70	010	10,77	1,20	4,68
23	08/20/2005	-68,65	48,70	0,50	1,17	0,23	0,42

Tableau B.2

Concentration en oxygène dissous, salinité et N* dans la colonne d'eau à la station 23

Station	Date mois/jour/an	Lon (°E)	Lat (°N)	Profondeur (m)	O_2 ($\mu mol\ l^{-1}$)	Salinité	N* ($\mu mol\ l^{-1}$)
23	08/20/2005	-68,65	48,70	327	62,98	34,55	-11,39
23	08/20/2005	-68,65	48,70	300	66,65	34,55	-5,99
23	08/20/2005	-68,65	48,70	250	70,18	34,47	-10,02
23	08/20/2005	-68,65	48,70	200	95,38	34,12	-8,18
23	08/20/2005	-68,65	48,70	150	134,08	33,65	-8,10
23	08/20/2005	-68,65	48,70	100	212,77	32,78	-5,99
23	08/20/2005	-68,65	48,70	050	337,95	32,06	-5,16
23	08/20/2005	-68,65	48,70	040	348,72	31,98	-5,51
23	08/20/2005	-68,65	48,70	030	357,87	31,21	-6,17
23	08/20/2005	-68,65	48,70	020	339,76	30,46	-4,53
23	08/20/2005	-68,65	48,70	010	331,75	29,23	-5,51
23	08/20/2005	-68,65	48,70	0,50	370,73	26,25	0,47

Tableau B.3

Concentration de NO_x^-, PO_4^- et SiO_2 dans la colonne d'eau à la station 25

Station	Date mois/jour/an	Lon (°E)	Lat (°N)	Profondeur (m)	NO_x^- ($\mu mol\ l^{-1}$)	PO_4^- ($\mu mol\ l^{-1}$)	SiO_2 ($\mu mol\ l^{-1}$)
25	08/21/2005	-69,47	48,22	287	26,66	2,69	43,67
25	08/21/2005	-69,47	48,22	250	24,59	2,47	39,54
25	08/21/2005	-69,47	48,22	200	24,37	2,46	38,91
25	08/21/2005	-69,47	48,22	150	22,89	2,28	31,17
25	08/21/2005	-69,47	48,22	100	20,58	1,97	24,03
25	08/21/2005	-69,47	48,22	075	17,72	1,70	16,96
25	08/21/2005	-69,47	48,22	050	13,75	1,09	10,00
25	08/21/2005	-69,47	48,22	040	12,36	1,31	7,54
25	08/21/2005	-69,47	48,22	030	11,26	1,22	6,51
25	08/21/2005	-69,47	48,22	020	9,82	1,12	5,14
25	08/21/2005	-69,47	48,22	010	10,00	1,05	7,29
25	08/21/2005	-69,47	48,22	0,50	6,72	0,78	5,58

Tableau B.4

Concentration en oxygène dissous, salinité et N* dans la colonne d'eau à la station 25

Station	Date mois/jour/an	Lon (°E)	Lat (°N)	Profondeur (m)	O_2 ($\mu mol\ l^{-1}$)	Salinité	N* ($\mu mol\ l^{-1}$)
25	08/21/2005	-69,47	48,22	287	67,06	34,40	-13,48
25	08/21/2005	-69,47	48,22	250	67,35		-11,95
25	08/21/2005	-69,47	48,22	200	71,34		-12,14
25	08/21/2005	-69,47	48,22	150	106,53		-10,63
25	08/21/2005	-69,47	48,22	100	157,01	33,29	-7,96
25	08/21/2005	-69,47	48,22	075	208,46	32,97	-6,54
25	08/21/2005	-69,47	48,22	050	272,70	32,34	-0,82
25	08/21/2005	-69,47	48,22	040	293,12	32,08	-5,78
25	08/21/2005	-69,47	48,22	030	305,95	31,88	-5,32
25	08/21/2005	-69,47	48,22	020	317,72	31,34	-5,25
25	08/21/2005	-69,47	48,22	010	310,70	30,37	-3,82
25	08/21/2005	-69,47	48,22	0,50	333,87	29,62	-2,81

Tableau B.5
Concentration de NO_x^-, PO_4^- et SiO_2 dans la colonne d'eau à la station 24

Station	Date mois/jour/an	Lon (°E)	Lat (°N)	Profondeur (m)	NO_x^- ($\mu mol\ l^{-1}$)	PO_4^- ($\mu mol\ l^{-1}$)	SiO_2 ($\mu mol\ l^{-1}$)
24	08/21/2005	-69,28	48,43	295	26,67	2,77	47,90
24	08/21/2005	-69,28	48,43	250	24,21	2,50	40,19
24	08/21/2005	-69,28	48,43	200	23,54	2,32	36,50
24	08/21/2005	-69,28	48,43	150	20,90	2,07	34,25
24	08/21/2005	-69,28	48,43	100	18,65	1,77	21,20
24	08/21/2005	-69,28	48,43	060	13,18	1,34	11,60
24	08/21/2005	-69,28	48,43	050	13,98	1,39	10,37
24	08/21/2005	-69,28	48,43	040	13,94	1,38	10,68
24	08/21/2005	-69,28	48,43	030	13,27	1,30	10,00
24	08/21/2005	-69,28	48,43	020	12,46	1,23	9,12
24	08/21/2005	-69,28	48,43	010	11,70	1,18	8,52
24	08/21/2005	-69,28	48,43	0,50	7,28	0,85	6,06

Tableau B.6
Concentration en oxygène dissous, salinité et N* dans la colonne d'eau à la station 24

Station	Date mois/jour/an	Lon (°E)	Lat (°N)	Profondeur (m)	O_2 ($\mu mol\ l^{-1}$)	Salinité	N* ($\mu mol\ l^{-1}$)
24	08/21/2005	-69,28	48,43	295	67,19	34,51	-14,79
24	08/21/2005	-69,28	48,43	250	72,55	34,38	-12,86
24	08/21/2005	-69,28	48,43	200	76,88	34,16	-10,68
24	08/21/2005	-69,28	48,43	150	121,83	33,90	-9,35
24	08/21/2005	-69,28	48,43	100	209,40	33,18	-6,85
24	08/21/2005	-69,28	48,43	060	301,95	32,35	-5,32
24	08/21/2005	-69,28	48,43	050	296,08	32,06	-5,28
24	08/21/2005	-69,28	48,43	040	294,27	31,71	-5,24
24	08/21/2005	-69,28	48,43	030	303,87	31,50	-4,59
24	08/21/2005	-69,28	48,43	020	313,03	31,10	-4,29
24	08/21/2005	-69,28	48,43	010	323,79	30,65	-4,35
24	08/21/2005	-69,28	48,43	0,50	361,59	29,04	-3,49

Tableau B.7
Concentration de NO_x^-, PO_4^- et SiO_2 dans la colonne d'eau à la station 22

Station	Date mois/jour/an	Lon (°E)	Lat (°N)	Profondeur (m)	NO_x^- ($\mu mol\ l^{-1}$)	PO_4^- ($\mu mol\ l^{-1}$)	SiO_2 ($\mu mol\ l^{-1}$)
22	08/22/2005	-68,09	48,93	300	26,17	2,41	42,15
22	08/22/2005	-68,09	48,93	250	24,14	2,36	35,76
22	08/22/2005	-68,09	48,93	200	18,92	2,02	30,10
22	08/22/2005	-68,09	48,93	175	23,07	2,29	33,46
22	08/22/2005	-68,09	48,93	140	21,78	1,96	24,19
22	08/22/2005	-68,09	48,93	100	18,02	1,68	15,86
22	08/22/2005	-68,09	48,93	050	6,04	0,93	5,67
22	08/22/2005	-68,09	48,93	040	7,97	0,99	1,78
22	08/22/2005	-68,09	48,93	030	10,55	1,08	5,87
22	08/22/2005	-68,09	48,93	020	8,49	0,87	5,76
22	08/22/2005	-68,09	48,93	010	8,85	0,81	5,82
22	08/22/2005	-68,09	48,93	0,50	7,90	0,83	5,89

Tableau B.8
Concentration en oxygène dissous, salinité et N* dans la colonne d'eau à la station 22

Station	Date mois/jour/an	Lon (°E)	Lat (°N)	Profondeur (m)	O_2 ($\mu mol\ l^{-1}$)	Salinité	N* ($\mu mol\ l^{-1}$)
22	08/22/2005	-68,09	48,93	300	77,79	34,60	-9,56
22	08/22/2005	-68,09	48,93	250	74,10	34,41	-10,68
22	08/22/2005	-68,09	48,93	200	89,31	34,20	-10,43
22	08/22/2005	-68,09	48,93	175	107,39	34,03	-10,65
22	08/22/2005	-68,09	48,93	140	145,95	33,65	-6,63
22	08/22/2005	-68,09	48,93	100	214,13	33,22	-5,90
22	08/22/2005	-68,09	48,93	050	387,43	31,91	-5,89
22	08/22/2005	-68,09	48,93	040	363,85	31,29	-5,05
22	08/22/2005	-68,09	48,93	030	331,96	30,11	-3,79
22	08/22/2005	-68,09	48,93	020	357,33	28,84	-2,59
22	08/22/2005	-68,09	48,93	010	356,75	27,73	-1,19
22	08/22/2005	-68,09	48,93	0,50	366,19	27,38	-2,53

Tableau B.9

Concentration de NO_x^-, PO_4^- et SiO_2 dans la colonne d'eau à la station 21

Station	Date mois/jour/an	Lon (°E)	Lat (°N)	Profondeur (m)	NO_x^- ($\mu mol\ l^{-1}$)	PO_4^- ($\mu mol\ l^{-1}$)	SiO_2 ($\mu mol\ l^{-1}$)
21	08/23/2005	-67,28	49,12	312	26,43	2,36	41,29
21	08/23/2005	-67,28	49,12	250	24,23	1,49	31,82
21	08/23/2005	-67,28	49,12	200	19,59	1,81	21,90
21	08/23/2005	-67,28	49,12	175	28,48	1,93	25,48
21	08/23/2005	-67,28	49,12	140	18,54	1,73	16,66
21	08/23/2005	-67,28	49,12	120	16,20	1,52	12,38
21	08/23/2005	-67,28	49,12	100	14,37	1,39	9,57
21	08/23/2005	-67,28	49,12	040	7,42	0,96	3,73
21	08/23/2005	-67,28	49,12	030	7,03	0,94	0,65
21	08/23/2005	-67,28	49,12	020	5,84	0,87	0,08
21	08/23/2005	-67,28	49,12	010	2,75	0,58	0,00
21	08/23/2005	-67,28	49,12	0,50	1,22	0,39	0,00

Tableau B.10

Concentration en oxygène dissous, salinité et N* dans la colonne d'eau à la station 21

Station	Date mois/jour/an	Lon (°E)	Lat (°N)	Profondeur (m)	O_2 ($\mu mol\ l^{-1}$)	Salinité	N* ($\mu mol\ l^{-1}$)
21	08/23/2005	-67,28	49,12	312	80,71	34,62	-8,42
21	08/23/2005	-67,28	49,12	250	81,82	34,43	3,26
21	08/23/2005	-67,28	49,12	200	105,55	34,07	-6,52
21	08/23/2005	-67,28	49,12	175	130,62	33,86	0,52
21	08/23/2005	-67,28	49,12	140	193,25	33,45	-6,24
21	08/23/2005	-67,28	49,12	120	249,82	33,07	-5,16
21	08/23/2005	-67,28	49,12	100	281,58	32,73	-4,95
21	08/23/2005	-67,28	49,12	040	376,04	31,98	-5,03
21	08/23/2005	-67,28	49,12	030	378,75	31,83	-5,03
21	08/23/2005	-67,28	49,12	020	395,62	31,67	-5,25
21	08/23/2005	-67,28	49,12	010	408,01	31,40	-3,57
21	08/23/2005	-67,28	49,12	0,50	422,41	29,95	-2,12

Tableau B.11
Concentration de NO_x^-, PO_4^- et SiO_2 dans la colonne d'eau à la station R6c

Station	Date mois/jour/an	Lon (°E)	Lat (°N)	Profondeur (m)	NO_x^- ($\mu mol\ l^{-1}$)	PO_4^- ($\mu mol\ l^{-1}$)	SiO_2 ($\mu mol\ l^{-1}$)
R6c	08/23/2005	-66,37	49,57		26,03	2,23	36,83
R6c	08/23/2005	-66,37	49,57		23,92	2,05	30,41
R6c	08/23/2005	-66,37	49,57		19,69	1,80	21,99
R6c	08/23/2005	-66,37	49,57		22,58	1,97	24,27
R6c	08/23/2005	-66,37	49,57		20,00	1,76	23,80
R6c	08/23/2005	-66,37	49,57		13,87	1,41	17,94
R6c	08/23/2005	-66,37	49,57		14,47	1,39	7,81
R6c	08/23/2005	-66,37	49,57		12,29	1,26	6,59
R6c	08/23/2005	-66,37	49,57		9,92	1,09	7,14
R6c	08/23/2005	-66,37	49,57		0,41	0,26	3,53
R6c	08/23/2005	-66,37	49,57		6,00	0,85	0,00
R6c	08/23/2005	-66,37	49,57		0,43	0,37	0,00

Tableau B.12
Concentration en N* dans la colonne d'eau à la station R6c

Station	Date mois/jour/an	Lon (°E)	Lat (°N)	Profondeur (m)	O_2 ($\mu mol\ l^{-1}$)	Salinité	N* ($\mu mol\ l^{-1}$)
R6c	08/23/2005	-66,37	49,57				-6,80
R6c	08/23/2005	-66,37	49,57				-6,03
R6c	08/23/2005	-66,37	49,57				-6,17
R6c	08/23/2005	-66,37	49,57				-6,05
R6c	08/23/2005	-66,37	49,57				-5,21
R6c	08/23/2005	-66,37	49,57				-5,73
R6c	08/23/2005	-66,37	49,57				-4,84
R6c	08/23/2005	-66,37	49,57				-4,89
R6c	08/23/2005	-66,37	49,57				-4,58
R6c	08/23/2005	-66,37	49,57				-0,87
R6c	08/23/2005	-66,37	49,57				-4,75
R6c	08/23/2005	-66,37	49,57				-2,52

Tableau B.13
Concentration de NO_x^-, PO_4^- et SiO_2 dans la colonne d'eau à la station 20

Station	Date mois/jour/an	Lon (°E)	Lat (°N)	Profondeur (m)	NO_x^- ($\mu mol\ l^{-1}$)	PO_4^- ($\mu mol\ l^{-1}$)	SiO_2 ($\mu mol\ l^{-1}$)
20	08/24/2005	-66,33	49,43	315	28,10	2,36	40,69
20	08/24/2005	-66,33	49,43	250	19,84	1,83	23,42
20	08/24/2005	-66,33	49,43	200	23,42	2,08	29,37
20	08/24/2005	-66,33	49,43	175	21,32	1,84	19,62
20	08/24/2005	-66,33	49,43	140	24,18	2,20	31,19
20	08/24/2005	-66,33	49,43	120	19,39	1,24	17,38
20	08/24/2005	-66,33	49,43	100	17,26	1,61	12,02
20	08/24/2005	-66,33	49,43	040	11,77	1,17	6,41
20	08/24/2005	-66,33	49,43	030	5,13	0,89	0,77
20	08/24/2005	-66,33	49,43	020	5,74	0,84	0,00
20	08/24/2005	-66,33	49,43	010	1,11	0,24	0,00
20	08/24/2005	-66,33	49,43	0,50	0,02	0,15	0,00

Tableau B.14
Concentration en oxygène dissous, salinité et N* dans la colonne d'eau à la station 20

Station	Date mois/jour/an	Lon (°E)	Lat (°N)	Profondeur (m)	O_2 ($\mu mol\ l^{-1}$)	Salinité	N* ($\mu mol\ l^{-1}$)
20	08/24/2005	-66,33	49,43	315	90,67	34,68	-6,72
20	08/24/2005	-66,33	49,43	250	84,36	34,40	-6,55
20	08/24/2005	-66,33	49,43	200	99,39	34,11	-6,97
20	08/24/2005	-66,33	49,43	175	110,77	33,99	-5,18
20	08/24/2005	-66,33	49,43	140	153,56	33,72	-8,12
20	08/24/2005	-66,33	49,43	120	205,31	33,35	2,51
20	08/24/2005	-66,33	49,43	100	242,26	33,05	-5,68
20	08/24/2005	-66,33	49,43	040	340,43	31,86	-4,09
20	08/24/2005	-66,33	49,43	030	390,61	31,58	-6,24
20	08/24/2005	-66,33	49,43	020	388,88	31,01	-4,84
20	08/24/2005	-66,33	49,43	010	403,40	30,11	0,17
20	08/24/2005	-66,33	49,43	0,50	395,77	29,79	0,60

Tableau B.15

Concentration de NO_x^-, PO_4^- et SiO_2 dans la colonne d'eau à la station 18

Station	Date mois/jour/an	Lon (°E)	Lat (°N)	Profondeur (m)	NO_x^- ($\mu mol\ l^{-1}$)	PO_4^- ($\mu mol\ l^{-1}$)	SiO_2 ($\mu mol\ l^{-1}$)
18	08/24/2005	-64,26	49,27	370	25,81	1,91	30,67
18	08/24/2005	-64,26	49,27	340	23,35	1,83	24,55
18	08/24/2005	-64,26	49,27	300	24,89	1,92	24,63
18	08/24/2005	-64,26	49,27	250	24,09	1,86	26,66
18	08/24/2005	-64,26	49,27	200	17,61	1,72	20,64
18	08/24/2005	-64,26	49,27	150	21,67	1,85	19,36
18	08/24/2005	-64,26	49,27	100	12,28	1,19	9,90
18	08/24/2005	-64,26	49,27	075	8,80	0,78	3,08
18	08/24/2005	-64,26	49,27	050	4,16	0,87	0,03
18	08/24/2005	-64,26	49,27	035	3,03	0,77	0,00
18	08/24/2005	-64,26	49,27	020	2,19	0,47	0,00
18	08/24/2005	-64,26	49,27	0,50	0,64	0,17	0,00

Tableau B.16

Concentration en oxygène dissous, salinité et N* dans la colonne d'eau à la station 18

Station	Date mois/jour/an	Lon (°E)	Lat (°N)	Profondeur (m)	O_2 ($\mu mol\ l^{-1}$)	Salinité	N* ($\mu mol\ l^{-1}$)
18	08/24/2005	-64,26	49,27	370	155,29	34,83	-1,92
18	08/24/2005	-64,26	49,27	340	154,79	34,83	-3,09
18	08/24/2005	-64,26	49,27	300	144,33	34,78	-2,94
18	08/24/2005	-64,26	49,27	250	121,26	34,63	-2,78
18	08/24/2005	-64,26	49,27	200	99,56	34,25	-6,96
18	08/24/2005	-64,26	49,27	150	166,98	33,59	-5,07
18	08/24/2005	-64,26	49,27	100	316,46	32,47	-3,84
18	08/24/2005	-64,26	49,27	075	377,84	32,11	-0,85
18	08/24/2005	-64,26	49,27	050	398,60	31,57	-6,79
18	08/24/2005	-64,26	49,27	035	405,44	31,03	-6,40
18	08/24/2005	-64,26	49,27	020	373,43	29,90	-2,36
18	08/24/2005	-64,26	49,27	0,50	377,03	28,69	0,79

Tableau B.17
Concentration de NO_x^-, PO_4^- et SiO_2 dans la colonne d'eau à la station R8d

Station	Date mois/jour/an	Lon (°E)	Lat (°N)	Profondeur (m)	NO_x^- ($\mu mol\ l^{-1}$)	PO_4^- ($\mu mol\ l^{-1}$)	SiO_2 ($\mu mol\ l^{-1}$)
R8d	08/24/2005	-64,09	49,49	280	26,54	2,13	34,13
R8d	08/24/2005	-64,09	49,49	200	23,89	1,29	25,75
R8d	08/24/2005	-64,09	49,49	175	23,18	1,85	25,03
R8d	08/24/2005	-64,09	49,49	150	19,88	1,37	17,92
R8d	08/24/2005	-64,09	49,49	100	14,17	1,42	10,57
R8d	08/24/2005	-64,09	49,49	075	9,27	1,00	4,14
R8d	08/24/2005	-64,09	49,49	050	3,75	0,63	0,07
R8d	08/24/2005	-64,09	49,49	040	5,10	0,86	0,00
R8d	08/24/2005	-64,09	49,49	030	3,33	0,77	0,00
R8d	08/24/2005	-64,09	49,49	020	2,65	0,60	0,00
R8d	08/24/2005	-64,09	49,49	010	2,17	0,62	0,00
R8d	08/24/2005	-64,09	49,49	0,50	0,53	0,18	0,00

Tableau B.18
Concentration en salinité et N* dans la colonne d'eau à la station R8d

Station	Date mois/jour/an	Lon (°E)	Lat (°N)	Profondeur (m)	O_2 ($\mu mol\ l^{-1}$)	Salinité	N* ($\mu mol\ l^{-1}$)
R8d	08/24/2005	-64,09	49,49	280		34,65	-4,57
R8d	08/24/2005	-64,09	49,49	200		34,23	6,16
R8d	08/24/2005	-64,09	49,49	175		33,88	-3,58
R8d	08/24/2005	-64,09	49,49	150		33,50	0,92
R8d	08/24/2005	-64,09	49,49	100		32,61	-5,59
R8d	08/24/2005	-64,09	49,49	075		32,18	-3,87
R8d	08/24/2005	-64,09	49,49	050		31,85	-3,41
R8d	08/24/2005	-64,09	49,49	040		31,68	-5,76
R8d	08/24/2005	-64,09	49,49	030		31,30	-6,13
R8d	08/24/2005	-64,09	49,49	020		30,87	-4,10
R8d	08/24/2005	-64,09	49,49	010		29,35	-4,82
R8d	08/24/2005	-64,09	49,49	0,50		28,68	0,57

Tableau B.19
Concentration de NO_x^-, PO_4^- et SiO_2 dans la colonne d'eau à la station R7f

Station	Date mois/jour/an	Lon (°E)	Lat (°N)	Profondeur (m)	NO_x^- ($\mu mol\ l^{-1}$)	PO_4^- ($\mu mol\ l^{-1}$)	SiO_2 ($\mu mol\ l^{-1}$)
R7f	08/24/2005	-65,20	50,02	193	24,70	2,16	31,74
R7f	08/24/2005	-65,20	50,02	175	22,42	1,98	24,96
R7f	08/24/2005	-65,20	50,02	150	20,44	1,79	19,36
R7f	08/24/2005	-65,20	50,02	125	12,44	1,31	11,50
R7f	08/24/2005	-65,20	50,02	100	14,92	1,42	9,75
R7f	08/24/2005	-65,20	50,02	065	11,08	1,17	5,44
R7f	08/24/2005	-65,20	50,02	050	7,48	0,86	2,56
R7f	08/24/2005	-65,20	50,02	040	4,78	0,83	0,00
R7f	08/24/2005	-65,20	50,02	030	3,96	0,83	0,00
R7f	08/24/2005	-65,20	50,02	020	2,18	0,54	0,00
R7f	08/24/2005	-65,20	50,02	010	2,89	0,70	0,00
R7f	08/24/2005	-65,20	50,02	0,50	0,80	0,15	0,00

Tableau B.20
Concentration en oxygène dissous, salinité et N* dans la colonne d'eau à la station R7f

Station	Date mois/jour/an	Lon (°E)	Lat (°N)	Profondeur (m)	O_2 ($\mu mol\ l^{-1}$)	Salinité	N* ($\mu mol\ l^{-1}$)
R7f	08/24/2005	-65,20	50,02	193	110,19	34,02	-6,90
R7f	08/24/2005	-65,20	50,02	175	122,56	33,88	-6,29
R7f	08/24/2005	-65,20	50,02	150	170,84	33,44	-5,26
R7f	08/24/2005	-65,20	50,02	125	219,97	33,18	-5,65
R7f	08/24/2005	-65,20	50,02	100	283,44	32,81	-4,92
R7f	08/24/2005	-65,20	50,02	065	346,19	32,23	-4,80
R7f	08/24/2005	-65,20	50,02	050	379,72	32,07	-3,46
R7f	08/24/2005	-65,20	50,02	040	404,66	31,87	-5,59
R7f	08/24/2005	-65,20	50,02	030	398,63	31,47	-6,49
R7f	08/24/2005	-65,20	50,02	020	410,92	30,53	-3,60
R7f	08/24/2005	-65,20	50,02	010	356,65	29,35	-5,36
R7f	08/24/2005	-65,20	50,02	0,50	344,96	27,82	1,30

Tableau B.21
Concentration de NO_x^-, PO_4^- et SiO_2 dans la colonne d'eau à la station R7d

Station	Date mois/jour/an	Lon (°E)	Lat (°N)	Profondeur (m)	NO_x^- ($\mu mol\ l^{-1}$)	PO_4^- ($\mu mol\ l^{-1}$)	SiO_2 ($\mu mol\ l^{-1}$)
R7d	08/25/2005	-65,20	49,75	288	25,69	2,19	37,40
R7d	08/25/2005	-65,20	49,75	250	23,66	2,01	29,13
R7d	08/25/2005	-65,20	49,75	200	23,93	1,99	29,44
R7d	08/25/2005	-65,20	49,75	150	21,68	1,67	22,37
R7d	08/25/2005	-65,20	49,75	100	15,65	1,46	13,10
R7d	08/25/2005	-65,20	49,75	075	9,14	1,08	6,12
R7d	08/25/2005	-65,20	49,75	050	8,50	1,03	2,95
R7d	08/25/2005	-65,20	49,75	040	6,24	0,91	1,90
R7d	08/25/2005	-65,20	49,75	030	4,38	0,84	0,08
R7d	08/25/2005	-65,20	49,75	020	2,25	0,60	0,00
R7d	08/25/2005	-65,20	49,75	010	0,61	0,34	0,00
R7d	08/25/2005	-65,20	49,75	0,50	0,00	0,26	0,00

Tableau B.22
Concentration en salinité et N* dans la colonne d'eau à la station R7d

Station	Date mois/jour/an	Lon (°E)	Lat (°N)	Profondeur (m)	O_2 ($\mu mol\ l^{-1}$)	Salinité	N* ($\mu mol\ l^{-1}$)
R7d	08/25/2005	-65,20	49,75	288		34,67	-6,47
R7d	08/25/2005	-65,20	49,75	250		34,59	-5,59
R7d	08/25/2005	-65,20	49,75	200		34,36	-4,99
R7d	08/25/2005	-65,20	49,75	150		33,80	-2,17
R7d	08/25/2005	-65,20	49,75	100		33,05	-4,88
R7d	08/25/2005	-65,20	49,75	075		32,72	-5,18
R7d	08/25/2005	-65,20	49,75	050		32,15	-5,10
R7d	08/25/2005	-65,20	49,75	040		31,94	-5,44
R7d	08/25/2005	-65,20	49,75	030		31,63	-6,09
R7d	08/25/2005	-65,20	49,75	020		30,49	-4,39
R7d	08/25/2005	-65,20	49,75	010		30,36	-1,96
R7d	08/25/2005	-65,20	49,75	0,50		29,82	-1,20

Tableau B.23

Concentration de NO_x^-, PO_4^- et SiO_2 dans la colonne d'eau à la station 19

Station	Date mois/jour/an	Lon (°E)	Lat (°N)	Profondeur (m)	NO_x^- ($\mu mol\ l^{-1}$)	PO_4^- ($\mu mol\ l^{-1}$)	SiO_2 ($\mu mol\ l^{-1}$)
19	08/25/2005	-65,20	49,49	350	25,20	2,00	33,52
19	08/25/2005	-65,20	49,49	300	23,10	1,91	30,52
19	08/25/2005	-65,20	49,49	250	23,65	2,12	35,15
19	08/25/2005	-65,20	49,49	200	23,22	2,02	27,58
19	08/25/2005	-65,20	49,49	150	21,12	1,79	21,85
19	08/25/2005	-65,20	49,49	100	15,27	1,24	13,46
19	08/25/2005	-65,20	49,49	075	12,86	1,23	7,41
19	08/25/2005	-65,20	49,49	050	9,46	1,08	4,29
19	08/25/2005	-65,20	49,49	030	5,07	0,60	1,20
19	08/25/2005	-65,20	49,49	020	0,93	0,46	0,00
19	08/25/2005	-65,20	49,49	010	0,17	0,20	0,00
19	08/25/2005	-65,20	49,49	0,50	0,00	0,32	0,00

Tableau B.24

Concentration en oxygène dissous, salinité et N* dans la colonne d'eau à la station 19

Station	Date mois/jour/an	Lon (°E)	Lat (°N)	Profondeur (m)	O_2 ($\mu mol\ l^{-1}$)	Salinité	N* ($\mu mol\ l^{-1}$)
19	08/25/2005	-65,20	49,49	350	123,63	34,78	-3,93
19	08/25/2005	-65,20	49,49	300	114,82	34,77	-4,51
19	08/25/2005	-65,20	49,49	250	86,03	34,62	-7,43
19	08/25/2005	-65,20	49,49	200	91,74	34,28	-6,16
19	08/25/2005	-65,20	49,49	150	137,82	33,87	-4,66
19	08/25/2005	-65,20	49,49	100	250,32	33,01	-1,60
19	08/25/2005	-65,20	49,49	075	299,08	32,61	-3,95
19	08/25/2005	-65,20	49,49	050	351,76	32,19	-4,94
19	08/25/2005	-65,20	49,49	030	391,72	31,69	-1,57
19	08/25/2005	-65,20	49,49	020	455,87	31,16	-3,60
19	08/25/2005	-65,20	49,49	010	363,13	29,00	-0,15
19	08/25/2005	-65,20	49,49	0,50	356,26	28,35	-2,26

Tableau B.25

Concentration de NO_x^- et de PO_4^- dans la colonne d'eau à la station 23

Station	Date mois/jour/an	Lon (°E)	Lat (°N)	Profondeur (m)	NO_x^- ($\mu mol\ l^{-1}$)	PO_4^- ($\mu mol\ l^{-1}$)
23	06/11/2006	-68,65	48,70	330,0000	28,56	2,50
23	06/11/2006	-68,65	48,70	300,0000	25,84	2,38
23	06/11/2006	-68,65	48,70	250,0000	26,00	2,29
23	06/11/2006	-68,65	48,70	200,0000	25,33	2,28
23	06/11/2006	-68,65	48,70	150,0000	21,31	1,88
23	06/11/2006	-68,65	48,70	100,0000	14,06	1,35
23	06/11/2006	-68,65	48,70	50,0000	12,24	1,11
23	06/11/2006	-68,65	48,70	40,0000	3,38	0,60
23	06/11/2006	-68,65	48,70	30,0000	3,97	0,56
23	06/11/2006	-68,65	48,70	20,0000	4,13	0,48
23	06/11/2006	-68,65	48,70	10,0000	7,63	0,66
23	06/11/2006	-68,65	48,70	0,5000	6,41	0,59

Tableau B.26

Concentration en oxygène dissous, salinité et N* dans la colonne d'eau à la station 23

Station	Date mois/jour/an	Lon (°E)	Lat (°N)	Profondeur (m)	O_2 ($\mu mol\ l^{-1}$)	Salinité	N* ($\mu mol\ l^{-1}$)
23	06/11/2006	-68,65	48,70	330,0000	65,05	34,55	-8,54
23	06/11/2006	-68,65	48,70	300,0000	65,74	34,55	-9,26
23	06/11/2006	-68,65	48,70	250,0000	65,26	34,47	-7,78
23	06/11/2006	-68,65	48,70	200,0000	66,31	34,12	-8,23
23	06/11/2006	-68,65	48,70	150,0000	67,24	33,65	-5,85
23	06/11/2006	-68,65	48,70	100,0000	66,63	32,78	-4,65
23	06/11/2006	-68,65	48,70	50,0000	77,74	32,06	-2,67
23	06/11/2006	-68,65	48,70	40,0000	77,37	31,98	-3,26
23	06/11/2006	-68,65	48,70	30,0000	128,33	31,21	-2,04
23	06/11/2006	-68,65	48,70	20,0000	127,80	30,46	-0,73
23	06/11/2006	-68,65	48,70	10,0000	234,25	29,23	-0,09
23	06/11/2006	-68,65	48,70	0,5000	235,24	29,23	-0,11

Tableau B.27

Concentration de NO_x^- et de PO_4^- dans la colonne d'eau entre les stations A et F1-B

Station	Date mois/jour/an	Lon (°E)	Lat (°N)	Profondeur (m)	NO_x^- ($\mu mol\ l^{-1}$)	PO_4^- ($\mu mol\ l^{-1}$)
A	06/12/2006	-71,18	46,83	20,0000	28,06	0,22
B	06/12/2006	-70,87	46,96	10,0000	25,46	0,27
C	06/12/2006	-70,79	47,05	10,0000	27,15	0,21
D	06/12/2006	-70,67	47,13	10,0000	32,09	0,47
D-E	06/12/2006	-70,62	47,18	20,0000	28,43	0,74
D-E	06/12/2006	-70,62	47,18	14,0000	30,33	0,71
D-E	06/12/2006	-70,62	47,18	3,0000	30,35	0,65
E	06/13/2006	-70,56	47,24	25,0000	27,96	0,82
E	06/13/2006	-70,56	47,24	15,0000	27,03	2,93
E	06/13/2006	-70,56	47,24	3,0000	29,14	0,71
E-F	06/13/2006	-70,47	47,37	10,0000	28,08	0,78
E-F	06/13/2006	-70,47	47,37	3,0000	28,15	4,83
F2	06/13/2006	-70,35	47,43	50,0000	32,82	1,03
F2	06/13/2006	-70,35	47,43	30,0000	26,21	0,77
F2	06/13/2006	-70,35	47,43	3,0000	26,12	0,80
F1-A	06/13/2006	-70,28	47,41	45,0000	26,61	0,78
F1-A	06/13/2006	-70,28	47,41	11,0000	22,23	0,95
F1-A	06/13/2006	-70,28	47,41	3,0000	18,10	1,02
F1-B	06/13/2006	-70,28	47,41	43,0000	19,18	0,80
F1-B	06/13/2006	-70,28	47,41	11,5000	21,06	0,96
F1-B	06/13/2006	-70,28	47,41	3,0000	27,35	1,05

Tableau B. 28
Concentration en oxygène dissous, salinité et N* dans la colonne d'eau entre les stations A et F1-B

Station	Date mois/jour/an	Lon (°E)	Lat (°N)	Profondeur (m)	O_2 ($\mu mol\ l^{-1}$)	Salinité	N* ($\mu mol\ l^{-1}$)
A	06/12/2006	-71,18	46,83	20,0000	270,96	0,11	27,51
B	06/12/2006	-70,87	46,96	10,0000	272,85	0,11	24,08
C	06/12/2006	-70,79	47,05	10,0000	281,38	0,11	26,71
D	06/12/2006	-70,67	47,13	10,0000	278,96	0,11	27,41
D-E	06/12/2006	-70,62	47,18	20,0000	290,65	7,90	19,45
D-E	06/12/2006	-70,62	47,18	14,0000	289,08	6,00	21,90
D-E	06/12/2006	-70,62	47,18	3,0000	287,94	3,40	22,91
E	06/13/2006	-70,56	47,24	25,0000	294,29	13,80	17,69
E	06/13/2006	-70,56	47,24	15,0000		10,85	-16,90
E	06/13/2006	-70,56	47,24	3,0000	292,18	8,40	20,64
E-F	06/13/2006	-70,47	47,37	10,0000	292,04	10,74	18,47
E-F	06/13/2006	-70,47	47,37	3,0000	291,88	10,28	
F2	06/13/2006	-70,35	47,43	50,0000	294,61	13,00	19,22
F2	06/13/2006	-70,35	47,43	30,0000	293,00	11,70	16,76
F2	06/13/2006	-70,35	47,43	3,0000	291,82	9,70	16,24
F1-A	06/13/2006	-70,28	47,41	45,0000	296,41	23,40	17,00
F1-A	06/13/2006	-70,28	47,41	11,0000	297,30	18,52	9,94
F1-A	06/13/2006	-70,28	47,41	3,0000	294,98	12,50	4,75
F1-B	06/13/2006	-70,28	47,41	43,0000	296,41	22,70	9,29
F1-B	06/13/2006	-70,28	47,41	11,5000	297,30	20,70	8,67
F1-B	06/13/2006	-70,28	47,41	3,0000	294,98	13,01	13,50

Tableau B. 29

Concentration de NO_x^- et de PO_4^- dans la colonne d'eau entre les stations G et K

Station	Date mois/jour/an	Lon (°E)	Lat (°N)	Profondeur (m)	NO_x^- ($\mu mol\ l^{-1}$)	PO_4^- ($\mu mol\ l^{-1}$)
G	06/14/2006	-70,18	47,52	85,0000	14,76	1,07
G	06/14/2006	-70,18	47,52	41,0000	17,52	0,98
G	06/14/2006	-70,18	47,52	20,0000	22,40	0,98
G	06/14/2006	-70,18	47,52	3,0000	24,02	0,84
H	06/14/2006	-70,00	47,60	40,0000	15,11	1,08
H	06/14/2006	-70,00	47,60	30,0000	18,07	1,03
H	06/14/2006	-70,00	47,60	10,0000	23,32	0,88
H	06/14/2006	-70,00	47,60	3,0000	24,46	0,84
I	06/14/2006	-69,90	47,76	86,0000	21,39	0,90
I	06/14/2006	-69,90	47,76	70,0000	13,72	1,11
I	06/14/2006	-69,90	47,76	51,0000	14,94	1,02
I	06/14/2006	-69,90	47,76	30,0000	16,77	1,00
I	06/14/2006	-69,90	47,76	19,5000	17,34	0,99
I	06/14/2006	-69,90	47,76	11,0000	17,88	0,96
I	06/14/2006	-69,90	47,76	3,0000	19,04	0,93
J	06/14/2006	-69,78	47,92	114,0000	13,68	1,13
J	06/14/2006	-69,78	47,92	70,0000	12,84	1,10
J	06/14/2006	-69,78	47,92	50,0000	13,54	1,08
J	06/14/2006	-69,78	47,92	32,0000	14,60	1,03
J	06/14/2006	-69,78	47,92	10,0000	16,84	0,92
J	06/14/2006	-69,78	47,92	3,0000	18,11	0,93
J	06/14/2006	-69,78	47,92	0,5000	17,60	0,98
K	06/15/2006	-69,43	48,10	95,0000	18,92	1,69
K	06/15/2006	-69,43	48,10	70,0000	14,05	1,36
K	06/15/2006	-69,43	48,10	50,0000	14,61	1,43
K	06/15/2006	-69,43	48,10	30,0000	14,48	1,32
K	06/15/2006	-69,43	48,10	20,0000	13,06	1,12
K	06/15/2006	-69,43	48,10	10,0000	13,96	1,09
K	06/15/2006	-69,43	48,10	3,0000	14,95	0,98
K	06/15/2006	-69,43	48,10	0,5000	14,90	0,96

Tableau B.30

Concentration en oxygène dissous, salinité et N* dans la colonne d'eau entre les stations G et K

Station	Date mois/jour/an	Lon (°E)	Lat (°N)	Profondeur (m)	O_2 ($\mu mol\ l^{-1}$)	Salinité	N* ($\mu mol\ l^{-1}$)
G	06/14/2006	-70,18	47,52	85,0000	289,37	23,40	0,56
G	06/14/2006	-70,18	47,52	41,0000	297,92	23,50	4,77
G	06/14/2006	-70,18	47,52	20,0000	297,64	27,06	9,67
G	06/14/2006	-70,18	47,52	3,0000	298,17	17,20	13,50
H	06/14/2006	-70,00	47,60	40,0000	290,70	25,90	0,76
H	06/14/2006	-70,00	47,60	30,0000	293,00	24,30	4,49
H	06/14/2006	-70,00	47,60	10,0000		16,80	12,22
H	06/14/2006	-70,00	47,60	3,0000	296,28	15,75	13,94
I	06/14/2006	-69,90	47,76	86,0000	286,31	28,00	9,86
I	06/14/2006	-69,90	47,76	70,0000		27,50	-1,12
I	06/14/2006	-69,90	47,76	51,0000		26,50	1,50
I	06/14/2006	-69,90	47,76	30,0000	295,79	24,70	3,65
I	06/14/2006	-69,90	47,76	19,5000		23,70	4,43
I	06/14/2006	-69,90	47,76	11,0000		22,70	5,44
I	06/14/2006	-69,90	47,76	3,0000	291,68	20,30	7,00
J	06/14/2006	-69,78	47,92	114,0000	284,41	29,81	-1,52
J	06/14/2006	-69,78	47,92	70,0000		29,50	-1,83
J	06/14/2006	-69,78	47,92	50,0000		28,50	-0,83
J	06/14/2006	-69,78	47,92	32,0000	291,96	26,80	1,05
J	06/14/2006	-69,78	47,92	10,0000		22,97	5,05
J	06/14/2006	-69,78	47,92	3,0000	301,66	22,10	6,19
J	06/14/2006	-69,78	47,92	0,5000		22,10	4,88
K	06/15/2006	-69,43	48,10	95,0000	189,97	33,04	-5,23
K	06/15/2006	-69,43	48,10	70,0000		32,40	-4,80
K	06/15/2006	-69,43	48,10	50,0000	248,88	32,20	-5,32
K	06/15/2006	-69,43	48,10	30,0000		31,50	-3,80
K	06/15/2006	-69,43	48,10	20,0000		28,90	-1,89
K	06/15/2006	-69,43	48,10	10,0000		26,13	-0,66
K	06/15/2006	-69,43	48,10	3,0000	295,25	24,90	2,23
K	06/15/2006	-69,43	48,10	0,5000		24,92	2,44

Tableau B.31
Concentration de NO_x^- et de PO_4^- dans la colonne d'eau à la station 25

Station	Date mois/jour/an	Lon (°E)	Lat (°N)	Profondeur (m)	NO_x^- ($\mu mol\ l^{-1}$)	PO_4^- ($\mu mol\ l^{-1}$)
25	06/15/2006	-69,38	48,29	311,0000	21,52	2,12
25	06/15/2006	-69,38	48,29	200,0000	23,19	2,15
25	06/15/2006	-69,38	48,29	149,0000	20,68	1,91
25	06/15/2006	-69,38	48,29	100,0000	13,17	1,31
25	06/15/2006	-69,38	48,29	70,0000	11,18	1,16
25	06/15/2006	-69,38	48,29	41,0000	9,88	1,01
25	06/15/2006	-69,38	48,29	20,0000	10,82	0,95
25	06/15/2006	-69,38	48,29	3,0000	12,85	0,85
25	06/15/2006	-69,38	48,29	0,5000	12,54	0,85

Tableau B.32
Concentration en oxygène dissous, salinité et N* dans la colonne d'eau à la station 25

Station	Date mois/jour/an	Lon (°E)	Lat (°N)	Profondeur (m)	O_2 ($\mu mol\ l^{-1}$)	Salinité	N* ($\mu mol\ l^{-1}$)
25	06/15/2006	-69,38	48,29	311,0000	63,32	34,41	-9,55
25	06/15/2006	-69,38	48,29	200,0000		34,05	-8,25
25	06/15/2006	-69,38	48,29	149,0000		33,52	-6,91
25	06/15/2006	-69,38	48,29	100,0000		32,42	-4,88
25	06/15/2006	-69,38	48,29	70,0000	288,58	31,54	-4,41
25	06/15/2006	-69,38	48,29	41,0000		30,09	-3,39
25	06/15/2006	-69,38	48,29	20,0000		28,03	-1,41
25	06/15/2006	-69,38	48,29	3,0000	304,79	25,30	2,15
25	06/15/2006	-69,38	48,29	0,5000		25,20	1,92

Tableau B.33

Concentration de NO_x^- et de PO_4^- dans la colonne d'eau à la station 21

Station	Date mois/jour/an	Lon (°E)	Lat (°N)	Profondeur (m)	NO_x^- ($\mu mol\ l^{-1}$)	PO_4^- ($\mu mol\ l^{-1}$)
21	08/06/2006	-67,28	49,11	312	28,75	2,25
21	08/06/2006	-67,28	49,11	298	24,71	2,00
21	08/06/2006	-67,28	49,11	250	24,51	2,20
21	08/06/2006	-67,28	49,11	200	17,94	1,53
21	08/06/2006	-67,28	49,11	175	16,79	1,48
21	08/06/2006	-67,28	49,11	122	9,37	1,05
21	08/06/2006	-67,28	49,11	60	8,04	0,93
21	08/06/2006	-67,28	49,11	40	6,67	0,81
21	08/06/2006	-67,28	49,11	30	5,57	0,60
21	08/06/2006	-67,28	49,11	21	11,17	0,84
21	08/06/2006	-67,28	49,11	11	7,61	0,54
21	08/06/2006	-67,28	49,11	1	1,95	0,19

Tableau B.34

Concentration en oxygène dissous, salinité et N* dans la colonne d'eau à la station 21

Station	Date mois/jour/an	Lon (°E)	Lat (°N)	Profondeur (m)	O_2 ($\mu mol\ l^{-1}$)	Salinité	N* ($\mu mol\ l^{-1}$)
21	08/06/2006	-67,28	49,11	312	74,55	34,68	-4,28
21	08/06/2006	-67,28	49,11	298	46,40	34,68	-4,42
21	08/06/2006	-67,28	49,11	250	57,33	34,42	-7,86
21	08/06/2006	-67,28	49,11	200	84,11	34,18	-3,59
21	08/06/2006	-67,28	49,11	175	96,08	33,89	-4,00
21	08/06/2006	-67,28	49,11	122	181,94	33,04	-4,56
21	08/06/2006	-67,28	49,11	60		31,91	-3,96
21	08/06/2006	-67,28	49,11	40		31,54	-3,44
21	08/06/2006	-67,28	49,11	30	260,41	30,95	-1,20
21	08/06/2006	-67,28	49,11	21	243,99	29,52	0,65
21	08/06/2006	-67,28	49,11	11	288,07	28,59	1,89
21	08/06/2006	-67,28	49,11	1	293,38	26,84	1,83

Tableau B.35
Concentration de NO_x^- et de PO_4^- dans la colonne d'eau à la station 18

Station	Date mois/jour/an	Lon (°E)	Lat (°N)	Profondeur (m)	NO_x^- ($\mu mol\ l^{-1}$)	PO_4^- ($\mu mol\ l^{-1}$)
18	08/07/2006	-64,26	49,29	370	26,14	1,81
18	08/07/2006	-64,26	49,29	330	14,28	1,26
18	08/07/2006	-64,26	49,29	270	25,69	1,82
18	08/07/2006	-64,26	49,29	230	21,45	1,56
18	08/07/2006	-64,26	49,29	150	13,11	1,15
18	08/07/2006	-64,26	49,29	100	12,99	1,12
18	08/07/2006	-64,26	49,29	60	5,47	0,71
18	08/07/2006	-64,26	49,29	40	3,80	0,63
18	08/07/2006	-64,26	49,29	30	1,78	0,30
18	08/07/2006	-64,26	49,29	15	1,65	0,26
18	08/07/2006	-64,26	49,29	5	0,00	0,09
18	08/07/2006	-64,26	49,29	1	0,00	0,06

Tableau B.36
Concentration en oxygène dissous, salinité et N* dans la colonne d'eau à la station 18

Station	Date mois/jour/an	Lon (°E)	Lat (°N)	Profondeur (m)	O_2 ($\mu mol\ l^{-1}$)	Salinité	N* ($\mu mol\ l^{-1}$)
18	08/07/2006	-64,26	49,29	370	122,42	34,80	0,11
18	08/07/2006	-64,26	49,29	330	117,77	34,79	-3,06
18	08/07/2006	-64,26	49,29	270	98,56	34,68	-0,51
18	08/07/2006	-64,26	49,29	230	81,04	34,47	-0,64
18	08/07/2006	-64,26	49,29	150	137,27	33,60	-2,38
18	08/07/2006	-64,26	49,29	100	250,63	32,72	-1,99
18	08/07/2006	-64,26	49,29	60	320,78	31,94	-2,92
18	08/07/2006	-64,26	49,29	40	324,14	31,47	-3,33
18	08/07/2006	-64,26	49,29	30	301,57	30,50	-0,18
18	08/07/2006	-64,26	49,29	15	272,51	28,95	0,34
18	08/07/2006	-64,26	49,29	5	270,73	28,90	1,52
18	08/07/2006	-64,26	49,29	1	278,41	28,90	1,94

Tableau B.37
Concentration de NO_x^- et de PO_4^- dans la colonne d'eau à la station 19

Station	Date mois/jour/an	Lon (°E)	Lat (°N)	Profondeur (m)	NO_x^- ($\mu mol\ l^{-1}$)	PO_4^- ($\mu mol\ l^{-1}$)
19	08/08/2006	-65,19	49,48	360	26,09	1,85
19	08/08/2006	-65,19	49,48	300	23,91	1,74
19	08/08/2006	-65,19	49,48	225	24,68	1,94
19	08/08/2006	-65,19	49,48	200	24,02	1,87
19	08/08/2006	-65,19	49,48	150	17,64	1,40
19	08/08/2006	-65,19	49,48	100	14,66	1,23
19	08/08/2006	-65,19	49,48	70	8,16	0,86
19	08/08/2006	-65,19	49,48	40	5,31	0,73
19	08/08/2006	-65,19	49,48	20	5,64	0,65
19	08/08/2006	-65,19	49,48	10	1,52	0,26
19	08/08/2006	-65,19	49,48	5	0,10	0,07
19	08/08/2006	-65,19	49,48	1	0,05	0,03

Tableau B.38
Concentration en oxygène dissous, salinité et N* dans la colonne d'eau à la station 19

Station	Date mois/jour/an	Lon (°E)	Lat (°N)	Profondeur (m)	O_2 ($\mu mol\ l^{-1}$)	Salinité	N* ($\mu mol\ l^{-1}$)
19	08/08/2006	-65,19	49,48	360	108,22	34,76	-0,67
19	08/08/2006	-65,19	49,48	300	95,98	34,68	-1,05
19	08/08/2006	-65,19	49,48	225	72,88	34,41	-3,43
19	08/08/2006	-65,19	49,48	200	80,52	34,21	-3,00
19	08/08/2006	-65,19	49,48	150	137,36	33,57	-1,88
19	08/08/2006	-65,19	49,48	100	266,79	33,77	-2,12
19	08/08/2006	-65,19	49,48	70	292,58	32,07	-2,64
19	08/08/2006	-65,19	49,48	40	308,15	31,63	-3,47
19	08/08/2006	-65,19	49,48	20	291,57	30,56	-1,78
19	08/08/2006	-65,19	49,48	10	268,54	29,10	0,27
19	08/08/2006	-65,19	49,48	5	271,05	27,92	1,83
19	08/08/2006	-65,19	49,48	1	267,19	27,92	2,42

Tableau B.39
Concentration de NO_x^- et de PO_4^- dans la colonne d'eau à la station 20

Station	Date mois/jour/an	Lon (°E)	Lat (°N)	Profondeur (m)	NO_x^- ($\mu mol\ l^{-1}$)	PO_4^- ($\mu mol\ l^{-1}$)
20	08/09/2006	-66,33	49,42	319	25,96	1,94
20	08/09/2006	-66,33	49,42	260	23,88	1,81
20	08/09/2006	-66,33	49,42	210	24,09	1,99
20	08/09/2006	-66,33	49,42	150	22,44	1,84
20	08/09/2006	-66,33	49,42	100	18,06	1,43
20	08/09/2006	-66,33	49,42	70	13,96	1,19
20	08/09/2006	-66,33	49,42	40	7,77	0,85
20	08/09/2006	-66,33	49,42	30	5,58	0,74
20	08/09/2006	-66,33	49,42	20	3,58	0,56
20	08/09/2006	-66,33	49,42	10	0,03	0,19
20	08/09/2006	-66,33	49,42	5	0,01	0,10
20	08/09/2006	-66,33	49,42	1	0,00	0,11

Tableau B.40
Concentration en oxygène dissous, salinité et N* dans la colonne d'eau à la station 20

Station	Date mois/jour/an	Lon (°E)	Lat (°N)	Profondeur (m)	O_2 ($\mu mol\ l^{-1}$)	Salinité	N* ($\mu mol\ l^{-1}$)
20	08/09/2006	-66,33	49,42	319	96,78	34,75	-2,20
20	08/09/2006	-66,33	49,42	260	85,99	34,68	-2,24
20	08/09/2006	-66,33	49,42	210	71,41	34,43	-4,90
20	08/09/2006	-66,33	49,42	150	101,57	33,91	-4,12
20	08/09/2006	-66,33	49,42	100	174,99	33,27	-1,95
20	08/09/2006	-66,33	49,42	70	234,46	32,72	-2,21
20	08/09/2006	-66,33	49,42	40	309,72	32,06	-3,01
20	08/09/2006	-66,33	49,42	30	327,52	31,80	-3,34
20	08/09/2006	-66,33	49,42	20	337,44	31,35	-2,53
20	08/09/2006	-66,33	49,42	10	296,95	29,31	-0,16
20	08/09/2006	-66,33	49,42	5	287,26	29,32	1,29
20	08/09/2006	-66,33	49,42	1	286,90	29,32	1,20

Tableau B.41
Concentration de NO_x^- et de PO_4^- dans la colonne d'eau à la station 22

Station	Date mois/jour/an	Lon (°E)	Lat (°N)	Profondeur (m)	NO_x^- ($\mu mol\ l^{-1}$)	PO_4^- ($\mu mol\ l^{-1}$)
22	08/10/2006	-68,09	48,94	301	25,99	2,14
22	08/10/2006	-68,09	48,94	250	23,34	1,96
22	08/10/2006	-68,09	48,94	200	23,18	2,01
22	08/10/2006	-68,09	48,94	150	21,96	1,87
22	08/10/2006	-68,09	48,94	100	17,43	1,48
22	08/10/2006	-68,09	48,94	60	10,18	1,01
22	08/10/2006	-68,09	48,94	40	5,72	0,71
22	08/10/2006	-68,09	48,94	30	8,43	0,79
22	08/10/2006	-68,09	48,94	20	8,74	0,69
22	08/10/2006	-68,09	48,94	10	7,81	0,53
22	08/10/2006	-68,09	48,94	5	7,87	0,55
22	08/10/2006	-68,09	48,94	1	7,07	0,45

Tableau B.42
Concentration en oxygène dissous, salinité et N* dans la colonne d'eau à la station 22

Station	Date mois/jour/an	Lon (°E)	Lat (°N)	Profondeur (m)	O_2 ($\mu mol\ l^{-1}$)	Salinité	N* ($\mu mol\ l^{-1}$)
22	08/10/2006	-68,09	48,94	301	69,64	34,65	-5,30
22	08/10/2006	-68,09	48,94	250	67,17	34,52	-5,13
22	08/10/2006	-68,09	48,94	200	71,19	34,20	-6,06
22	08/10/2006	-68,09	48,94	150	89,63	33,87	-5,12
22	08/10/2006	-68,09	48,94	100	167,09	33,14	-3,29
22	08/10/2006	-68,09	48,94	60	232,19	32,20	-3,03
22	08/10/2006	-68,09	48,94	40	296,38	31,06	-2,70
22	08/10/2006	-68,09	48,94	30	262,91	30,27	-1,29
22	08/10/2006	-68,09	48,94	20	272,64	28,80	0,56
22	08/10/2006	-68,09	48,94	10	265,75	26,74	2,24
22	08/10/2006	-68,09	48,94	5	276,78	25,80	2,01
22	08/10/2006	-68,09	48,94	1	284,39	25,36	2,79

Tableau B.43
Concentration de NO_x^- et de PO_4^- dans la colonne d'eau à la station TCA

Station	Date mois/jour/an	Lon (°E)	Lat (°N)	Profondeur (m)	NO_x^- ($\mu mol\ l^{-1}$)	PO_4^- ($\mu mol\ l^{-1}$)
TCA	08/17/2006	-61,82	49,68	270	26,28	1,97
TCA	08/17/2006	-61,82	49,68	250	24,14	1,72
TCA	08/17/2006	-61,82	49,68	225	24,19	1,68
TCA	08/17/2006	-61,82	49,68	200	23,75	1,70
TCA	08/17/2006	-61,82	49,68	150	19,77	1,48
TCA	08/17/2006	-61,82	49,68	100	11,75	1,00
TCA	08/17/2006	-61,82	49,68	50	4,45	0,64
TCA	08/17/2006	-61,82	49,68	40	2,17	0,51
TCA	08/17/2006	-61,82	49,68	30	1,36	0,55
TCA	08/17/2006	-61,82	49,68	20	0,07	0,36
TCA	08/17/2006	-61,82	49,68	10	0,00	0,20
TCA	08/17/2006	-61,82	49,68	1	0,00	0,14

Tableau B.44
Concentration en oxygène dissous, salinité et N* dans la colonne d'eau à la station TCA

Station	Date mois/jour/an	Lon (°E)	Lat (°N)	Profondeur (m)	O_2 ($\mu mol\ l^{-1}$)	Salinité	N* ($\mu mol\ l^{-1}$)
TCA	08/17/2006	-61,82	49,68	270	105,79	34,59	-2,35
TCA	08/17/2006	-61,82	49,68	250	107,72	34,59	-0,47
TCA	08/17/2006	-61,82	49,68	225	111,93	34,48	0,14
TCA	08/17/2006	-61,82	49,68	200	115,92	34,35	-0,53
TCA	08/17/2006	-61,82	49,68	150	162,95	33,76	-1,00
TCA	08/17/2006	-61,82	49,68	100	272,66	32,91	-1,34
TCA	08/17/2006	-61,82	49,68	50	338,63	32,07	-2,96
TCA	08/17/2006	-61,82	49,68	40	354,15	31,96	-3,09
TCA	08/17/2006	-61,82	49,68	30	361,16	31,82	-4,50
TCA	08/17/2006	-61,82	49,68	20	374,00	31,70	-2,84
TCA	08/17/2006	-61,82	49,68	10	274,00	30,74	-0,31
TCA	08/17/2006	-61,82	49,68	1	270,88	30,75	0,66

Tableau B. 45
Concentration de NO_x^- et de PO_4^- dans la colonne d'eau à la station CA

Station	Date mois/jour/an	Lon (°E)	Lat (°N)	Profondeur (m)	NO_x^- ($\mu mol\ l^{-1}$)	PO_4^- ($\mu mol\ l^{-1}$)
CA	08/17/2006	-60,85	49,54	280	25,65	1,84
CA	08/17/2006	-60,85	49,54	250	23,58	1,67
CA	08/17/2006	-60,85	49,54	225	23,66	1,64
CA	08/17/2006	-60,85	49,54	200	21,91	1,55
CA	08/17/2006	-60,85	49,54	150	14,79	1,18
CA	08/17/2006	-60,85	49,54	100	9,13	0,86
CA	08/17/2006	-60,85	49,54	50	3,54	0,59
CA	08/17/2006	-60,85	49,54	40	2,10	0,50
CA	08/17/2006	-60,85	49,54	30	0,57	0,55
CA	08/17/2006	-60,85	49,54	20	0,06	0,41
CA	08/17/2006	-60,85	49,54	10	0,00	0,17
CA	08/17/2006	-60,85	49,54	1	0,00	0,06

Tableau B.46
Concentration en oxygène dissous, salinité et N* dans la colonne d'eau à la station CA

Station	Date mois/jour/an	Lon (°E)	Lat (°N)	Profondeur (m)	O_2 ($\mu mol\ l^{-1}$)	Salinité	N* ($\mu mol\ l^{-1}$)
CA	08/17/2006	-60,85	49,54	280	124,34	34,68	-0,96
CA	08/17/2006	-60,85	49,54	250	115,00	34,61	-0,30
CA	08/17/2006	-60,85	49,54	225	116,00	34,47	0,29
CA	08/17/2006	-60,85	49,54	200	127,00	34,19	0,01
CA	08/17/2006	-60,85	49,54	150	173,00	33,15	-1,11
CA	08/17/2006	-60,85	49,54	100	280,00	32,65	-1,69
CA	08/17/2006	-60,85	49,54	50	350,00	32,07	-2,95
CA	08/17/2006	-60,85	49,54	40	364,00	31,91	-3,03
CA	08/17/2006	-60,85	49,54	30	375,00	31,81	-5,37
CA	08/17/2006	-60,85	49,54	20	375,00	31,69	-3,68
CA	08/17/2006	-60,85	49,54	10	275,00	30,20	0,21
CA	08/17/2006	-60,85	49,54	1	273,00	30,25	1,89

Tableau B.47
Concentration de NO_x^- et de PO_4^- dans la colonne d'eau à la station CE

Station	Date mois/jour/an	Lon (°E)	Lat (°N)	Profondeur (m)	NO_x^- ($\mu mol\ l^{-1}$)	PO_4^- ($\mu mol\ l^{-1}$)
CE	08/18/2006	-59,26	49,80	245	24,80	1,71
CE	08/18/2006	-59,26	49,80	225	22,54	1,57
CE	08/18/2006	-59,26	49,80	200	24,40	1,76
CE	08/18/2006	-59,26	49,80	150	16,10	1,28
CE	08/18/2006	-59,26	49,80	125	12,75	1,05
CE	08/18/2006	-59,26	49,80	100	9,61	0,87
CE	08/18/2006	-59,26	49,80	50	2,69	0,48
CE	08/18/2006	-59,26	49,80	40	1,73	0,63
CE	08/18/2006	-59,26	49,80	30	0,62	0,61
CE	08/18/2006	-59,26	49,80	20	0,06	0,27
CE	08/18/2006	-59,26	49,80	10	0,00	0,14
CE	08/18/2006	-59,26	49,80	1	0,00	0,15

Tableau B.48
Concentration en oxygène dissous, salinité et N* dans la colonne d'eau à la station CE

Station	Date mois/jour/an	Lon (°E)	Lat (°N)	Profondeur (m)	O_2 ($\mu mol\ l^{-1}$)	Salinité	N* ($\mu mol\ l^{-1}$)
CE	08/18/2006	-59,26	49,80	245	126,01	34,56	0,29
CE	08/18/2006	-59,26	49,80	225	127,00	34,43	0,40
CE	08/18/2006	-59,26	49,80	200	110,00	34,27	-0,92
CE	08/18/2006	-59,26	49,80	150	214,00	33,51	-1,40
CE	08/18/2006	-59,26	49,80	125	270,00	33,03	-1,19
CE	08/18/2006	-59,26	49,80	100	309,00	32,68	-1,47
CE	08/18/2006	-59,26	49,80	50	361,00	31,91	-2,16
CE	08/18/2006	-59,26	49,80	40	356,00	31,87	-5,43
CE	08/18/2006	-59,26	49,80	30	338,00	31,67	-6,32
CE	08/18/2006	-59,26	49,80	20	266,00	31,50	-1,39
CE	08/18/2006	-59,26	49,80	10	265,00	30,75	0,67
CE	08/18/2006	-59,26	49,80	1	266,00	30,74	0,55

Tableau B.49
Concentration de NO_x^- et de PO_4^- dans la colonne d'eau à la station TCE

Station	Date mois/jour/an	Lon (°E)	Lat (°N)	Profondeur (m)	NO_x^- ($\mu mol\ l^{-1}$)	PO_4^- ($\mu mol\ l^{-1}$)
TCE	08/18/2006	-58,11	50,47	270	26,04	1,98
TCE	08/18/2006	-58,11	50,47	250	24,07	1,80
TCE	08/18/2006	-58,11	50,47	225	24,56	1,78
TCE	08/18/2006	-58,11	50,47	200	23,10	1,63
TCE	08/18/2006	-58,11	50,47	150	15,84	1,20
TCE	08/18/2006	-58,11	50,47	100	10,59	0,92
TCE	08/18/2006	-58,11	50,47	50	3,56	0,54
TCE	08/18/2006	-58,11	50,47	40	1,36	0,41
TCE	08/18/2006	-58,11	50,47	30	0,02	0,49
TCE	08/18/2006	-58,11	50,47	20	0,01	0,20
TCE	08/18/2006	-58,11	50,47	10	0,00	0,15
TCE	08/18/2006	-58,11	50,47	1	0,00	0,15

Tableau B.50
Concentration en oxygène dissous, salinité et N* dans la colonne d'eau à la station TCE

Station	Date mois/jour/an	Lon (°E)	Lat (°N)	Profondeur (m)	O_2 ($\mu mol\ l^{-1}$)	Salinité	N* ($\mu mol\ l^{-1}$)
TCE	08/18/2006	-58,11	50,47	270	93,55	34,49	-2,69
TCE	08/18/2006	-58,11	50,47	250	96,27	34,49	-1,87
TCE	08/18/2006	-58,11	50,47	225	99,00	34,39	-0,97
TCE	08/18/2006	-58,11	50,47	200	125,66	34,22	-0,06
TCE	08/18/2006	-58,11	50,47	150	214,00	33,42	-0,40
TCE	08/18/2006	-58,11	50,47	100	294,00	32,73	-1,20
TCE	08/18/2006	-58,11	50,47	50	356,00	31,98	-2,25
TCE	08/18/2006	-58,11	50,47	40	367,00	31,82	-2,31
TCE	08/18/2006	-58,11	50,47	30	359,00	31,72	-4,91
TCE	08/18/2006	-58,11	50,47	20	293,00	30,81	-0,25
TCE	08/18/2006	-58,11	50,47	10	270,00	30,87	0,53
TCE	08/18/2006	-58,11	50,47	1	270,00	30,87	0,50

Tableau B.51
Concentration de NO_x^- et de PO_4^- dans la colonne d'eau à la station 16

Station	Date mois/jour/an	Lon (°E)	Lat (°N)	Profondeur (m)	NO_x^- ($\mu mol\ l^{-1}$)	PO_4^- ($\mu mol\ l^{-1}$)
16	08/20/2006	-60,73	48,40	420	22,02	1,49
16	08/20/2006	-60,73	48,40	350	20,79	1,31
16	08/20/2006	-60,73	48,40	275	21,63	1,33
16	08/20/2006	-60,73	48,40	250	21,31	1,33
16	08/20/2006	-60,73	48,40	200	19,37	1,30
16	08/20/2006	-60,73	48,40	150	16,14	1,19
16	08/20/2006	-60,73	48,40	100	8,89	0,81
16	08/20/2006	-60,73	48,40	50	2,71	0,44
16	08/20/2006	-60,73	48,40	40	0,84	0,53
16	08/20/2006	-60,73	48,40	30	0,00	0,14
16	08/20/2006	-60,73	48,40	20	0,00	0,08
16	08/20/2006	-60,73	48,40	1	0,00	0,07

Tableau B.52
Concentration en oxygène dissous, salinité et N* dans la colonne d'eau à la station 16

Station	Date mois/jour/an	Lon (°E)	Lat (°N)	Profondeur (m)	O_2 ($\mu mol\ l^{-1}$)	Salinité	N* ($\mu mol\ l^{-1}$)
16	08/20/2006	-60,73	48,40	420	196,58	34,86	1,12
16	08/20/2006	-60,73	48,40	350	195,22	34,85	2,70
16	08/20/2006	-60,73	48,40	275	174,85	34,74	3,26
16	08/20/2006	-60,73	48,40	250	176,18	34,68	2,98
16	08/20/2006	-60,73	48,40	200	181,18	34,33	1,52
16	08/20/2006	-60,73	48,40	150	217,62	33,60	-0,01
16	08/20/2006	-60,73	48,40	100	322,78	32,56	-1,19
16	08/20/2006	-60,73	48,40	50	375,48	31,80	-1,38
16	08/20/2006	-60,73	48,40	40	347,00	31,06	-4,80
16	08/20/2006	-60,73	48,40	30	339,00	30,25	0,58
16	08/20/2006	-60,73	48,40	20	285,00	30,24	1,57
16	08/20/2006	-60,73	48,40	1	257,00	30,24	1,73

Tableau B.53
Concentration de NO_x^- et de PO_4^- dans la colonne d'eau à la station 17

Station	Date mois/jour/an	Lon (°E)	Lat (°N)	Profondeur (m)	NO_x^- ($\mu mol\ l^{-1}$)	PO_4^- ($\mu mol\ l^{-1}$)
17	08/20/2006	-63,12	48,97	390	23,35	1,58
17	08/21/2006	-63,12	48,97	350	21,41	1,41
17	08/21/2006	-63,12	48,97	285	22,71	1,50
17	08/21/2006	-63,12	48,97	250	23,28	1,68
17	08/21/2006	-63,12	48,97	200	20,00	1,49
17	08/21/2006	-63,12	48,97	150	14,35	1,15
17	08/21/2006	-63,12	48,97	100	8,58	0,77
17	08/21/2006	-63,12	48,97	50	4,60	0,59
17	08/21/2006	-63,12	48,97	30	2,38	0,46
17	08/21/2006	-63,12	48,97	20	1,10	0,57
17	08/21/2006	-63,12	48,97	10	0,08	0,20
17	08/21/2006	-63,12	48,97	1	0,00	0,05

Tableau B.54
Concentration en oxygène dissous, salinité et N* dans la colonne d'eau à la station 17

Station	Date mois/jour/an	Lon (°E)	Lat (°N)	Profondeur (m)	O_2 ($\mu mol\ l^{-1}$)	Salinité	N* ($\mu mol\ l^{-1}$)
17	08/20/2006	-63,12	48,97	390	162,12	34,82	1,03
17	08/21/2006	-63,12	48,97	350	158,00	34,82	1,76
17	08/21/2006	-63,12	48,97	285	138,78	34,70	1,69
17	08/21/2006	-63,12	48,97	250	113,00	34,42	-0,66
17	08/21/2006	-63,12	48,97	200	159,00	33,76	-0,96
17	08/21/2006	-63,12	48,97	150	242,00	33,19	-1,09
17	08/21/2006	-63,12	48,97	100	333,00	32,76	-0,81
17	08/21/2006	-63,12	48,97	50	351,00	31,91	-1,99
17	08/21/2006	-63,12	48,97	30	348,00	31,69	-2,06
17	08/21/2006	-63,12	48,97	20	344,00	31,35	-5,18
17	08/21/2006	-63,12	48,97	10	264,00	29,33	-0,20
17	08/21/2006	-63,12	48,97	1	266,00	29,30	2,15

Tableau B.55

Concentration de nitrate et nitrite, phosphate, ammonium et silice dans les eaux porales de la carotte prise à la station 22 en 2006

Profondeur (cm)	NO_3+NO_2 ($\mu mol\ l^{-1}$)	PO_4 ($\mu mol\ l^{-1}$)	NH_4 ($\mu mol\ l^{-1}$)	SiO_2 ($\mu mol\ l^{-1}$)
-0,42	25,37	2,43	0,00	45,67
-0,21	23,41	2,22	0,00	40,44
0,00	23,87	2,28	0,00	42,90
0,21	18,71	3,21	0,33	84,44
0,43	13,51	4,05	0,62	147,48
0,65	11,08	4,54	0,53	156,30
0,87	7,90	4,66	1,53	161,22
1,08	5,97	5,07	3,26	155,11
1,30	4,74	5,32	4,14	242,24
1,52	4,98	5,27	4,25	231,62
1,76	7,34	6,22	7,25	244,88
2,04	6,70	6,13	6,45	269,70
2,26	4,84	6,27	6,28	262,32
2,47	4,91	6,38	6,91	250,56
2,69	5,44	6,83	7,17	279,52
2,91	7,48	6,94	8,27	259,08
3,13	6,66	7,55	8,96	272,59
3,34	4,63	8,07	9,54	295,96
3,56	2,51	7,94	9,25	294,77
3,78	2,10	8,73	8,72	306,38
3,99	0,78	9,37	9,46	309,22
4,21	0,18	8,98	10,59	269,25
4,43	0,30	9,65	12,13	377,46
4,66	0,33	20,12	35,92	182,92
3	0,61	8,92	3,55	176,95
6	2,69	10,64	8,77	212,96
9	1,74	28,23	26,41	270,16
12	2,53	33,13	34,41	286,35
15	1,89	42,97	42,06	312,35
18	1,13	37,77	48,57	339,20
21	2,88	31,37	54,07	332,42
30	1,09	33,80	59,13	207,70

Tableau B.56
Concentration de nitrate et nitrite, phosphate, ammonium et silice dans les eaux porales de la carotte prise à la station 21 en 2006

Profondeur (cm)	NO_3+NO_2 ($\mu mol\ l^{-1}$)	PO_4 ($\mu mol\ l^{-1}$)	NH_4 ($\mu mol\ l^{-1}$)	SiO_2 ($\mu mol\ l^{-1}$)
-1,29	28,60	2,23	0,00	41,88
-1,08	25,16	2,16	0,00	40,08
-0,87	25,39	2,24	0,00	41,82
-0,65	25,52	2,31	0,00	43,51
-0,44	24,98	2,40	0,71	47,70
-0,23	23,77	2,61	0,77	59,48
0,00	22,52	2,91	0,72	75,72
0,21	18,61	3,53	0,91	105,40
0,43	13,97	4,18	0,89	153,03
0,66	10,53	4,37	1,58	154,68
0,89	7,14	4,54	0,88	166,10
1,14	5,17	4,80	1,93	163,74
1,38	2,86	5,02	2,66	182,90
1,64	2,20	5,25	2,96	215,97
1,89	1,93	5,49	3,55	204,83
2,15	1,36	5,49	4,32	199,19
2,42	1,90	5,54	4,39	216,53
2,68	4,13	7,51	9,55	231,64
2,95	3,21	6,86	9,52	242,17
3,22	1,91	7,23	8,51	232,74
3,55	0,47	7,59	12,29	241,70
2,50	2,00			
5,50	0,79	15,12	11,20	242,49
8,50	0,47	9,17	17,67	328,76
11,50	1,56			
14,50	0,96	34,50	29,86	302,33
17,50	0,79	37,73	41,31	287,93
20,50	1,53			
23,50	1,39			
26,50	0,64	45,67	71,68	391,57
29,50	0,53	49,59	81,53	333,46

Tableau B.57
Concentration de nitrate et nitrite, phosphate, ammonium et silice dans les eaux porales de la carotte prise à la station 20 en 2006

Profondeur (cm)	NO_3+NO_2 ($\mu mol\ l^{-1}$)	PO_4 ($\mu mol\ l^{-1}$)	NH_4 ($\mu mol\ l^{-1}$)	SiO_2 ($\mu mol\ l^{-1}$)
-0,65	28,08	2,16	0,00	37,69
-0,44	24,19	2,04	0,00	32,17
-0,22	24,81	2,14	0,00	33,46
0,00	24,64	2,16	0,28	34,51
0,22	20,73	3,29	0,79	80,61
0,45	18,28	3,52	0,74	108,83
0,68	12,96	3,92	0,87	129,41
0,91	8,97	4,95	2,30	149,41
1,16	6,75	5,41	3,75	178,84
1,42	5,05	5,91	5,21	190,64
1,71	3,43	6,32	6,24	191,23
1,97	2,10	6,77	7,06	200,89
2,24	1,73	7,02	7,30	196,04
2,51	1,78	7,91	8,13	198,86
2,78	1,53	8,48	9,67	208,33
3,05	2,17	10,23	11,06	197,18
3,33	2,48	8,76	9,41	204,61
3,61	1,89	9,22	10,40	213,08
3,89	1,72	8,78	10,11	204,76
4,17	1,67	9,92	10,61	221,46
4,45	1,69	9,66	11,74	200,35
4,73	1,50	9,31	11,14	189,50
5,01	1,34	9,09	11,43	193,12
5,30	1,11	9,80	13,17	227,16
5,59	0,70	9,13	15,72	204,86

Tableau B.58

Concentration de nitrate et nitrite, phosphate, ammonium et silice dans les eaux porales de la carotte prise à la station 20 en 2006 à l'aide de céramique poreuse

Profondeur (cm)	NO_3+NO_2 ($\mu mol\ l^{-1}$)	PO_4 ($\mu mol\ l^{-1}$)	NH_4 ($\mu mol\ l^{-1}$)	SiO_2 ($\mu mol\ l^{-1}$)
3,50	0,36	10,70	2,86	186,77
6,50	0,60	17,24	11,96	195,87
9,50	0,26	16,16	27,28	215,66
12,50	0,24	19,77	36,38	256,72
15,50	0,20	24,33	44,75	241,62
18,50	0,19	22,49	52,02	271,32
21,50	0,38	18,61	58,56	236,27
24,50	0,22	19,57	61,42	270,67
27,50	0,29	19,32	67,32	265,06
30,50	0,50	21,03	73,48	233,13

Tableau B.59
Concentration de nitrate et nitrite, phosphate, ammonium et silice dans les eaux porales de la carotte prise à la station 19 en 2006

Profondeur (cm)	NO_3+NO_2 ($\mu mol\ l^{-1}$)	PO_4 ($\mu mol\ l^{-1}$)	NH_4 ($\mu mol\ l^{-1}$)	SiO_2 ($\mu mol\ l^{-1}$)
-1,07	29,52	1,83	0,00	32,17
-0,86	20,44	1,95	0,00	33,35
-0,65	23,58	1,90	0,00	32,29
-0,43	21,90	2,29	0,19	32,13
-0,22	21,69	2,91	0,54	60,21
0,00	19,09	2,73	0,22	69,63
0,21	17,82	3,48	0,30	116,53
0,43	12,32	4,09	3,27	145,37
0,66	10,42	4,34	6,98	152,75
0,89	7,30	4,85	7,96	169,26
1,14	5,97	5,22	10,64	204,26
1,38	4,39	6,04	13,49	243,41
1,64	3,65	6,41	16,58	244,45
1,89	2,59	7,41	17,13	243,90
2,15	2,82	7,75	17,35	262,04
2,42	2,64	7,46	18,13	254,16
2,68	1,95	7,65	18,10	274,33
3,04	0,93	7,22	19,61	263,77
3,30	0,55	7,11	20,75	279,48
3,56	0,74	7,37	21,32	271,50
3,84	0,54	6,75	20,40	242,62
4,11	0,32	6,71	20,09	279,38
4,39	0,19	6,82	21,31	284,04
4,66	0,08	6,60	19,72	282,21
4,94	0,10	7,47	11,15	292,21
5,30	0,15	7,56	10,74	301,68
5,58	0,07	7,30	22,20	297,22

Tableau B.60

Concentration de nitrate et nitrite, phosphate, ammonium et silice dans les eaux porales de la carotte prise à la station 19 en 2006 à l'aide de céramique poreuse,

Profondeur (cm)	NO_3+NO_2 ($\mu mol\ l^{-1}$)	PO_4 ($\mu mol\ l^{-1}$)	NH_4 ($\mu mol\ l^{-1}$)	SiO_2 ($\mu mol\ l^{-1}$)
6,00	1,46	12,73	11,46	212,36
9,00	1,09	20,57	28,41	274,64
12,00	0,93	22,07	37,70	274,38
15,00	0,33	25,09	57,37	324,39
18,00	0,56	31,74	67,66	383,37
21,00	0,14	39,37	90,06	337,19
24,00	1,40			
27,00	0,18	44,41	119,85	470,62
30,00	0,24	44,32	128,88	450,24

Tableau B.61

Concentration de nitrate et nitrite, phosphate, ammonium et silice dans les eaux porales de la carotte prise à la station 18 en 2006

Profondeur (cm)	NO_3+NO_2 ($\mu mol\ l^{-1}$)	PO_4 ($\mu mol\ l^{-1}$)	NH_4 ($\mu mol\ l^{-1}$)	SiO_2 ($\mu mol\ l^{-1}$)
-0,87	24,85	2,12	0,00	39,32
-0,65	22,19	1,99	0,00	33,96
-0,43	22,48	2,08	0,00	35,99
-0,22	22,37	2,13	0,66	38,56
0,00	22,12	2,27	1,00	44,32
0,21	20,02	3,23	0,81	84,00
0,43	18,47	3,75	1,01	113,70
0,66	17,17	4,00	0,78	154,16
0,89	13,27	4,41	1,17	205,33
1,14	10,14	4,56	2,64	225,55
1,38	7,45	4,97	7,24	252,88
1,64	4,01	5,31	11,52	247,57
1,89	2,57	6,44	13,17	284,76
2,15	1,66	6,81	13,83	280,31
2,42	1,25	7,24	14,77	279,41
2,68	0,81	7,79	17,23	282,66
2,95	1,01	7,67	19,10	277,01
3,22	1,66	7,93	11,35	284,26
3,50	2,16	8,86	27,09	297,98
3,79	1,67	8,59	30,73	309,09
4,08	0,49	8,40	14,90	295,18
4,36	0,33	8,43	14,86	308,59
4,63	0,27	8,40	13,65	312,99
4,91	0,18	8,37	13,57	318,00
3,00		11,43	12,61	231,75
6,00	1,55	11,16	18,61	236,54
9,00	1,81	19,92	31,89	284,93
12,00	2,04	25,81	46,46	361,09
15,00	2,08	28,24	58,65	419,46
18,00	1,93	34,85	67,88	414,76
21,00	1,27	40,84	90,16	443,88
24,00	1,17	42,67	91,80	400,22
27,00	4,19	48,98	110,77	472,37

Tableau B.62
Concentration de nitrate et nitrite, phosphate, ammonium et silice dans les eaux porales de la carotte prise à la station 16 en 2006

Profondeur (cm)	NO_3+NO_2 ($\mu mol\ l^{-1}$)	PO_4 ($\mu mol\ l^{-1}$)	NH_4 ($\mu mol\ l^{-1}$)	SiO_2 ($\mu mol\ l^{-1}$)
-0,42	23,98	1,76	0,00	24,48
-0,21	21,08	1,58	0,00	20,90
0,00	21,16	1,56	0,00	21,18
0,21	22,12	2,16	0,21	59,64
0,43	22,91	2,53	0,64	79,70
0,66	21,82	2,94	1,83	87,57
0,89	21,70	3,25	2,68	100,80
1,12	20,98	3,54	2,84	115,26
1,35	21,03	3,79	4,45	125,11
1,59	20,34	4,01	3,72	125,19
1,84	20,03	4,23	4,04	134,99
2,09	19,87	4,50	5,42	151,47
2,34	18,06	4,63	5,05	141,46
2,59	13,19	4,94	7,66	149,81
2,85	9,11	4,98	5,36	155,30
3,10	4,71	5,22	8,29	155,71
3,29	2,63	5,25	7,36	154,34
1,00	13,54	4,74	3,18	200,93
6,00	4,88	12,31	7,80	313,80
11,00	0,29	15,95	12,76	368,78
16,00	0,17	17,13	16,37	403,96
21,00	0,45	16,94	19,66	404,44
26,00	0,72	15,26	18,90	387,71
31,00	0,82	13,41	22,71	361,80

Tableau B.63
Concentration de nitrate et nitrite, phosphate, ammonium et silice dans les eaux porales de la carotte prise à la station TCA en 2006

Profondeur (cm)	NO_3+NO_2 ($\mu mol\ l^{-1}$)	PO_4 ($\mu mol\ l^{-1}$)	NH_4 ($\mu mol\ l^{-1}$)	SiO_2 ($\mu mol\ l^{-1}$)
-1,28	26,40	1,96	0,00	28,81
-1,07	24,61	1,83	0,00	23,73
-0,86	24,84	1,82	0,00	24,13
-0,64	24,40	1,83	0,03	24,88
-0,43	24,72	1,86	0,03	25,96
-0,22	24,10	0,81	0,04	39,77
0,00	22,17	2,13	0,04	61,13
0,21	16,96	2,53	0,50	95,07
0,43	15,19	2,97	1,45	114,03
0,66	10,81	3,46	2,27	121,81
0,89	7,92	3,66	6,49	129,24
1,14	5,76	3,87	7,23	136,98
1,38	5,39	4,39	8,98	136,11
1,64	7,39	4,61	12,22	151,85
1,91	8,67	4,64	13,79	155,32
2,24	7,29	5,02	16,69	162,98
2,56	4,86	5,44	19,20	172,45
2,83	4,64	5,34	8,87	166,90
3,10	6,47	4,77	20,35	166,25
3,47	3,64	4,93	19,38	205,70
3,78	1,75	5,22	21,34	205,60
4,09	1,21	5,09	21,41	210,98
4,42	1,06	5,15	22,46	217,17
4,69	0,51	5,34	23,97	207,89
5,00	1,14	9,19	32,51	332,80
10,00	1,07	20,22	42,27	153,59
15,00	0,98	36,67	50,00	190,45
20,00	1,04	29,25	55,12	189,40
25,00	2,10	21,77	56,32	173,65
30,00	1,49	21,60	60,98	183,22
36,00	1,64	26,36	78,37	210,09

Tableau B.64
Concentration de nitrate et nitrite, phosphate, ammonium et silice dans les eaux porales de la carotte prise à la station TCE en 2006

Profondeur (cm)	NO_3+NO_2 ($\mu mol\ l^{-1}$)	PO_4 ($\mu mol\ l^{-1}$)	NH_4 ($\mu mol\ l^{-1}$)	SiO_2 ($\mu mol\ l^{-1}$)
-0,86	26,86	2,27	0,00	29,39
-0,65	24,67	2,00	0,00	27,01
-0,44	25,11	2,09	0,00	27,97
-0,22	22,59	2,43	0,20	39,26
0,00	21,90	3,22	1,28	67,84
0,21	16,29	4,22	2,93	94,09
0,43	14,79	3,87	1,54	105,35
0,66	11,79	3,58		113,53
0,89	8,85	4,44	5,01	130,98
1,14	4,83	6,30	10,97	159,48
1,38	5,02	6,11	13,77	145,11
1,64	7,54	7,19	21,16	154,12
1,89	10,12	7,97	17,97	157,42
2,15	13,72	8,56	19,55	144,49
2,42	14,87	7,58	25,31	150,13
2,68	10,31	7,56	23,32	160,91
2,95	2,60	7,48	14,94	147,75
3,22	3,71	7,17	18,00	175,01
3,50	1,75	6,55	16,93	180,16
3,77	3,65	6,84	20,46	185,99
4,05	3,93	6,82	23,81	192,33
4,30	5,89	7,17	30,21	199,47
4,49	2,74	7,58	32,50	183,67

Tableau B.65

Concentration de nitrate et nitrite, phosphate, ammonium et silice dans les eaux porales de la carotte prise à la station 23(a) en 2005

Profondeur (cm)	NO_3+NO_2 ($\mu mol\ l^{-1}$)	PO_4 ($\mu mol\ l^{-1}$)	NH_4 ($\mu mol\ l^{-1}$)	SiO_2 ($\mu mol\ l^{-1}$)
-0,17	25,29	3,16	0,12	37,06
0,00	22,86	4,87	1,25	44,39
0,17	21,48	6,64	1,53	144,83
0,34	18,12	8,47	2,86	34,80
0,47	13,09	5,62	3,82	42,72
0,54				
0,69	9,93	4,10	4,00	40,36
0,84	6,55	4,26	1,77	41,19
0,87				
1,05	4,69	4,30	1,89	42,64
1,22	3,96	4,24	2,55	44,70
1,38	4,14	4,26	2,40	41,39
1,55	3,63	4,32	2,86	50,18
1,62				
1,84	4,93	4,50	6,19	33,57

Tableau B.66

Concentration de nitrate et nitrite, phosphate, ammonium et silice dans les eaux porales de la carotte prise à la station 23(b) en 2005

Profondeur (cm)	NO_3+NO_2 ($\mu mol\ l^{-1}$)	PO_4 ($\mu mol\ l^{-1}$)	NH_4 ($\mu mol\ l^{-1}$)	SiO_2 ($\mu mol\ l^{-1}$)
0,00	24,85	3,04	0,00	40,78
0,18	21,50	3,40	0,00	47,83
0,36	18,48	4,31	0,74	74,28
0,65	13,79	7,08	5,14	132,58
0,85	11,50	4,65	0,00	127,72
1,06	8,03	5,23	0,00	157,04
1,27	6,00	5,13	0,00	163,23
1,49	6,49	4,94	2,68	177,20
1,76	4,57	5,27	1,73	182,16
2,03	2,91	4,90	3,90	216,92
2,26	1,70	5,21	1,68	201,38
2,40				
2,66	1,74	7,88	7,32	207,60
2,94	1,21	6,69	6,22	212,93
2,99				
3,36	1,81	5,65	4,12	211,87
3,91	1,18	5,38	5,08	213,03
4,46	0,55	5,60	6,01	223,68
5,02	0,47	5,84	14,60	230,54

Tableau B.67
Concentration de nitrate et nitrite, phosphate, ammonium et silice dans les eaux porales de la carotte prise à la station 24 en 2005

Profondeur (cm)	NO_3+NO_2 ($\mu mol\ l^{-1}$)	PO_4 ($\mu mol\ l^{-1}$)	NH_4 ($\mu mol\ l^{-1}$)	SiO_2 ($\mu mol\ l^{-1}$)
-1,11	25,67	3,20	0,00	28,11
-0,99				
-0,74	23,80	2,60	0,00	23,85
-0,49	23,78	2,57	0,00	24,57
-0,25	23,70	2,57	0,00	25,71
0,00	23,43	2,59	0,00	25,53
0,15	22,69	2,71	0,00	30,22
0,28	21,46	3,34	0,00	33,70
0,32				
0,45	17,30	3,45	0,00	49,03
0,57	10,85	3,58	0,00	74,28
0,72				
0,86	9,12	3,93	0,00	100,36
0,99	6,29	4,09	1,31	109,99
1,13	14,77	4,26	1,92	112,39
1,28	23,90	4,38	3,09	123,11
1,42	23,11	4,36	4,76	122,83
1,57	14,87	4,25	6,05	130,23
1,71	13,76	4,46	8,30	126,97
2,02	9,46	4,65	15,52	138,54
2,33	16,56	5,67	20,17	145,54
3,38	4,89	4,81	36,35	140,72

Tableau B.68
Concentration de nitrate et nitrite, phosphate, ammonium et silice dans les eaux porales de la carotte prise à la station E5 en 2005

Profondeur (cm)	NO_3+NO_2 ($\mu mol\ l^{-1}$)	PO_4 ($\mu mol\ l^{-1}$)	NH_4 ($\mu mol\ l^{-1}$)	SiO_2 ($\mu mol\ l^{-1}$)
-1,04	25,53	2,63	0,00	30,02
-0,65	23,37	2,53	0,00	28,58
-0,28	11,21	1,45	0,55	12,37
0,00	23,43	2,79	0,00	34,20
0,06				
0,20	20,07	3,35	0,00	41,97
0,35	17,61	3,47	0,00	57,14
0,49	15,10	3,47	0,00	63,69
0,64	12,48	3,82	0,00	71,61
0,74				
0,80				
0,95	8,01	3,93	0,00	95,35
1,10	6,49	3,98	0,00	102,19
1,27	7,66	4,04	0,00	108,35
1,43	5,04	4,22	1,18	121,36
1,50				
1,66	3,69	4,73	1,48	120,48
1,83	2,97	5,08	2,37	111,24
2,00	2,75	7,25	8,31	145,66
2,17	2,41	8,11	14,22	139,25
2,42	1,48	9,73	20,24	157,01
2,69	1,14	11,24	21,09	148,42
3,04	1,22	13,19	32,50	160,11
3,39	1,85	13,11	30,30	157,16
3,74	1,85	13,00	32,92	159,06

APPENDICE C

DONNÉES PRÉSENTÉES DANS LE CHAPITRE III

Tableau C.1

Concentration et composition isotopique des nitrates à la station de Lévis entre juin 2006 et mai 2007

Date	NO_3 ($\mu mol\ l^{-1}$)	$\delta^{15}N$ (‰)	écart type (‰)	$\delta^{18}O$ (‰)	écart type (‰)
28 juin 2006	25,38	6,92	0,23	3,73	0,43
12 juillet 2006	26,27	6,96	0,07	3,74	0,93
26 juillet 2006	13,46	7,23	0,08	3,18	0,25
9 août 2006	20,88	7,48	0,12	3,31	0,59
23 août 2006	11,63	7,21	0,04	2,23	0,10
8 septembre 2006	13,05	6,99	0,24	2,49	0,17
22 septembre 2006	15,63	5,42	0,03	3,47	0,11
6 octobre 2006	19,45	6,56	0,00	4,13	0,17
20 octobre 2006	20,77	6,97	0,00	3,76	0,37
2 novembre 2006	35,31	7,21	0,00	4,03	0,40
14 novembre 2006	31,30	7,13	0,05	4,49	0,18
27 novembre 2006	28,61	6,01	0,19	4,67	1,25
10 janvier 2007	43,82	6,63	0,13	4,44	0,11
29 janvier 2007	30,14	5,49	0,06	5,00	0,39
11 février 2007	29,25	4,88	0,10	5,07	0,12
19 février 2007	28,30	4,72	0,01	5,34	0,50
5 mars 2007	30,12	4,94	0,14	4,73	0,16
21 mars 2007	34,52	4,12	0,07	8,64	0,03
3 avril 2007	35,73	5,01	0,28	7,08	0,33
10 avril 2007	36,19	5,73	0,06	5,88	0,73
16 avril 2007	35,46	6,13	0,02	4,94	0,39
22 avril 2007	37,56	6,12	0,27	3,40	0,23
9 mai 2007	23,02	5,35	0,20	3,90	0,02

Tableau C.2
Concentration et composition isotopique des nitrates à la station de Lévis entre mai 2007 et juillet 2008

Date	NO_3 ($\mu mol\ l^{-1}$)	$\delta^{15}N$ (‰)	écart type (‰)	$\delta^{18}O$ (‰)	écart type (‰)
20 mai 2007	24,80	5,39	0,04	5,41	0,10
3 juin 2007	27,96	6,33	0,01	4,80	0,10
18 juin 2007	25,02	5,49	0,09	4,50	0,20
3 juillet 2007	21,56	6,35	0,01	4,00	0,29
18 juillet 2007	20,77	6,91	0,00	4,60	0,03
30 juillet 2007	16,50	7,17	0,05	3,38	0,01
13 août 2007	12,75	7,29	0,01	3,07	0,09
4 octobre 2007	12,70	7,03	0,07	3,18	0,31
29 novembre 2007	25,54	6,52	0,19	4,75	0,11
26 décembre 2007	25,03	5,78	0,29	4,43	0,01
31 janvier 2008	30,53	5,41	0,13	5,13	0,42
7 mars 2008	27,93	4,81	0,02	5,49	0,10
28 mars 2008	28,53	4,95	0,13	5,96	0,24
4 avril 2008	31,70	4,45	0,70	6,46	0,13
24 avril 2008	32,39	5,34	0,19	4,71	0,12
20 mai 2008	19,13	5,40	0,03	5,58	0,17
17 juin 2008	32,91	6,65	0,27	3,71	0,06
2 juillet 2008	22,34	6,36	0,22	3,40	0,07

Tableau C.3

Débit, $\delta^{18}O$ de l'eau et $\delta^{18}O$ modélisé des nitrates à la station de Lévis entre juin 2006 et mai 2007

Date	Débit ($m^3\ s^{-1}$)	$\delta^{18}O_{H2O}$ (‰)	$\delta^{18}O_{NO3}$ modélisé (‰)
28 juin 2006	11672	-8,46	1,69
12 juillet 2006	10526	-8,63	1,59
26 juillet 2006	10526		
9 août 2006	10536	-7,98	1,98
23 août 2006	10536	-7,59	2,22
8 septembre 2006	10163	-7,48	2,29
22 septembre 2006	10163	-7,37	2,36
6 octobre 2006	13110	-8,06	1,94
20 octobre 2006	13110	-8,22	1,84
2 novembre 2006	14714	-9,57	1,01
14 novembre 2006	14714	-9,03	1,34
27 novembre 2006	14714	-8,75	1,51
10 janvier 2007	10358	-9,5	1,05
29 janvier 2007	10358		
11 février 2007	9899	-8,54	1,64
19 février 2007	9899	-8,2	1,85
5 mars 2007	12775	-8,82	1,47
21 mars 2007	12775	-9,92	0,79
3 avril 2007	15293	-9,37	1,13
10 avril 2007	15293	-9,55	1,02
16 avril 2007	15293	-11,16	0,03
22 avril 2007	15293	-9,99	0,75
9 mai 2007	12571	-9,36	1,14

Tableau C.4

Débit, $\delta^{18}O$ de l'eau et $\delta^{18}O$ modélisé des nitrates à la station de Lévis entre mai 2007 et juillet 2008

Date	Débit ($m^3 s^{-1}$)	$\delta^{18}O_{H2O}$ (‰)	$\delta^{18}O_{NO3}$ modélisé (‰)
20 mai 2007	12571	-8,75	1,51
3 juin 2007	11726	-8,74	1,52
18 juin 2007	11726	-8,04	1,95
3 juillet 2007	10363	-7,98	1,98
18 juillet 2007	10363	-8,3	1,79
30 juillet 2007	10363	-8,06	1,94
13 août 2007	9634	-7,63	2,20
4 octobre 2007	9926	-7,29	2,41
29 novembre 2007	9672	-8,11	1,90
26 décembre 2007	9772	-8,23	1,83
31 janvier 2008	10521	-8,78	1,49
7 mars 2008	11972	-8,55	1,63
28 mars 2008	11972	-8,53	1,65
4 avril 2008	17566	-8,66	1,57
24 avril 2008	17566	-11,7	-0,30
20 mai 2008	16773	-9,56	1,01
17 juin 2008		-8,83	1,46
2 juillet 2008		-9,04	1,33

APPENDICE D

DONNÉES DE LA CAROTTE CR06-TCE

L'appendice D contient les données micropaléontologiques et géochimiques que j'ai produites à partir d'une carotte échantillonnée en 2006 à la tête du Chenal Esquiman (CR06-TCE). La carotte a été prélevée à 50°28,362 N et 58°06,628 W sous une profondeur d'eau de 282 m. Le très faible taux de sédimentation nous a empêché de l'utiliser pour la problématique abordée dans cette thèse. Par contre les données produites seront utilisées ultérieurement pour retracer la variabilité naturelle du système Saint-Laurent. L'abondance relative élevée des foraminifères benthiques *Brizalina subaenariensis* et *Oridorsalis umbonata,* ainsi que les valeurs enrichies de la composition isotopique des foraminifères benthiques *Globobulimina auriculata*, nous indiquent des conditions benthiques relativement chaudes et marquées par une faible oxygénation au cours de l'histoire postglaciaire. Il sera donc important de compléter l'analyse de cette carotte afin de mieux comprendre les causes possibles, naturelles ou anthropogéniques, de l'hypoxie de l'estuaire maritime du Saint-Laurent.

Tableau D.1

Données géochimiques des sédiments de la carotte CR06-TCE

Profondeur (cm)	$CaCO_3$ (%)	C_{org} (%)	C/N	$\delta^{13}C_{org}$ (‰)	$\delta^{15}N_{org}$ (‰)
0,5	7,50	2,15	11,10	-22,75	7,32
1,5	5,69	2,26	12,07	-22,66	7,13
2,5	7,44	2,14	11,23	-22,62	7,08
3,5	8,49	2,06	10,62	-22,74	7,00
4,5	8,00	2,09	11,26	-22,76	7,15
5,5	8,54	2,03	11,19	-22,71	7,16
6,5	8,72	1,88	10,65	-22,57	7,16
7,5	9,22	1,84	9,91	-22,65	7,35
8,5	9,55	1,79	9,98	-22,60	7,18
9,5	10,72	1,70	9,13	-22,56	7,13
10,5	8,66	1,84	10,87	-22,64	7,17
11,5	8,08	1,79	11,22	-22,52	7,12
12,5	9,04	1,59	10,78	-22,59	7,07
13,5	9,01	1,65	10,96	-22,66	7,15
14,5	8,85	1,60	10,95	-22,68	7,12
15,5	9,12	1,39	10,75	-22,76	6,95
16,5	8,75	1,43	11,64	-22,76	7,48
17,5	8,91	1,36	11,39	-22,78	7,38
18,5	8,13	1,57	11,90	-22,73	6,85
19,5	9,52	1,30	10,97	-22,69	7,36
20,5	9,34	1,43	11,63	-22,74	7,38
21,5	9,10	1,37	10,72	-22,70	7,37
22,5	9,24	1,31	11,25	-22,75	7,47
23,5	9,49	1,30	11,94	-22,88	7,33
24,5	9,55	1,37	11,37	-22,86	7,27
25,5	9,70	1,17	12,43	-23,02	7,25
26,5	9,47	1,22	11,87	-23,02	7,29
27,5	9,38	1,28	12,64		7,31
28,5	10,39	1,12	11,70	-22,94	7,22
29,5	10,21	1,16	12,83	-22,98	7,20
30,5	9,92	1,16	12,55	-23,05	7,16
31,5	10,46	1,10	12,03	-22,98	7,21
32,5	11,12	1,10	12,56	-22,99	7,20
33,5	10,23	1,13	11,69	-23,01	7,17
34,5	10,67	1,06	11,38	-22,98	7,14

Tableau D.2
Composition isotopique de *Globobulimina auriculata* (foraminifère benthique) dans la carotte CR06-TCE

Profondeur (cm)	$\delta^{13}C$ (‰)	$\delta^{18}O$ (‰)
0,5	-1,06	2,98
1,5	-1,27	3,02
2,5	-1,04	3,09
3,5	-0,82	3,64
4,5	-0,95	3,28
5,5	-1,20	3,06
6,5	-0,73	3,69
7,5	-0,85	3,19
8,5	-0,49	3,74
9,5	-0,83	3,55
10,5	-1,07	3,32
11,5	-1,01	3,12
12,5	-0,91	3,09
13,5	-0,99	3,37
14,5	-0,84	2,95
15,5	-0,71	3,21
16,5	-0,85	3,02
17,5	-1,12	3,14
18,5	-1,02	2,99
19,5	-0,64	2,61
20,5	-0,85	2,96
21,5	-0,81	3,15
22,5	-0,79	3,08
23,5	-1,09	2,95
24,5	-0,71	2,87
25,5	-0,88	2,85
26,5	-0,87	3,06
27,5	-0,93	2,64
28,5		
29,5	-0,86	2,85
30,5		
31,5		
32,5	-1,06	2,68
33,5	-0,64	3,36
34,5		

Tableau D.3
Abondance des foraminifères benthiques dans la carotte CR06-TCE

Profondeur	Nb d'individus			Concentrations	
(cm)	>250 µm	150-250 µm	Total	(Nb/cm^3)	(Nb/g)
0,5	30	135	165	33	76
1,5	44	153	197	39	65
2,5	28	103	131	26	49
3,5	57	129	186	37	59
4,5	47	93	140	28	45
5,5	61	141	202	40	70
6,5	48	130	178	36	53
7,5	113	224	337	67	96
8,5	100	215	315	63	91
9,5	128	381	509	102	148
10,5	122	279	401	80	132
11,5	348	390	738	148	217
12,5	396	596	992	198	288
13,5	131	270	401	80	121
14,5	109	188	297	59	90
15,5	30	116	146	29	45
16,5	66	176	242	48	71
17,5	33	68	101	20	31
18,5	22	70	92	18	26
19,5	0	0	0	0	0
20,5	35	95	130	26	36
21,5	46	190	236	47	83
22,5	77	314	391	78	118
23,5	20	39	59	12	16
24,5	34	148	182	33	51
25,5	36	106	142	28	36
26,5	8	46	54	11	17
27,5	12	58	70	14	20
28,5	22	45	67	13	17
29,5	18	52	70	14	19
30,5	11	44	55	11	15
31,5	20	76	96	19	24
32,5	18	63	81	16	20
33,5	14	51	65	13	17
34,5	19	40	59	12	16

Tableau D.4
Pourcentage des espèces dominantes de foraminifères benthiques dans la carotte CR06-TCE (1 de 4)

Profondeur (cm)	*Brizalina subaenariensis* (%)	*Bulimina exilis* (%)	*Bulimina marginata* (%)
0,5	12	10	36
1,5	7	9	41
2,5	6	4	48
3,5	6	9	37
4,5	1	4	39
5,5	2	3	43
6,5	4	1	44
7,5	2	1	51
8,5	1	2	47
9,5	0	1	61
10,5	1	2	54
11,5	0	2	38
12,5	0	1	39
13,5	0	1	48
14,5	0	0	49
15,5	2	2	53
16,5	0	1	57
17,5	0	2	47
18,5	0	0	78
19,5			
20,5	0	1	56
21,5	1	1	58
22,5	1	2	47
23,5	2	2	59
24,5	6	3	54
25,5	20	1	28
26,5	6	4	44
27,5	10	4	40
28,5	7	0	54
29,5	6	0	47
30,5	7	0	53
31,5	13	0	48
32,5	15	0	44
33,5	18	0	38
34,5	15	0	41

Tableau D.5
Pourcentage des espèces dominantes de foraminifères benthiques dans la carotte CR06-TCE (2 de 4)

Profondeur (cm)	*Glandulina* spp. (%)	*Globobulimina auriculata* (%)	*Lagena* sp. (%)
0,5	1	7	1
1,5	0	9	0
2,5	0	15	1
3,5	2	9	1
4,5	2	14	0
5,5	1	12	1
6,5	4	12	1
7,5	2	12	1
8,5	2	13	1
9,5	0	12	1
10,5	0	13	1
11,5	2	20	0
12,5	1	15	1
13,5	1	16	2
14,5	2	17	3
15,5	3	9	3
16,5	3	12	2
17,5	5	17	6
18,5	2	4	3
19,5			
20,5	4	12	4
21,5	4	8	0
22,5	1	5	1
23,5	10	8	2
24,5	1	8	4
25,5	4	4	3
26,5	2	6	6
27,5	4	4	1
28,5	3	0	1
29,5	4	1	4
30,5	2	2	4
31,5	1	2	1
32,5	1	5	0
33,5	5	3	0
34,5	0	10	0

Tableau D.6
Pourcentage des espèces dominantes de foraminifères benthiques dans la carotte CR06-TCE (3 de 4)

Profondeur (cm)	*Cibicides* spp. (%)	*Elphidium excavatum* (%)	*Nonionella labradorica* (%)
0,5	0	3	7
1,5	1	2	8
2,5	1	3	5
3,5	0	2	5
4,5	0	2	12
5,5	1	1	10
6,5	1	2	8
7,5	1	2	10
8,5	1	2	9
9,5	1	3	7
10,5	0	2	10
11,5	0	2	18
12,5	0	4	22
13,5	0	3	16
14,5	0	0	19
15,5	0	5	14
16,5	0	5	10
17,5	0	5	16
18,5	0	1	5
19,5			
20,5	2	5	15
21,5	0	4	12
22,5	1	7	17
23,5	0	2	15
24,5	1	4	9
25,5	4	5	17
26,5	6	4	7
27,5	6	7	14
28,5	6	4	16
29,5	6	10	11
30,5	5	9	15
31,5	4	9	10
32,5	2	7	17
33,5	5	5	18
34,5	8	2	15

Tableau D.7
Pourcentage des espèces dominantes de foraminifères benthiques dans la carotte CR06-TCE (4 de 4)

Profondeur (cm)	*Oridorsalis umbonata* (%)	*Cassidulina* sp. (%)	*Islandiella norcrossi* (%)	*Uvigerina* sp. (%)	Indéterminés (%)
0,5	7	12	2	1	2
1,5	8	9	0	5	1
2,5	5	5	0	3	3
3,5	5	15	1	4	3
4,5	6	11	0	2	5
5,5	3	13	0	4	4
6,5	2	15	1	1	3
7,5	0	14	1	1	3
8,5	0	17	1	3	2
9,5	0	10	1	1	1
10,5	0	13	0	1	1
11,5	0	17	1	0	0
12,5	0	13	3	0	0
13,5	0	8	6	0	0
14,5	0	7	1	0	0
15,5	0	6	1	1	0
16,5	0	4	5	0	0
17,5	0	2	1	0	0
18,5	0	3	1	1	0
19,5					
20,5	0	2	2	0	0
21,5	0	7	4	0	0
22,5	0	12	6	1	0
23,5	0	0	0	0	0
24,5	0	2	7	0	1
25,5	9	1	4	0	0
26,5	7	0	7	2	0
27,5	4	0	4	0	0
28,5	4	0	1	0	1
29,5	6	0	4	0	0
30,5	2	0	2	0	0
31,5	8	0	2	0	1
32,5	4	0	4	0	0
33,5	2	0	6	0	0
34,5	2	2	3	2	0

APPENDICE E

DONNÉES ISOTOPIQUES DES NITRATES DANS L'ESTUAIRE MOYEN ET MARITIME

Tableau E.1

Composition isotopique des nitrates dissous aux stations A à G

Station	Profondeur	$\delta^{15}N$	Écart type	$\delta^{18}O$	Écart type
A	20	6,03	0,08	4,73	0,45
B	10	6,06	0,08	3,83	0,12
C	10	5,94	0,02	3,98	0,04
D	10	5,04		4,18	0,27
D-E	20	5,30		4,15	0,74
D-E	14	5,39		3,86	0,51
D-E	3	5,84	0,07	3,90	0,37
E	25	5,55	0,28	5,12	0,25
E	15	5,60	0,14	3,92	0,22
E	3	5,22	0,26	3,83	0,49
E-F	10	5,55	0,12	3,96	0,28
E-F	3	5,35	0,12	4,11	0,17
F2	50	5,60	0,09		
F2	30	5,56		3,34	0,17
F2	3	5,59		3,95	0,45
F1-A	45	5,44		3,78	0,33
F1-A	11	5,28		3,99	0,26
F1-A	3	5,19		4,27	0,18
F1-B	43	5,45		4,38	0,55
F1-B	12	5,59		4,51	
F1-B	3	5,70		3,75	
G	85	5,32		4,30	
G	41	5,45		4,54	
G	20	5,39		5,38	
G	3	5,47		3,79	

Tableau E.2
Composition isotopique des nitrates dissous aux stations I à K

Station	Profondeur	$\delta^{15}N$	Écart type	$\delta^{18}O$	Écart type
I	51	5,18		4,62	
I	30	4,91		5,27	
I	20	5,15		4,25	
I	11	4,97		4,54	
I	3	6,09		4,16	
J	114	5,22		4,60	
J	70	4,97		5,07	
J	50	5,94		4,93	
J	32	5,76			
J	10	5,45		4,31	
J	3	5,52		4,67	0,54
J	1	5,42		4,24	
K	95	5,70		3,99	
K	70	5,67			
K	50	6,00		5,42	0,34
K	30	6,01		5,48	
K	20	5,84		5,50	
K	10	5,84		5,27	
K	3	5,95		4,52	
K	1	5,83		4,70	0,38

Tableau E.3
Composition isotopique des nitrates dissous à la station 25

Station	Profondeur	$\delta^{15}N$	Écart type	$\delta^{18}O$	Écart type
25	311	6,30	0,01	4,22	0,02
25	200	6,50	0,04	4,12	0,12
25	149	6,03	0,04	3,98	0,43
25	100	5,67	0,15	4,03	1,15
25	70	5,34		4,20	1,07
25	41	5,28	0,05	4,37	1,16
25	20	4,44		4,71	0,69
25	3	5,63	0,17	4,73	0,52
25	1	5,81		4,95	0,73

Tableau E.4
Composition isotopique des nitrates dissous à la station 23

Station	Profondeur	$\delta^{15}N$	Écart type	$\delta^{18}O$	Écart type
23	330	6,25	0,03	5,65	0,52
23	300	6,34	0,02	5,70	0,18
23	250	6,25	0,06	5,34	0,46
23	200	6,27	0,06	4,97	0,01
23	150	6,11	0,07	4,55	0,42
23	100	5,63	0,22	5,01	0,17
23	50	5,03	0,13	8,81	0,10
23	40	5,92		9,17	
23	30	6,23		7,15	
23	20	7,96		9,93	
23	10	6,95	0,33	7,30	0,26
23	1	7,75	0,16	8,68	0,33

Tableau E.5
Composition isotopique des nitrates dissous à la station 21

Station	Profondeur	$\delta^{15}N$	Écart type	$\delta^{18}O$	Écart type
21	312	5,95	0,15	4,74	0,76
21	298	5,96	0,17	5,05	1,07
21	250	6,16	0,04	5,15	1,02
21	200	5,76	0,10	5,01	1,24
21	175	5,74	0,13	4,68	1,35
21	122	5,60	0,15	4,30	1,77
21	60	4,01	0,09	3,99	0,83
21	40	3,65	0,19	3,95	0,36
21	30	4,47	0,07	4,08	0,02
21	21	5,64	0,10	4,02	0,03
21	11	6,75	0,14	4,68	0,22

Tableau E.6
Composition isotopique des nitrates dissous à la station 18

Station	Profondeur	$\delta^{15}N$	Écart type	$\delta^{18}O$	Écart type
18	370	6,01	0,15	4,68	
18	330	5,37			
18	270	5,73	0,06	4,94	0,31
18	230	6,18	0,03	4,28	0,02
18	150	5,85	0,29	3,60	0,17
18	100	5,61	0,05	4,49	
18	50	4,10		5,09	
18	10			4,92	

Tableau E.7
Composition isotopique des nitrates dissous à la station 16

Station	Profondeur	$\delta^{15}N$	Écart type	$\delta^{18}O$	Écart type
16	420	5,12		4,73	0,57
16	350	5,22		4,50	0,58
16	275	5,52		5,10	0,74
16	250	5,42		4,90	0,63
16	200	5,21		5,06	0,41
16	150	5,18		4,67	
16	100	5,09		4,95	

Tableau E.8
Composition isotopique des nitrates dissous à la station TCE

Station	Profondeur	$\delta^{15}N$	Écart type	$\delta^{18}O$	Écart type
TCE	270	5,81		4,25	0,16
TCE	250	5,83		4,28	0,10
TCE	225	5,48		3,95	0,16
TCE	200	5,62		4,04	0,03
TCE	150	5,46		3,63	0,10
TCE	100			3,62	
TCE	50	6,03			

Tableau E.9
Composition isotopique des nitrates dissous à la station TCA

Station	Profondeur	$\delta^{15}N$	Écart type	$\delta^{18}O$	Écart type
TCA	270	5,64	0,10	3,39	0,10
TCA	250	5,48	0,30	3,56	0,19
TCA	225	5,41	0,01	4,49	1,07
TCA	200	5,58	0,01	3,65	
TCA	150	5,36	0,35	2,84	
TCA	100	5,46	0,44	2,45	
TCA	50	4,28	0,18	3,89	0,31

APPENDICE F

RECENT CHANGES IN BOTTOM WATER OXYGENATION AND TEMPERATURE IN THE GULF OF ST. LAWRENCE: MICROPALEONTOLOGICAL AND GEOCHEMICAL EVIDENCE

Linda Genovesi[1], Anne de Vernal[1*], Benoît Thibodeau[1], Claude Hillaire-Marcel[1], Taoufik Radi[1], Alfonso Mucci[2], Denis Gilbert[3]

*Corresponding author e-mail: devernal.anne@uqam.ca

[1] GEOTOP, Université du Québec à Montréal, CP 8888, Succursale Centre-Ville, Montreal, Quebec, Canada, H3C 3P8, Tel: +1-514-987-4080; Fax: +1-514-987-3635

[2] GEOTOP & Earth and Planetary Science, University McGill, 3450 University Street, Montreal, Quebec, Canada, H3A 2A7

[3] Institut Maurice-Lamontagne, Pêches et Océans Canada, 850, route de la Mer, CP 1000, Mont-Joli, Quebec, Canada, G5H 3Z4

Article soumis en Août 2010 à la revue *Limnology & oceanography*

Abstract

Micropaleontological and geochemical analyses of a sediment core collected in the Laurentian Trough of the Gulf of St. Lawrence were carried out to reconstruct temporal variations in pelagic productivity and benthic condition. Dinoflagellate cyst assemblages reveal relatively uniform pelagic conditions over the last centuries. Similarly, geochemical (organic C, C_{org}/N) and isotopic (δ^{13}Corg, δ^{15}N) data suggest that organic matter fluxes to the seafloor have been relatively constant over the same period. Nevertheless, significant changes are recorded in the benthic foraminifer assemblages. The greater relative abundances of *Cassidulina laevigata* and *Brizalina subaenariensis* in the upper centimetre of the core indicate a recent decrease of oxygen concentrations in bottom water. A decrease in the relative abundance of *Nonionellina labradorica,* concomitant with a greater relative abundance of *Oridorsalis umbonatus* in the upper 8 cm of the core indicates a significant warming in bottom water, which is consistent with the hypothesis that the contribution of Labrador Current water, relative to North Atlantic central water, to the water entering the Laurentian Trough through Cabot Strait has waned over the years. Change in bottom water properties is further constrained by decrease of the isotopic (δ^{18}O) composition of *Bulimina exilis* shells by 0.4‰, which would correspond to a warming of approximately 1.4°C, over the last century. These results demonstrate that recent oxygen depletion in the bottom waters of the Gulf of St. Lawrence is

driven mostly by increased bottom water temperatures and/or changes in bottom water origin rather than an increased productivity of the surface waters.

Introduction

Eutrophication is often identified as the main cause of bottom water hypoxia in coastal environments (e.g., Cloern, 2001). In the Lower St. Lawrence Estuary, direct measurements have documented a progressive depletion of dissolved oxygen (DO) in bottom waters, from ~125 to 65 μmol L^{-1} over the last 70 years (Gilbert et al., 2005), which is consistent with micropaleontological and geochemical analyses of sediment cores showing clear evidence of oxygen depletion since the 1960s (Thibodeau et al., 2006). Whereas one half to two thirds of the oxygen depletion as been ascribed to a change in the ocean circulation in the northwest Atlantic and, thus, variations in the water properties (DO, temperature, salinity) of the bottom waters that enter the Gulf and St. Lawrence Estuary through Cabot Strait (Gilbert et al., 2005), the remainder as been associated with increased organic carbon fluxes to the seafloor due to anthropogenic eutrophication (Thibodeau et al., 2006). As shown by Thibodeau et al. (2006) and Gilbert et al. (2007), the enhanced use of agricultural fertilizers in the St. Lawrence River drainage basin is concurrent with the depletion of bottom water oxygen concentrations in the LSLE. However, an increase in bottom water

temperatures, leading to increased respiration rates, could also explain the recent decrease of dissolved oxygen concentrations (Gilbert et al., 2005).

In order to determine if the eutrophication and hypoxia extend seaward to the Gulf, we analyzed a core collected in the central part of the Gulf of St. Lawrence (GSL) (Fig. 1).

Micropaleontological, geochemical and isotopic proxies were used to estimate changes historical in primary productivity and bottom water conditions in the GSL.

Oceanographic context

The GSL is a semi-enclosed sea on the eastern coast of Canada, which was described in detail by Dickie and Trites (1983). The dominant bathymetric feature in the Gulf and Lower St. Lawrence Estuary (LSLE) is the Laurentian Channel (or Trough), a submarine valley that extends 1240 km landward from the Atlantic continental shelf, through the GSL and ends at the mouth of the Saguenay Fjord near Tadoussac (Figure 1). Depths throughout the Laurentian Trough exceed 200 m and reach 480 m at Cabot Strait.

The average annual primary production in the GSL was estimated at 210 $gCm^{-2}yr^{-1}$ in the 1950-1960s (Steven, 1974). Satellite data also served to evaluating primary productivity. It was estimated at 186 $gC\ m^{-2}\ yr^{-1}$ from the Coastal Zone Color Scanner (CZCS) program applied to observations from 1978 to 1989 (Antoine et al., 1996), and was estimated at 293 $gC\ m^{-2}\ yr^{-1}$ based on the MODerate resolution Imaging Spectroradiometer (MODIS) program using the model of Behrenfeld and

Falkowski (1997) and observations from 2002 to 2005 (data archived at the address http://daac.gsfc.nasa.gov). The discrepancies between the productivity data sets could be related to the difference in the CZCS and MODIS data acquisition processes and/or productivity variations through time (see Radi and de Vernal, 2008). Despite uncertainties in annual productivity estimates, the observations indicate high primary production on regional scale, especially when taking into account the short ice-free season from April to December (Dickie and Trites, 1983).

In summer, the water column is characterized by three distinct layers. The upper layer is 10 to 15 m thick; it is relatively warm and of low salinity (27 to 32). A cold intermediate layer (-0.5 to 1.0 °C) of salinity ranging 31.5 to 33, which formed at the surface during winter, extends to depths varying from 80 to 150 m. The deepest layer, which fills the Laurentian Channel, is characterized by warm temperatures (4 to 6°C) and high salinities (~ 34.6) (Dickie and Trites, 1983). The bottom waters originate from the edge of the continental shelf and are a mixture of cold and oxygen-rich waters from the Labrador Current (LCW) and warm and oxygen-poor North Atlantic central water (NACW) (Gilbert et al., 2005). They enter the Gulf through Cabot Strait and flow landward to the head of the Laurentian Channel in about 3 to 4 years (Gilbert, 2004). A permanent pycnocline separates the bottom waters from the intermediate and surface layers, inhibiting mixing and replenishment of oxygen from the atmosphere. As a result, bottom water, dissolved oxygen concentrations gradually decrease landward in response to the respiration of organic matter settling from the surface (Gilbert et al., 2005). The bottom water oxygen levels in the Gulf and St.

Lawrence Estuary of are therefore particularly sensitive to variations in organic fluxes and/or temperature.

Material and methods

Sampling

An undisturbed sediment core (COR0503-CL05-37BC) was recovered in 2005 at 409 m water depth in the Laurentian Channel, south of Anticosti Island (48°20'N, 61°30'W) on board the R/V Coriolis II using an Ocean Instrument Mark II box corer . The box core was subsampled by pushing a 10-cm diameter liner in the sediment. The 38 cm long push-core was mounted on a holding table, extruded with a hydraulic piston and subsampled at 0.5 cm intervals from 0 to 15 cm, and at 1 cm intervals for the remainder of the core.

Core chronology

Lead-210 activities of dried and crushed samples were obtained indirectly by measuring the decay rate of its daughter isotope ^{210}Po ($t_{1/2}$ = 138.4 days; α = 5.30 MeV) by alpha spectrometry. A Polonium-209 spike was added to the samples to determine the extraction and counting efficiency. Polonium was extracted and purified by chemical treatments (reacted sequentially with HCl, HNO_3, HF and H_2O_2) and deposited on a silver disk (Flynn, 1968). The $^{209\text{-}210}$Po activities were measured in a silicon surface-barrier α-spectrometer (EGG&ORTEC type 576A).

The ^{210}Pb activity profile of core COR0503-CL05-37BC was used to evaluate the supported ^{210}Pb fraction and the excess ^{210}Pb activities (Fig. 2). Hence, different sedimentation rates (under a constant rate supply assumption) were calculated using the radioactive decay constant (λ) of ^{210}Pb and the linear regression slope of the logarithmic function of excess ^{210}Pb below the mixed layer.

Cesium-137 was measured by γ-ray spectrometry at 661.6 keV with a Canberra low-background high-purity Ge well-detector. The reproducibility of ^{137}Cs activities was estimated at ± 1% by replicate analyses (n=6) of the standard reference material IAEA-300 (Baltic Sea sediment).

Micropaleontological analysis

Sediment samples were treated according to the procedure described by de Vernal et al. (1999). A known volume of humid sediments was weighed, dried at room temperature, and weighed once more to determine its water content. Wet sediments were sieved through 106 µm and 10 µm mesh sieves. The fraction greater than 106 µm was dried at room temperature, weighed and examined under a binocular microscope (x40). Calcareous and agglutinated foraminifera were hand-picked, counted and identified using the nomenclature of Rodrigues (1980). In this paper, we report the total concentration of benthic foraminifer shells and the relative abundance of the most abundant taxa.

The 10 μm to 106 μm fraction was submitted to a series of treatments, with hydrochloric acid (HCl 10%) and hydrofluoric acid (HF 49%) to dissolve carbonate and silica particles (for details see de Vernal et al., 1999). The residue was wet sieved through a 10 μm mesh and mounted between a slide and a cover in glycerine gel. The slides were examined under an optical microscope at 400x magnification and all palynomorphs were counted. Tablets of *Lycopodium* spores have previously been added to the samples to calculate the palynomorph concentrations. The nomenclature used for the identification of dinocysts is that of Rochon *et al.* (1999). Relative abundances (in percentages) of the main taxa are reported and the modern analogue technique (MAT) following the procedure described by Radi and de Vernal (2008), is used to reconstruct the primary productivity. The reference productivity databases used for reconstruction are those of CZCS (Antoine et al., 1996) and MODIS (http://daac.gsfc.nasa.gov). Validation exercises indicate that the accuracy of the reconstruction is ± 34 gC m^{-2} using CZCS, and ± 55 gC m^{-2} using MODIS (Radi and de Vernal, 2008). Details about other palynomorphs (pollen grains, spores, organic linings of foraminifera) identified in the sediment samples can be found in Genovesi (2009).

(a) Sediment Carbon and Nitrogen analyses ($\%C_{org}$, $\delta^{13}C$, C/N, $\delta^{15}N$)

Total carbon (TC) and total nitrogen (TN) concentrations of the dried, ground and homogenized samples were determined with a Carlo Erba™ NC 2500 elemental

analyzer. Inorganic carbon (IC) was analyzed independently using a UIC Coulometrics™ coulometer following acidification of the samples and CO_2 extraction. The organic carbon (OC) content was obtained from the difference between the total and inorganic carbon concentrations. Precision, as determined from replicate measurements of Organic Analytical Standard substances (Acetanilide, Atropine, Cyclohexanone-2.4-Dinitrophenyl-Hydrazone and Urea), is estimated at ± 0.1% for OC and ± 0.3% for N contents. The analytical reproducibility was ± 5%.

For the isotopic analyses of OC and nitrogen, sediment samples were acidified with a dilute HCl (1N) solution, dried at room temperature, ground and homogenized. The isotopic composition was measured with a Carlo Erba™ elemental analyzer online with a Micromass Isoprime™ mass spectrometer. Data are reported in δ (‰) with reference to V-PDB for carbon and atmospheric N_2 for nitrogen (Coplen, 1995). The analytical uncertainty is ± 0.1 ‰ for the $\delta^{13}C$ and 0.2 ‰ for the $\delta^{15}N$ values, as determined from replicate measurements of standard materials during analytical runs. The international standards IAEA-C6 sucrose and IAEA-N2 were measured several times during the isotopic analyses and yielded, respectively, an average value of $\delta^{13}C$ = -10.73 ± 0.02 ‰ for n=4 whereas the reported value is -10.8 ± 0.1 ‰ and $\delta^{15}N$ = 20.20 ± 0.24 ‰ for n=4 whereas the reported value is 20.41 ± 0.12 ‰.

Oxygen and carbon isotopes analyses in benthic foraminifer shells ($\delta^{18}O$, $\delta^{13}C$)

In each sample, approximately a dozen benthic foraminifer shells of *Bulimina exilis* were hand-picked from the 150-250 μm size fraction. The calcareous shells were roasted at ~200°C under vacuum for about 2 hours and analyzed with a Micromass Isoprime™ isotope ratio mass spectrometer in dual inlet mode coupled to a MultiCarb™ preparation system. CO_2 was extracted at 90°C by acidification with 100% H_3PO_4. Measurements were made with an internal reference carbonate material calibrated against the V-PDB scale. The analytical reproducibility based on replicate measurements of the internal standard material was routinely better than 0.05 %.

Results

Excess ^{210}Pb, ^{137}Cs activity and sedimentation rate

The ^{210}Pb profile follows a negative exponential trend with some variations (Fig. 2). The upper 2 cm could possibly respond to benthic mixing and/or illustrate large discrepancies in water content. They were therefore excluded for further calculations. In order to estimate the supported fraction of ^{210}Pb without data on parent isotopes such as ^{226}Ra, we used both the regional value of 1.89±0.05 dpm/g proposed by Zhang, (2000) and Jennane (1992), and the asymptotic trend in ^{210}Pb-activities (2.09±0.14 dpm/g) observed in the lower part of the cored sequence. The choice of one or the other of these values results in a important difference in the estimation of the unsupported fraction of ^{210}Pb ($^{210}Pb_{xs}$), thus in the calculation of a

mean sediment accumulation rate assuming constant sedimentary and ^{210}Pb fluxes (see Fig. 2). Sedimentation rate values of approximately 0.20 or 0.15 cm/a can be obtained, respectively. The ^{137}Cs measurements show an activity peak at ~4.25 cm (cf. Table 1), which can be assigned to the maximum input of artificial radionuclides originating from atmospheric nuclear testing at ca. 1963 (Jouanneau et al., 1999). Therefore, the lower sedimentation rate estimate of 0.15 cm/a as calculated from the asymptotic ^{210}Pb-trend at the base of the core seems more likely. Furthermore, the analysis of several sedimentary sequences from nearby sites in the Gulf of St. Lawrence yielded almost similar sedimentation rates (e.g., Silverberg et al., 1986; Jennane, 1992; Zhang, 2000). We will thus retain here a mean sedimentation rate of ~ 0.15 cm/a. However, as highlighted in the $Ln^{210}Pb_{xs}$ plot of figure 2, the actual sedimentation rate (and/or $^{210}Pb_{xs}$ flux) may have varied through time. This is particularly the case between 13 and 16 cm downcore, where the sediment depicts an almost reverse profile that may correspond to an abrupt sedimentological event. The supported ^{210}Pb fraction relates mostly to grain-size, mineralogical composition and organic carbon content of the sediment, which may vary, in the Gulf of St. Lawrence area, depending upon the proximal sediment sources (i.e., reworked Paleozoic shales, eroded Paleozoic carbonates, Goldthwait Sea sediments, etc.). Adding the large uncertainties deeper in the core, one must conclude that the extension of a precise chronology below the depth of 13-16 cm would be speculative. Since the subsequent micropaleontological and geochemical analyses were performed at 1 cm interval, we

may conclude at a ~ decadal resolution for the upper section of the core, i.e. down to the 13-16 cm layer, spanning approximately the last 100 years.

Dinocyst assemblages

The dinocyst concentrations (Fig. 3a) vary between 30 000 and 90 000 cysts g^{-1} and show high frequency oscillations but no clear trend. The dinocyst assemblages (Fig. 3b) are dominated by two taxa, *Pentapharsodinium dalei* and *Islandinium minutum* which, respectively, represent ~34% and ~30% of the assemblage. Other important species include *Operculodinium centrocarpum* (~13%), *Nematosphaeropsis labyrinthus* (~12%) and *Brigantedinium* spp. (5%). The following taxa were also present but only represented 2% or less of the assemblage: *Spiniferites elongatus, Spiniferites ramosus, Islandinium? cezare, Selenopemphix quanta, Spiniferites* spp., *Ataxiodinium choane, Alexandrium tamarense*. The relative abundances of each taxa show no significant trend, suggesting relatively uniform sea-surface conditions and pelagic productivity in the Gulf of St. Lawrence for the past few centuries. Nevertheless, we note a decrease in the relative abundance of heterotrophic taxa in the uppermost centimetre of the core, from ~30% to ~8% for *Islandinium minutum* and from ~5% to ~0.6% for *Brigantedinium* spp. This could reflect a very recent change of the trophic and/or hydrographic conditions (e.g., Radi and de Vernal, 2008).

Productivity estimates from MAT applied to dinocyst assemblages

Transfer functions based on the modern analogue technique using the productivity databases of Antoine et al. (1996) and MODIS (http://daac.gsfc.nasa.gov), were applied to reconstruct primary production. The results, using the data from Antoine et al. (1996), average around 182 gC m^{-2} yr^{-1} (Fig. 4a). These values are approximately 100 gC m^{-2} yr^{-1} lower than those obtained by using the MODIS database (283 gC m^{-2} yr^{-1}, Fig. 4b). As mentioned in the method section, there are discrepancies between the two reference data sets that may arise from the use of different algorithms, alternate data acquisition processes or discrepancies in productivity values between the 1980s and 2000s (Radi and de Vernal, 2008). There are differences in the reconstructions based on the two databases, but they both yield relatively uniform values of annual primary production, with some variations and no clear trend, suggesting uniform primary productivity throughout the core.

Geochemistry of sedimentary organic matter

The C_{org} content, C_{org}/N_{tot} weight ratio, $\delta^{13}C_{org}$ and $\delta^{15}N_{org}$ of core COR0503-CL05-37BC oscillate slightly with depth (Fig. 5). However, with the exception of the upper 6 cm, there are no systematic variations or trend. The values are typical of marine organic matter (Meyers, 1997) and lie in the lower range of values reported for the Laurentian Channel (Muzuka and Hillaire-Marcel, 1999). Variations within the upper 6 cm of the sediment core can be attributed to the preferential degradation

of nitrogen-rich autochthonous organic matter in the sediment during early diagenesis (Meyers, 1997; Muzuka and Hillaire-Marcel, 1999).

Benthic foraminifer assemblages

The total benthic foraminifer concentrations (Fig. 6a) vary from 4 to 21 tests g^{-1}, and average ~ 9.6 tests g^{-1}. The assemblages are dominated by calcareous taxa (Fig. 6b), except in the upper part of the core where agglutinated species are more abundant. Their relative and absolute abundances may result from a change in bottom water properties. It can also be due to selective preservation of agglutinated shells in surface and subsurface sediment. Because the particles forming the agglutinated tests are cemented together by organic matter, their resistance to diagenetic alteration, although difficult to quantify, is generally low (Murray, 1991). The abundance of agglutinated foraminifera in the upper part of the core could thus reflect change in the progression of hypoxia in bottom waters and a better preservation of their fragile shells under less oxidizing conditions (Barmawidjadja et al., 1995).

Among the calcareous taxa, the dominant species are *Bulimina exilis*, *Bulimina marginata*, *Elphidium excavatum*, *Nonionella labradorica* and *Oridorsalis umbonatus*. Secondary species include *Globobulimina auriculata*, *Quinqueloculina seminulum*, *Lagena* sp., *Brizalina subaenariensis*, *Cassidulina laevigata* and *Glandulina* sp. Several significant changes in the calcareous foraminifer assemblage are observed in the upper 8 cm of the core. The relative abundances of *Bulimina*

marginata, *Lagena* sp., *Quinqueloculina seminulum*, *Glandulina* sp. and *Elphidium excavatum* decrease significantly whereas the relative abundances of *Brizalina subaenariensis* and *Cassidulina laevigata* increase towards the sediment-water interface. These observations are consistent with the development of hypoxia in the GSL, as the latter species are generally associated with oxygen-depleted environments (e.g., Mendes et al., 2004; Murray, 1991; Sen Gupta and Machain-Castillo, 1993). Most notable, in the same interval, is the disappearance (from~30% to 0%) of *Nonionellina labradorica*, a species found in the cold waters of the Labrador Shelf (Bilodeau et al., 1994). This change is concomitant with the increase (from ~5 % to 30 %) in the relative abundance of *Oridorsalis umbonatus*, a species common in surface sediments bathed by warm waters of the North Atlantic (Bilodeau et al., 1994; Murray, 1991).

Isotopic composition of benthic foraminifer shells

The $\delta^{18}O$ of the calcareous shells of *Bulimina exilis* records a decreasing trend towards the top of the core, from which is particularly pronounced in the upper 16 cm depth. According to the paleotemperature equation of Shackleton (1974), the $\delta^{18}O$ variations correspond to temperature increases of 0.53°C from 16 to 37 cm and of 1.36°C from 16 cm to the top of the core. and/or a change in the isotopic composition of the ambient seawater.

$t = 16.9 - 4.38(\delta^{18}O_c - A) + 0.10(\delta^{18}O_c - A)^2$, with $A = (\delta^{18}O_w - 0.27)$

where t is the temperature (in °C) at the time of calcite precipitation, $\delta^{18}O_c$ is the isotopic composition of calcite (relative to V-PDB), and $\delta^{18}O_w$ is the isotopic composition of the ambient water (relative to SMOW). The value used for the isotopic composition of ambient water ($\delta^{18}O_w$) is 0.07 ‰, an average of $\delta^{18}O$ measurements from samples taken at depths between 350 and 450 m in the vicinity of the Gulf of St. Lawrence (data from the *Global Seawater $\delta^{18}O$ Database*; cf. Schmidt et al., 1999).

The $\delta^{13}C$ isotopic compositions of *Bulimina exilis* (Fig.7b) are more variable with depth than their $\delta^{18}O$ signatures. In the lower part of the core, from 10 to 37 cm, increase very slightly and smoothly with depth from ~ -1.63 ‰ to ~ -1.99 ‰ whereas, in the upper part of the core, $\delta^{13}C$ values decrease rapidly from the surface (~ -2.12 ‰) to a depth of ~6 cm (~ -2.37 ‰) and increase to ~ -2.12 ‰ to a depth of ~12 cm. *Bulimina exilis* is an endobenthic species and, thus, the $\delta^{13}C$ composition of its shell is responds to variations of the isotopic composition of the CO_2 produced by the decay of buried organic matter (Muzuka and Hillaire-Marcel, 1999). Therefore the $\delta^{13}C$ cannot be used to support any of the above mentioned processes or combination of processes invoked for explaining the change in oxygen isotope composition (i.e., an increase in temperature or a change in isotopic composition of ambient water).

Discussion

As was proposed for the LSLE (Gilbert et al., 2005; Thibodeau et al., 2006; Benoit et al., 2006), the recent development of hypoxic conditions in the bottom waters of the Gulf of St. Lawrence may, at least in part, be related to increased biogenic production and organic carbon fluxes to the deep waters and the seafloor. To verify this hypothesis, we examined several proxies of productivity, including the organic carbon content, its isotopic composition, the C_{org}:N_{tot} ratio, and organic walled microfossils. The organic carbon (Corg) content of the sediment shows a subtle increase towards the surface over the last 12 cm or century (Fig. 5a). This increase may reflect a greater flux of organic matter reaching the seafloor, a better preservation of the organic matter as dissolved oxygen concentrations became depleted in the overlying waters (Gelinas et al., 2001) or the progressive remineralization of the most reactive material over time (Meyers, 1997). The isotopic composition of organic carbon ($\delta^{13}C$) and nitrogen ($\delta^{15}N$) and the C/N ratio of organic matter indicate a steady source with fluxes predominantly from marine origin (e.g., Meyers, 1997). Consistent with the latter interpretation, the dinoflagellate cyst assemblages and concentrations do not vary significantly with depth, and the reconstruction of primary productivity suggests relatively uniform production throughout the period represented by the core (~ 200 years).. Hence, the change in bottom water conditions, independent from surface parameters, necessarily plays a determinant role on the development of hypoxia in the GSL..These findings contrasts

with the findings of Thibodeau et al. (2006) who, based on the same proxies, provided evidence for a recent increase in pelagic productivity in the LSLE.

The benthic foraminifer assemblages are indicators of benthic conditions during their life cycle including temperature, salinity, productivity and oxygenation (e.g., Barmawidjaja et al., 1995; Kaiho, 1994). They have also often been used as tracers of hypoxia (e.g., Osterman, 2003; Tsujimoto et al., 2006). Important changes in the foraminifer assemblage are recorded in the upper 8 cm of core COR0503-CL05-37BC. The relative abundance of certain species, such as *Bulimina marginata*, *Elphidium excavatum*, *Nonionellina labradorica*, *Lagena* sp., and *Glandulina* sp., decrease sharply or, in some cases, disappear towards the sediment-water interface. The reason for these changes in foraminifer abundances cannot be assessed unequivocally since the tolerance limits of these species to the physical and chemical properties of water masses are poorly known (Sen Gupta and Machain-Castillo, 1993). Nevertheless, the general decrease in species diversity must reflect a new imposed stress to this environment, such as hypoxia. This interpretation is consistent with the increased relative abundance of *Brizalina subaenariensis* and *Cassidulina laevigata* in the upper part of the core, as these two species are tolerant to low-oxygen concentrations (e.g., Mendes et al., 2004; Murray, 1991; Sen Gupta and Machain-Castillo, 1993). Therefore, we propose that the changes in foraminifer assemblages and relative abundances are a response to the decreasing dissolved oxygen level in bottom waters of the GSL. According to our age models, these changes may have

started between the 1940s and 1960s, consistent with the development of hypoxia in the LSLE described by Gilbert et al. (2005).

Gilbert et al. (2005, 2007) interpret the oxygen depletion in the LSLE as the response to two factors: an increase in the flux of organic matter from the surface to the seafloor, and a modification of the proportion of LCW and NACW entering the Laurentian Channel through Cabot Strait. Using temperature and salinity measurements of the LCW and NACW, they calculated that in the 1930s the waters entering the Laurentian Channel at Cabot Strait were composed of approximately 72% LCW and 28% NACW, but since the 1980s these proportions have changed to 53% LCW and 47% NACW. These waters would therefore be 1.65°C warmer (Gilbert et al., 2005). The change in the relative proportion of cold and oxygen-rich LCW to warm and oxygen-poor NACW is recorded both by the benthic foraminifer assemblages and their stable isotope composition. The relative abundance of *Nonionellina labradorica*, a species abundant in the Labrador Sea (Bilodeau et al., 1994), decreased by ~30% while *Oridorsalis umbonatus*, a species common under North Atlantic waters (Bilodeau et al., 1994; Murray, 1991), increased by ~25% over the past ~60 years. Furthermore, the $\delta^{18}O$ of benthic foraminifer shells indicates a shift in bottom water temperature. An increase of temperature of about 0.5°C is recorded from ~1730/1810 to ~1880/1910, followed by a warming of at least 1.4°C from the turn of the century (~1880/1910) to 2005. According to Gilbert et al. (2005, 2007), the increased bottom water temperature was accompanied by an increase in

salinity ($\Delta S_p \approx 0,.28$). Since the isotopic composition of the ambient water is dependent upon salinity (Ravelo and Hillaire-Marcel, 2007), the temperature change we calculated from $\delta^{18}O$ measurements may be underestimated. Nevertheless, the estimated increase in temperature of the bottom waters of the GSL is consistent with the historical measurements (~1.65°C, Gilbert et al., 2005). An increase of temperature in sub-surface waters of the North Atlantic and Labrador Sea during the last decades could also be invoked (Levitus et al., 2000).

Conclusion

Micropaleontological and geochemical analysis of sediment core COR0503-CL05-37BC collected in the Gulf of St. Lawrence shows no evidence of an increase in primary production over the last few centuries and the recent period of development of hypoxic conditions in the bottom waters. These data are more consistent with the hypothesis that dissolved oxygen depletion in the bottom waters of the GSL results from changes in the relative contributions of LCW and NACW to the waters that enter the Gulf through Cabot Strait from the edge of the Canadian continental shelf. These changes are accompanied by slight decreases in salinity ($\Delta S_p \approx 0.3$) and increases in temperature (~1.65°C) over the last 80 years. This interpretation is supported by variations of the benthic foraminifer assemblages recorded in the sediments, particularly by the concomitant decrease in the relative

abundance of *Nonionellina labradorica* and increase of *Oridorsalis umbonatus,* as well as by variations in the isotopic composition of benthic foraminifer shells, which indicate ~1.9°C warming of the bottom waters in the Gulf of St. Lawrence over the last century.

Our study demonstrates that the bottom water oxygenation in the Laurentian Channel is not only sensitive to eutrophication but also to temperature variations which accompanied changes in ocean circulation on the edge the continental shelf. These recent changes may be a manifestation of climate warming or natural cycles, only longer time series will tell.

References

Antoine, D., André, J-M., Morel, A. 1996. Estimation at global scale from satellite (coastal zone color scanner) chlorophyll. Global Biochem. Cy. **10**:57-69

Barmawidjaja, D.M., Van der Zwaan, G.J., Jorissen, F.J., Puskaric, S., 1995. 150 years of eutrophication in the northern Adriatic sea: Evidence from a benthic foraminifer record. Mar. Geol. **122**: 367-384

Benoit P., Gratton Y., Mucci A., 2006. Modeling of dissolved oxygen levels in the bottom waters of the Lower St. Lawrence Estuary: coupling of benthic and pelagic processes. Marine Chemistry **102:** 13-32.

Berhenfeld, M.J., Falkowski, P.G., 1997. Photosynthetic rates derived from satellite-based chlorophyll concentration. Limnol. Oceanogr. **42**: 1-20

Bilodeau, G., de Vernal, A., Hillaire-Marcel, C., 1994. Benthic foraminiferal assemblages in Labrador Sea sediments: relations with deep-water mass changes since deglaciation. Can. J. Earth Sci. **31**: 128-138.

Bratton, J.F., Colman, S.M., Seal, R.R., 2003. Eutrophication and carbon sources in Chesapeake Bay over the last 2700 yr: Human impacts in context. Geochim. Cosmochim. Ac. **67**: 3385-3402

Cloern, J.E., 2001. Our evolving conceptual model of the costal eutrophication problem. Mar. Ecol. Prog. Ser. **210**: 223-253

Coplen, T.B., 1995. Discontinuance of SMOW and Pdb. Nature **375**: 285

de Vernal, A., Henry, M., Bilodeau, G., 1999. Techniques de préparation et d'analyse en micropaléontologie. Les cahiers du GEOTOP.

Devillers, R., de Vernal, A., 2000. Distribution of dinoflagellate cysts in surface sediments of the northern North Atlantic in relation to nutrient content and productivity in surface waters. Mar. Geol. **166**: 103-124

Dickie, L.M., Trites, R.W., 1983. The Gulf of St. Lawrence. p. 403-425 *In* Ketchum, H. (Ed), Estuaries and enclosed seas. Elsevier Scientific Publishing company, Amsterdam-Oxford-New York

Flynn, W.W. 1968. The determination of low levels of polonium-210 in environmental materials. Anal. Chim. Acta **43**: 221-227

Genovesi, L. 2009. Indices micropaléontologiques et géochimiques de changements récents de l'oxygénation et la température des eaux profondes du Golfe du St-Laurent. Mémoire de maîtrise, Université du Québec à Montréal

Gilbert, D. 2004. Propagation of temperature signals from the northwest Atlantic continental shelf edge into the Laurentian Channel. ICES CM 2004/N:07

Gilbert, D., Sundby, B., Gobeil, C., Mucci, A., Tremblay, G-H., 2005. A seventy-two year record of diminishing deep-water oxygen in the St. Lawrence estuary: The northwest Atlantic connection. Limnol. Oceanogr. **50**: 1654-1666

Gilbert, D., Chabot, D., Archambault, P., Rondeau, B., Hébert, S. 2007. Appauvrissement en oxygène dans les eaux profondes du St-Laurent marin : causes possibles et impacts écologiques. Le Naturaliste Canadien, **131**: 67-75

Jennane, A. 1992. Application de la méthode du plomb-210 dans l'Estuaire maritime et le Golfe du St-Laurent. Taux de sédimentation, flux et modes d'ablation. Mémoire de maîtrise, Université du Québec à Montréal.

Jouanneau, J.M., Castaing, P., Grousset, F., Buat-Menard, P., Pedemay, P., 1999. Recording and chronology of a cadmium contamination by Cs-137 in the Gironde estuary (SW France). C.R. Acad. Sci. Sér. II, Sci. Terre Planètes **329**: 265-270

Kaiho, K., 1994. Benthic foraminiferal dissolved-oxygen index and dissolved-oxygen levels in the modern ocean. Geology **22**: 719-722

Levitus, S., Antonov, J. I., Boyer, T.P., Stephens, C. 2000. Warming of the world oceans. Science **287**: 2225-2229.

Mendes, I., Gonzalez, R., Dias, J.M.A., Lobo F., Martins V., 2004. Factors influencing recent benthic foraminifer distribution on the Guadiana shelf (Southwestern Iberia). Mar. Micropaleontol. **51**:171–192

Meyers, P.A., 1997. Organic geochemical proxies of paleoceanographic, paleolimnologic, and paleoclimatic processes. Org. Geochem. **27**: 213-250

Murray, J.W., 1991. Ecology and palaeoecology of benthic foraminifera. Longman Scientific & Technical

Muzuka, A.N.N., Hillaire-Marcel, C. 1999. Burial rates of organic matter along the eastern Canadian margin and stable isotope constraints on its origin and diagenetic evolution. Mar. Geol. **160**: 251-270

Osterman, L.E., 2003. Benthic foraminifers from the continental shelf and slope of the Gulf of Mexico: an indicator of shelf hypoxia. Estuar. Coast. Shelf S. **58**: 17-35

Radi, T., de Vernal, A., 2008. Dinocysts as proxy of primary productivity in mid-high latitudes of the Northern Hemisphere. Mar. Micropaleontol. **68**: 84-114

Radi, T., Pospelova, V., de Vernal, A., Barrie, J.V., 2007. Dinoflagellate cysts as indicators of water quality and productivity in British Columbia estuarine environments. Mar. Micropaleontol. **62**: 269-297

Ravelo, A.C., Hillaire-Marcel, C. 2007. The use of oxygen and carbon isotopes of foraminifera in paleoceanography. p. 735-760. *In* C. Hillaire-Marcel and A. de Vernal [eds], Develpments in marine geology Volume 1: Proxies in late Cenozoic paleoceanography.

Rochon, A., de Vernal, A., Turon, J-L., Matthiessen, J., Head, M.J., 1999. Distribution of recent dinoflagellate cysts in surface sediments from the North Atlantic ocean and adjacent seas in relation to sea-surface parameters. Am. Assoc. Stratigr. Palynol. Found. **35**

Rodrigues, C.G., 1980. Holocene microfauna and paleoceanography of the Gulf of St. Lawrence. Ph.D. Thesis. Carleton University

Schmidt, G.A., Bigg, G. R., Rohling, E. J. 1999. Global Seawater Oxygen-18 Database. http://data.giss.nasa.gov/o18data/

Sen Gupta B.K., Machain-Castillo, M.L. 1993. Benthic foraminifera in oxygen-poor habitats. Mar. Micropaleontol. **20**: 183-201

Shackleton, N.J., 1974. p.203-209. *In* J. Labeyrie [ed], Méthodes quantitatives d'études des variations du climat au cours du Pléistocène, Éditions du CNRS

Silverberg, N., Nguyen, H.V., Delibrias, G., Koide, M., Sundby, B., Yokoyama, Y., Chesselet, R., 1986. Radionuclide profiles, sedimentation rates, and bioturbation in modern sediments of the Laurentian through, Gulf of St. Lawrence. Oceanol. Acta, **9**: 285-290

Sorgente, D., Frignani, M., Langone, L., Ravaioli, M., 1999. Chronology of marine sediments : interpretation of activity-depth profiles of ^{210}Pb and other radioactive tracers, Part I. Technical Report n.54, Consiglio nazionale delle ricerche istituto per la geologia marina, Bologna.

Steven, D.M., 1974. Primary and secondary production in the Gulf of St. Lawrence. Mar. Sci. Centre, McGill Univ., Rep. **26**

Thibodeau, B., de Vernal, A., Mucci, A., 2006. Recent eutrophication and consequent hypoxia in the bottom waters of the Lower St. Lawrence Estuary: Micropaleontological and geochemical evidence. Mar. Geol. **231**: 37-50

Tsujimoto, A., Nomura, R., Yasuhara, M., Yamazaki, H., Yoshikawa, S. 2006. Impact of eutrophication on shallow marine benthic foraminifers over the last 150 years in Osaka Bay, Japan. Mar. Micropaleontol. **60**: 258-268

Zhang, D. 2000. Fluxes of short-lived radioisotopes in the marginal basins of eastern Canada. Ph.D. Thesis, Université du Québec à Montréal.

Acknowledgments

This study is a contribution to a strategic project of the National Sciences and Engineering Research Council of Canada (NSERC) entitled "Deep-water hypoxia and the sensitivity of the Lower St. Lawrence Estuary to Environmental change". Financial support from NSERC through the scholarship grants, ship time allocation and from FQRNT is also acknowledged.

Special thanks to Guy Bilodeau, Maryse Henry, Bassam Ghaleb and Christelle Not for their help and advice with the project.

RÉFÉRENCES

Anschutz, P., Sundby, B., Lefrançois, L., Luther III, G.W. and Mucci, A. 2000. Interactions between metal oxides and species of nitrogen and iodine in bioturbated marine sediments. Geochimica et Cosmochimica Acta 64(16), p. 2751-2763.

Baden, S.P., Pihl, L. and Rosenberg, R. 1990. Effects of oxygen depletion on the ecology, blood physiology and fishery of the Norway lobster Nephrops norvegicus. Mar. Ecol. Prog. Ser. 67, p. 141-155.

Belley, R., Archambault, P., Sundby, B., Gilbert, F. and Gagnon, J.M. 2010. Effects of hypoxia on benthic macrofauna and bioturbation in the Estuary and Gulf of St. Lawrence, Canada. Continental Shelf Research 30, 1302-1313.

Benoit, P., Gratton, Y. and Mucci, A. 2006. Modeling of dissolved oxygen levels in the bottom waters of the Lower St. Lawrence Estuary: coupling of benthic and pelagic processes. Marine Chemistry 102, p. 13-32.

Bograd, S.J., Castro, C.G., Di Lorenzo, E., Palacios, D.M., Bailey, H.R. and Gilly, W. 2008. The shoaling of the hypoxic boundary in the California Current. Geophys. Res. Let. 35

Bopp, L., Le Quéré, C., Heimann, M., Manning, A.C. and Monfray, P. 2002. Climate-induced oceanic oxygen fluxes: Implications for the contemporary carbon budget. Global Biogeochemical Cycles 16(2), p. 6-1.

Bourque, M. 2009. Variation spatio-temporelle de la macrofaune endobenthique dans la zone profonde du Saint-Laurent (Québec, Canada) en relation avec les conditions environnementales, Université du Québec à Rimouski, Rimouski, 94 pp.

Breitburg, D.L. 1992. Episodic hypoxia in Chesapeake bay: Interacting effects of recruitment, behavior, and physical disturbance. Ecological Monographs 62(4), p. 525-546.

Brown, C.A., Nelson, W.G., Boese, B.L., Dewitt, T.H., Eldridge, P.M., Kaldy, J.E., Lee Ii, H., Power, J.H. and Young, D.R. 2007. An approach to developing nutrient criteria for Pacific northwest estuaries A case study of Yaquina Estuary, EPA/600/R-07/046, Oregon, U.S. Environmental Protection Agency, p. 183.

Bugden, G.L. 1988. Oceanographic conditions in the deeper waters of the Gulf of St. Lawrence in relation to local and oceanic forcing. NAFO SCR Document 88/87.

Chan, F., Barth, J.A., Lubchenco, J., Kirincich, A., Weeks, H., Peterson, W.T. and Menge, B.A. 2008. Emergence of anoxia in the California current large marine ecosystem. Science 319(5865), p. 920.

Cloern, J.E. 2001. Our evolving conceptual model of the coastal eutrophication problem. Marine Ecology Progress Series 210, p. 223-253.

DeMenocal, P., Ortiz, J., Guilderson, T. and Sarnthein, M. 2000. Coherent high- and low-latitude climate variability during the holocene warm period. Science 288(5474), p. 2198-2202.

Diaz, R.J. 2001. Overview of hypoxia around the world. Journal of Environmental Quality 30(2), p. 275-281.

Diaz, R.J. and Rosenberg, R. 1995. Marine benthic hypoxia: a review of its ecological effects and the behavioural responses of benthic macrofauna. Oceanography and Marine Biology: an annual review. Vol. 33, p. 245-303.

Diaz, R.J. and Rosenberg, R. 2008. Spreading dead zones and consequences for marine ecosystems. Science 321(5891), p. 926-929.

Diaz, R.J., Solan, M. and Valente, R.M. 2004. A review of approaches for classifying benthic habitats and evaluating habitat quality. Journal of Environmental Management 73(3), p. 165-181.

Dickie, L.M. and Trites, R.W. 1983. The Gulf of St. Lawrence. Estuaries and Enclosed Seas, p. 403-425.

Dickson, B., Yashayaev, I., Meincke, J., Turrell, B., Dye, S. and Holfort, J. 2002. Rapid freshening of the deep North Atlantic Ocean over the past four decades. Nature 416(6883), p. 832-837.

Doney, S.C. and Jenkins, W.J. 1994. Ventilation of the deep western boundary current and abyssal western North Atlantic: estimates from tritium and ^{3}He distributions. Journal of Physical Oceanography 24(3), p. 638-659.

Druffel, E.R.M. 1997. Pulses of rapid ventilation in the North Atlantic surface ocean during the past century. Science 275(5305), p. 1454-1457.

Frölicher, T.L., Joos, F., Plattner, G.K., Steinacher, M. and Doney, S.C. 2009. Natural variability and anthropogenic trends in oceanic oxygen in a coupled carbon cycle-climate model ensemble. Global Biogeochemical Cycles 23(1)

Galloway, J.N., Dentener, F.J., Capone, D.G., Boyer, E.W., Howarth, R.W., Seitzinger, S.P., Asner, G.P., Cleveland, C.C., Green, P.A., Holland, E.A., Karl, D.M., Michaels, A.F., Porter, J.H., Townsend, A.R. and Vöosmarty, C.J. 2004. Nitrogen Cycles: Past, Present, and Future. Biogeochemistry 70(2), p. 153-226.

Galloway, J.N., Townsend, A.R., Erisman, J.W., Bekunda, M., Cai, Z., Freney, J.R., Martinelli, L.A., Seitzinger, S.P. and Sutton, M.A. 2008. Transformation of the nitrogen cycle: Recent trends, questions, and potential solutions. Science 320(5878), p. 889-892.

Genovesi, L., Thibodeau, B., de Vernal, A. and Hillaire-Marcel, C. 2008. Recent changes of bottom water oxygenation and temperature in the Gulf of St. Lawrence: micropaleontological and geochemical evidences, Water, Weather, and Climate: Science Informing Decisions. Canadian Meteorological and Oceanographic Society, Kelowna, B.C., pp. 17-18.

Gilbert, D., Rabalais, N.N., Diaz, R.J. and Zhang, J. 2009. Evidence for greater oxygen decline rates in the coastal ocean than in the open ocean. Biogeosciences Discuss 6, p. 9127-9160.

Gilbert, D., Sundby, B., Gobeil, C., Mucci, A. and Tremblay, G.H. 2005. A seventy-two-year record of diminishing deep-water oxygen in the St. Lawrence estuary: The northwest Atlantic connection. Limnology and Oceanography 50(5), p. 1654-1666.

Gillooly, J.F., Brown, J.H., West, G.B., Savage, V.M. and Charnov, E.L. 2001. Effects of size and temperature on metabolic rate. Science 293(5538), p. 2248-2251.

Greene, C.H. and Pershing, A.J. 2003. The flip-side of the North Atlantic Oscillation and modal shifts in slope-water circulation patterns. Limnology and Oceanography 48(1 I), p. 319-322.

Grey, S.M., Haines, K. and Troccoli, A. 2000. A study of temperature changes in the Upper North Atlantic: 1950-94. Journal of Climate 13(15), p. 2697-2711.

Ito, T. and Deutsch, C. 2010. A conceptual model for the temporal spectrum of oceanic oxygen variability. Geophysical Research Letters 37(3)

Katsev, S., Chaillou, G., Sundby, B. and Mucci, A. 2007. Effects of progressive oxygen depletion on sediment diagenesis and fluxes: A model for the lower St. Lawrence River Estuary. Limnology and Oceanography 52(6), p. 2555-2568.

Keeling, R.F. and Garcia, H.E. 2002. The change in oceanic O_2 inventory associated with recent global warming. Proceedings of the National Academy of Sciences of the United States of America 99(12), p. 7848-7853.

Keigwin, L.D. and Pickart, R.S. 1999. Slope water current over the Laurentian Fan on interannual to millennial time scares. Science 286(5439), p. 520-523.

Kendall, C., Elliott, E.M. and Wankel, S.D. 2007. Tracing anthropogenic inputs of nitrogen to ecosystems. Stable Isotopes in Ecology and Environmental Science, p. 375-449.

Lehmann, M.F., Sigman, D.M., McCorkle, D.C., Brunelle, B.G., Hoffmann, S., Kienast, M., Cane, G. and Clement, J. 2005. Origin of the deep Bering Sea nitrate deficit: Constraints from the nitrogen and oxygen isotopic composition of water column nitrate and benthic nitrate fluxes. Global Biogeochemical Cycles 19(4)

Levin, L.A., Ekau, W., Gooday, A.J., Jorissen, F., Middelburg, J.J., Naqvi, S.W.A., Neira, C., Rabalais, N.N. and Zhang, J. 2009. Effects of natural and human-induced hypoxia on coastal benthos. Biogeosciences 6, p. 2063-2098.

Marcus, N.H., Richmond, C., Sedlacek, C., Miller, G.A. and Oppert, C. 2004. Impact of hypoxia on the survival, egg production and population dynamics of Acartia tonsa Dana. Journal of Experimental Marine Biology and Ecology 301(2), p. 111-128.

Meehl, G.A. 2007. Global climate projections. Climate Change 2007: The Physical Science Basis, p. 747-845.

Nakata, K., Sugioka, S.I. and Hosaka, T. 1997. Hindcast of a Japan sea oil spill. Spill Science and Technology Bulletin 4(4), p. 219-229.

Paillet, J. and Arhan, M. 1996. Oceanic ventilation in the eastern North Atlantic. Journal of Physical Oceanography 26(10), p. 2036-2052.

Paillet, J. and Mercier, H. 1997. An inverse model of the eastern North Atlantic general circulation and thermocline ventilation. Deep-Sea Research Part I: Oceanographic Research Papers 44(8), p. 1293-1328.

Plattner, G.K., Joos, F. and Stocker, T.F. 2002. Revision of the global carbon budget due to changing air-sea oxygen fluxes. Global Biogeochemical Cycles 16(4), p. 43-51.

Poulin, P., Pelletier, E. and Saint-Louis, R. 2007. Seasonal variability of denitrification efficiency in northern salt marshes: An example from the St. Lawrence Estuary. Marine Environmental Research 63(5), p. 490-505.

Rabalais, N.N., Diaz, R.J., Levin, L.A., Turner, R.E., Gilbert, D. and Zhang, J. 2010. Dynamics and distribution of natural and human-caused hypoxia. Biogeosciences 7(2), p. 585-619.

Richmond, C., Marcus, N.H., Sedlacek, C., Miller, G.A. and Oppert, C. 2006. Hypoxia and seasonal temperature: Short-term effects and long-term implications for Acartia tonsa dana. Journal of Experimental Marine Biology and Ecology 328(2), p. 177-196.

Savenkoff, C., Vézina, A.F., Smith, P.C. and Han, G. 2001. Summer transports of nutrients in the Gulf of St. Lawrence estimated by inverse modelling. Estuarine, Coastal and Shelf Science 52(5), p. 565-587.

Silva, S.R., Ging, P.B., Lee, R.W., Ebbert, J.C., Tesoriero, A.J. and Inkpen, E.L. 2002. Forensic Applications of Nitrogen and Oxygen Isotopes in Tracing Nitrate Sources in Urban Environments. Environmental Forensics 3(2), p. 125-130.

Slowey, N.C. and Curry, W.B. 1992. Enhanced ventilation of the North Atlantic subtropical gyre thermocline during the last glaciation. Nature 358(6388), p. 665-668.

Taylor, J.C. and Miller, J.M. 2001. Physiological performance of juvenile southern flounder, Paralichthys lethostigma (Jordan and Gilbert, 1884), in chronic and episodic hypoxia. Journal of Experimental Marine Biology and Ecology 258(2), p. 195-214.

Thibodeau, B., de Vernal, A. and Mucci, A. 2006. Recent eutrophication and consequent hypoxia in the bottom waters of the Lower St. Lawrence Estuary: Micropaleontological and geochemical evidence. Marine Geology 231(1-4), p. 37-50.

Tunnicliffe, V. 1981. High species diversity and abundance of the epibenthic community in an oxygen-deficient basin. Nature 294(5839), p. 354-356.

Turner, R.E. and Rabalais, N.N. 1994. Coastal eutrophication near the Mississippi river delta. Nature 368(6472), p. 619-621.

Ueda, N., Tsutsumi, H., Yamada, M., Hanamoto, K. and Montani, S. 2000. Impacts of oxygen-deficient water on the macrobenthic fauna of Dokai Bay and on adjacent intertidal flats, in Kitakyushu, Japan. Marine Pollution Bulletin 40(11), p. 906-913.

Wang, F., Juniper, S.K., Pelegrí, S.P. and Macko, S.A. 2003. Denitrification in sediments of the Laurentian Trough, St. Lawrence Estuary, Québec, Canada. Estuarine, Coastal and Shelf Science 57(3), p. 515-522.

Wankel, S.D., Kendall, C., Francis, C.A. and Paytan, A. 2006. Nitrogen sources and cycling in the San Francisco Bay estuary: A nitrate dual isotopic composition approach. Limnology and Oceanography 51(4), p. 1654-1664.

Wankel, S.D., Kendall, C. and Paytan, A. 2009. Using nitrate dual isotopic composition ^{15}N and ^{18}O as a tool for exploring sources and cycling of nitrate in an estuarine system: Elkhorn Slough, California. Journal of Geophysical Research G: Biogeosciences 114(1)